2013

Patterns and Pathways of Wetland Sedimentation and Landscape Change in Coastal Louisiana

Andrew William Tweel
Louisiana State University and Agricultural and Mechanical College

PATTERNS AND PATHWAYS OF WETLAND SEDIMENTATION AND LANDSCAPE CHANGE IN COASTAL LOUISIANA

A Dissertation

Submitted to the Graduate Faculty of the
Louisiana State University and
Agricultural and Mechanical College
in partial fulfillment of the
requirements for the degree of
Doctor of Philosophy

in

The Department of Oceanography and Coastal Sciences

by
Andrew William Tweel
B.A., Colorado College, 2004
May 2013

To those devoid of imagination a blank place on the map is a useless waste;

to others, the most valuable part

-Aldo Leopold

ACKNOWLEDGEMENTS

I thank everyone who has helped me along the way. The mapping and archival work presented here was greatly facilitated by R. Hampton Peele, John M. Anderson, David J. Morgan, and the Government Documents and Special Collections staff at the Louisiana State University Library. Samuel J. Bentley provided guidance and facilities for the sediment grain size analysis, as well as helpful discussion of storm surge sediment transport. I am grateful for working with the other lab members here, including Erick M. Swenson, Charles S. Milan, James M. Lee, and Giovanna M. McClenachan. Christopher M. Swarzenski provided helpful discussion of coastal wetland soil processes. I would like to thank Robert P. Gambrell, Michael S. Kearney, Bruce G. Sharky, and Lei Wang for serving on my committee and for providing helpful comments and suggestions.

Support for this research was provided by a Louisiana Board of Regents Fellowship for the first four years and a Shell Graduate Fellowship for the final year.

I would also like to thank everyone that I explored coastal Louisiana with, especially Gary W. Peterson.

I am exceptionally grateful to have had the guidance of R. Eugene Turner for my dissertation research. He was always available and eager to answer questions and discuss ideas. He also provided generous support to attend conferences and participate in field trips including many low altitude flights over the Louisiana coast. I cannot thank him enough.

TABLE OF CONTENTS

ABSTRACT

Coastal Louisiana wetlands exist in a dynamic physical environment and retracted dramatically in the last century. Here I examine the spatial and temporal variability of this landscape with an emphasis on the interactions between anthropogenic landscape modifications and geological processes.

The Mississippi River watershed underwent drastic changes during the past 200 years, beginning with widespread land clearing and, later, large-scale reservoir construction. These modifications caused increases in suspended sediment concentrations, then sharp decreases, and have remained relatively stable since 1960. I show how changes in land area of the Mississippi River birdfoot delta reflect these fluctuations, and that they are distinct from the timing of land losses elsewhere along the coast.

The deposition of inorganic sediments elsewhere along the coast is driven primarily by marine processes. I quantified the total amount and spatial distribution of mineral sediment following recent hurricanes and found that Hurricanes Katrina, Rita, and Gustav deposited an estimated 68, 48, and 21 million metric tons (MMT), respectively. I used the observed sediment deposition patterns away from the coast and storm track to estimate a long-term tropical cyclone sedimentation rate (5.6 MMT yr^{-1}) for coastal Louisiana wetlands, which accounts for the majority of inorganic sediments in soils of the abandoned delta lobes and chenier plain.

I applied geographically weighted regression as a supplement to a traditional regression of geological and anthropogenic factors to further explore patterns of landscape variability. I found that the patterns of interior wetland loss are strongly related to the density of dredged canals, and that this relationship varies spatially. Canals closer to the coast, for example, are more strongly correlated to land loss than those found further inland.

The research presented here raises new questions about how physical, chemical, and biological systems interact and regulate coastal systems, and how these driving factors can vary considerably over relatively short distances. The success of coastal restoration in Louisiana and elsewhere will be greatly aided if this spatial variability and remaining scientific uncertainties are included in planning and implementation schemes.

CHAPTER 1
INTRODUCTION

Coastal Variability in Time and Space

The Louisiana coastal landscape contains an array of wetland types that can be found in other deltas and coastal areas throughout the world. There are hardwood swamps, floating marshes, organic-rich freshwater and intermediate marshes, mineral-rich salt marshes, oak ridges, barrier islands, and actively expanding sandy freshwater marshes within a hundred kilometers of each other. The dynamics of these ecosystems are subject to the influences of their physical, geological, and biological context. The large size of the Mississippi River Basin (MRB; 3.2×10^6 km^2), for example, yields massive amounts of sediments (145×10^6 t yr^{-1}, Meade and Moody 2010) compared to most other coastal areas (Dearing et al. 2003) which, in turn, have built a large coastal plain (19,500 km^2 in 1932, Couvillion et al. 2011) that is blanketed by a thin (< 1 to 6 m) veneer of predominantly organic wetland soils (Kosters 1989, Chabreck 1972). The considerable discharge from the Mississippi River (580 km^3 yr^{-1}, Meade and Moody 2010), combined with the relatively low astronomical tides of the Gulf of Mexico (~ 0.3 m at Grand Isle), has resulted in a river-dominated delta forming at its current mouth, in the form of a long birdfoot reaching out over the continental shelf (Coleman 1981). This delta morphology is in great contrast to wave-dominated deltas (e.g., Nile delta or the Sao Francisco in Brazil), where wave action reworks much of the sediment into a smoothed shoreline (Coleman 1981), or tide-dominated deltas (e.g., Ganges) where strong tides dominate sediment transport, carving a series of linear channels in a fragmented delta.

Although the geomorphology of the world's major river deltas varies quite a bit, their formation initiated as sea level rise began to decelerate at the beginning of the Holocene epoch ca. 7,500 ybp as continental glaciation was ending (Stanley and Warne 1994). During

deglaciation the Mississippi River began a transition from a braided, gravelly course to a more entrenched alluvial river (Fisk 1944), and the receding glaciers gave way to a much larger drainage basin (Brown and Kennett 1998). Sea level rose rapidly while this was occurring and led to increased sediment deposition within the river valleys and on the newly inundated continental shelf (Kolb and Van Lopik 1966). This deposition continued until sea level rise slowed down, allowing sediments to accumulate on the shallower continental shelf, forming a delta. The river gradient decreased as this delta expanded, and the Mississippi River eventually abandoned the enlarged delta in favor of a more efficient path to the Gulf (Kolb and Van Lopik 1966). This deltaic shifting occurred roughly every 1000 years and left behind a platform of sediments that are still undergoing various stages of the subsidence, compaction, and marine reworking. At any given point in delta development, roughly 20% of the deltaic plain was actively growing, while the remainder was in a transgressive phase (Coleman 1988).

Sediments left behind by former delta lobes provide the platform for marsh development on this ‘hiatal’ surface (Kolb and Van Lopik 1966), and the complex geomorphology of active and decaying deltas supports a variety of wetland types at the surface. Existing soil conditions in the interior portions of long-abandoned deltas indicate that freshwater marsh plants have maintained elevation by accretion of organic material. The salt and brackish marsh peats located toward the Gulf are also dominated by organic processes, but are punctuated by peaks in mineral content indicative of greater marine influence (Chabreck 1972, Turner et al. 2002, Turner et al. 2007). The soils of active deltas are dominated by fluvial sedimentation. The active delta environment is particularly dynamic, and changes in marsh type and wetland conversion to open water (wetland loss) or back occur throughout the landscape.

Recent Changes and Stressors

These changes in wetland loss and gain in Louisiana have been an ongoing throughout its recent geologic history (Roberts 1997), but the net loss rates have accelerated during historic times (Dunbar et al. 1992). Despite decades of scientific research, there are still many uncertainties as to the causes of wetland loss, especially on a coast-wide scale. Much of this uncertainty stems from the complexity of Louisiana's coastal systems combined with its long history of human intervention, making it sometimes problematic to identify causal factors. On a geologic time-scale, the coastal landscape is subject to the shifting Mississippi River. Extensive peats in abandoned delta lobes indicate that elevation was maintained by organic processes long before river leveeing occurred (Kolb and Van Lopik 1966). On shorter time scales, coastal wetlands are exposed to storm surge and riverine flooding events, tropical cyclones, subsurface faulting, drought stress, eustatic sea level rise and deltaic subsidence (isostatic).

Humans began to modify the coastal landscape in a significant way as early as the 18th century. Beginning with small private levees and trappers' canals, these modifications expanded dramatically over the past two centuries (Davis 1973). Canals dredged for oil and gas production and their adjacent spoil banks are perhaps the most visible landscape alteration, and accounted for approximately 10% of direct land losses coastwide between 1932 and 1990 (Britsch and Dunbar 1993). Spoil banks impact adjacent wetlands by altering sheet flow hydrology, and can cause changes in hydroperiod (Swenson and Turner 1987). Since Louisiana is a microtidal system, seemingly small changes to marsh flooding regimes can have larger impacts on their ability to accrete vertically than otherwise similar macrotidal marshes (Friedrichs and Perry 2001, Kirwan et al. 2010).

There have been in excess of 50,000 oil wells drilled in the Louisiana coastal zone, and over 18,000 of these have been drilled in wetlands and are no longer productive (SONRIS 2010, Figure A.1, page 131). Most of these were built with a dredged access canal. There were 134 km^2 of canals dredged in Barataria Basin by 2001, adding approximately 5,300 km in additional shoreline (originally mapped at 1:62,500 scale). For perspective, this length equals the distance between Florida and Alaska. The shoreline length for Barataria Basin in 1932 was approximately 6,675 km (measured from Britsch and Dunbar 2006). The shoreline length in Barataria Basin (canals plus all other post-1932 land loss) in 2001 was 13,965 km (Table A.1). Accordingly, the mean distance to shoreline in Barataria Basin decreased from 750 m in 1932 to 267 m in 2001, and the mean patch size decreased from 5.3 km^2 to 0.5 km^2 in the same interval (Table A.1).

The coastal area is also subject to varying nutrient and sediment inputs from intensive land use in the Mississippi River watershed (Turner and Rabalais 1994, Raymond et al. 2008). Large-scale “eat-outs” by rodents or waterfowl may lead to plant stress and eventual wetland loss in some areas (O’Neil 1949). Additionally, the construction of a continuous levee system along the Mississippi River curtailed overbank flooding events (Kesel 1989). These impacts are discussed in greater detail in several scientific reports (e.g., Boesch et al. 1994, Turner 1990).

A Priority Determination of the Causes of Recent Wetland Losses

A key factor determining whether or not a wetland will become open water is the rate at which net sediment accretion occurs. The type of accretion that sustains the wetlands varies across the coast. Soils are more organic inland, less organic towards the coast, and highly mineral in the birdfoot and Atchafalaya deltas. Much uncertainty remains, however, as to the

relative contributions of factors (natural or anthropogenic) that drive these patterns and how they relate to wetland formation and loss on this coast.

The processes involved in wetland loss are complex, but can be grouped into three main categories: edge erosion, submergence, and direct human loss (Craig et al. 1979). These three processes are not isolated from each other, which further complicates studies of wetland loss. One type of wetland loss, for example, may make the surrounding wetlands more vulnerable to additional loss. Also, the direct loss via canal construction is spatially related to the indirect loss of wetlands (Turner 1997), and is attributed to subsequent changes in hydrology via increased frequency of flooding and drying events (Swenson and Turner 1987) that can cause plant stress (Mendelssohn and McKee 1988). Similarly, wetland loss that initially begins by submergence, can reach an alternative equilibrium as open water (Simenstad et al. 2000) that can cause further loss via edge erosion (Fearnley et al. 2009, Nyman et al. 1994). Due to the number of possible factors, considerable uncertainty remains as to the relative contributions of the numerous stressors to wetland loss. One way to approach this problem of multi-stressor interactions is to conduct a coast-wide multivariate analysis to identify which factors are most related to wetland loss in various areas, and to help provide a framework for further research of specific processes or coastal areas. Several previous studies have attempted to quantify the contribution of various factors to wetland loss patterns (Deegan et al. 1984, Turner 1997, Cowan and Turner 1988, Day et al. 2000), but the results were not consistent among studies.

One possible explanation for this variability between land loss studies is that they utilized different analysis methods and spatial scales. Furthermore, traditional ordinary least squares regression may not be the most appropriate tool for quantifying spatial relationships (Brundson et al. 1996) as this approach cannot always account for relationships that vary across the study

area. For instance, marshes of a certain soil type may be more sensitive to a given stressor than marshes of another soil type. This varying relationship is referred to as spatial non-stationarity. Geographically weighted regression (GWR) is an analysis method that allows for the possibility of data non-stationarity (Brundson et al. 1996). Use of this method may help more precisely characterize land loss patterns and identify what variables are most correlated to land loss across the landscape.

How data are classified presents another potential source of variability. Coast-wide wetland loss measurements are often generalized into a coast-wide loss rate changing over time; but the geography of the coastal plain is highly variable- both ecologically and geologically. One area characterized by a unique soil type and geomorphology is the Mississippi River birdfoot delta (MRBD), which also experienced earlier and higher rates of wetland loss than other areas of the coast (Britsch and Dunbar 1993). Much of this loss was the same land that expanded as four large subdeltas beginning around 1850 (Wells and Coleman 1987). The timing of this expansion corresponded to a period of rapid agricultural development in the Mississippi River basin, where widespread upland erosion was common. Subsequently, large reservoir construction greatly reduced sediment supply. The timing of these changes in relationship to land loss has yet to be investigated, and could help build a more complete model for coastal restoration and for understanding the processes that drive coastal land loss.

Although the soils are distinctly more organic than the highly mineral soils of the birdfoot delta, the deltaic plain marshes have higher mineral content nearer the Gulf (Chabreck 1972). Recent tropical cyclones affecting Louisiana have drawn attention from wetland scientists for both their potential to cause wetland loss (Barras 2006), and for extensive sediment deposition (Turner et al. 2006, McKee and Cherry 2009). Sediment inputs to wetlands are the focus of

much wetland research in and outside of Louisiana (e.g., Louisiana: Blum and Roberts 2009, Chesapeake: Stevenson et al. 1988, Sacramento delta: Reed 2002, Gulf of Mexico: Callaway et al. 1997), but the inputs from tropical cyclone events are difficult to quantify at an event scale. Although the influx of sediment from these storms appears considerable, the quantification of the role that hurricanes play in contributing sediment to coastal wetlands over a longer time scale, and how sediment deposition may relate to meteorological characteristics of a given event remain only loosely constrained. Understanding the dynamics of sediment input to coastal wetlands, and its incorporation into the model for a coastal wetland sediment budget, is an important component of successful wetland restoration.

Research Goals and Questions

The research described herein attempts to constrain the uncertainty of land change processes on a coast-wide scale and also in several more focused areas. I developed a multi-scale spatial database of geologic and ecological variables for Barataria Basin to provide a broad basis for understanding landscape-scale patterns in wetland loss. I quantify how geological and anthropogenic characteristics of a given landscape influence wetland loss, and how these relationships vary spatially by using quantitative geographic comparisons. Other chapters focus on more specific areas to quantify sediment sources to coastal wetlands and how these sources vary spatially and temporally. The outcome of this research is intended to be an improved scientific understanding of how wetland sedimentation varies spatially, how it is affected by anthropogenic landscape modification, and how it is related to patterns of landscape change.

The primary research questions investigated are:

1. How have changes in the Mississippi River suspended sediment load influenced land area in the birdfoot delta and how do these changes relate to patterns observed elsewhere on

the coast? This question is addressed in chapter two and was published in 2012 (Tweel and Turner 2012a).

2. How much mineral sediment was deposited by hurricanes in Louisiana wetlands during 2005 and 2008 and how does this deposition vary spatially? This question is addressed in chapter 3 and was published in 2012 (Tweel and Turner 2012b).
3. How do these depositional events relate to long-term trends in hurricane landfall and wetland sediment characteristics? This question is addressed in chapter four and has been submitted for publication (Tweel and Turner *submitted*).
4. What variables are related to the patterns of land loss in coastal Louisiana wetlands and how do these relationships vary across the landscape?
5. Is geographically weighted regression a suitable tool for identifying variability in ecosystem response to stressors? Questions four and five are addressed in chapter five.

A concluding chapter (Chapter six) summarizes the cumulative impact of the answers to these questions within the context of coastal restoration and future sustainability.

References

Barras, J. A. 2006. Land Area Change in Coastal Louisiana after the 2005 Hurricanes—a Series of Three Maps. US Geological Survey open-file report 1274.

Blum, M. D. and H. H. Roberts. 2009. Drowning of the Mississippi Delta Due to Insufficient Sediment Supply and Global Sea-Level Rise. Nature Geoscience 2:488-491.

Brown, P. A. and J. P. Kennett. 1998. Megaflood Erosion and Meltwater Plumbing Changes During Last North American Deglaciation Recorded in Gulf of Mexico Sediments. Geology 26:599-602.

Brunsdon, C., S. Fotheringham, and M. Charlton. 2002. Geographically Weighted Regression. Journal of the Royal Statistical Society: Series D (The Statistician) 47:431-443.

Callaway, J. C., R. D. DeLaune, and W. H. Patrick Jr. 1997. Sediment Accretion Rates from Four Coastal Wetlands Along the Gulf of Mexico. Journal of Coastal Research 13:181-191.

Chabreck, R. H. 1972. Vegetation, Water and Soil Characteristics of the Louisiana Coastal Region. Louisiana Agricultural Experiment Station Bulletin 664. 72 p.

Coleman, J. M. 1981. Deltas: Processes of Deposition & Models for Exploration. Burgess Publishing, Minneapolis, Minnesota. 124 p.

Coleman, J. M. 1988. Dynamic Changes and Processes in the Mississippi River Delta. Geological Society of America Bulletin 100:999-1015.

Couvillion, B. R., J. A. Barras, G. D. Steyer, W. Sleavin, M. Fischer, H. Beck, N. Trahan, B. Griffin, and D. Heckman. 2011. Land Area Change in Coastal Louisiana (1932 to 2010). US Department of the Interior, US Geological Survey. 12 p.

Cowan, J. H. and R. E. Turner. 1988. Modeling Wetland Loss in Coastal Louisiana: Geology, Geography, and Human Modifications. Environmental Management 12:827-838.

Craig, N. J., R. E. Turner, and J. W. Day. 1979. Land Loss in Coastal Louisiana (USA). Environmental Management 3:133-144.

Davis, D. W. 1973. Louisiana Canals and Their Influence on Wetland Development. Ph. D. Dissertation. Louisiana State University and Agricultural and Mechanical College.

Day, J. W., L. D. Britsch, S. R. Hawes, G. P. Shaffer, D. J. Reed, and D. Cahoon. 2000. Pattern and Process of Land Loss in the Mississippi Delta: A Spatial and Temporal Analysis of Wetland Habitat Change. Estuaries and Coasts 23:425-438.

Dearing, J. A. and R. T. Jones. 2003. Coupling Temporal and Spatial Dimensions of Global Sediment Flux through Lake and Marine Sediment Records. Global and Planetary Change 39:147-168.

Deegan, L. A., H. M. Kennedy, and C. Neill. 1984. Natural Factors and Human Modifications Contributing to Marsh Loss in Louisiana's Mississippi River Deltaic Plain. Environmental Management 8:519-527.

Dunbar, J. B., L. Britsch, and E. Kemp. 1992. Land Loss Rates: Louisiana Coastal Plain. US Army Engineer Waterways Experiment Station, Vicksburg, Mississippi. Report GO-90-2, Part 3.

Fearnley, S., S. Penland, and L. D. Britsch. 2009. Mapping the Geomorphology and Processes of Coastal Land Loss in the Pontchartrain Basin: 1932 to 1990 and 1990 to 2001. Journal of Coastal Research 54:48-58.

Fisk, H. N. 1944. Geological Investigation of the Alluvial Valley of the Lower Mississippi River. US Army Corps of Engineers, Mississippi River Commission, Vicksburg, Mississippi. 78 p.

Friedrichs, C. T. and J. E. Perry. 2001. Tidal Salt Marsh Morphodynamics: A Synthesis. Journal of Coastal Research SI 27:7-37.

Kesel, R. H. 1989. The Role of the Mississippi River in Wetland Loss in Southeastern Louisiana, USA. Environmental Geology 13:183-193.

Kirwan, M. L., G. R. Guntenspergen, A. D'Alpaos, J. T. Morris, S. M. Mudd, and S. Temmerman. 2010. Limits on the Adaptability of Coastal Marshes to Rising Sea Level. Geophysical Research Letters 37:L23401.

Kolb, C. R. and J. R. van Lopik. 1966. Depositional Environments of the Mississippi River Deltaic Plain Region-Southeastern Louisiana. LS Shirley and JA Ragsdale, eds. Deltas in their Geologic Framework. Houston Geological Society. p. 17-61.

Kosters, E. C. 1989. Organic-Clastic Facies Relationships and Chronostratigraphy of the Barataria Interlobe Basin, Mississippi Delta Plain. Journal of Sedimentary Research 59:98-113.

McKee, K. L. and J. A. Cherry. 2009. Hurricane Katrina Sediment Slowed Elevation Loss in Subsiding Brackish Marshes of the Mississippi River Delta. Wetlands 29:2-15.

Meade, R. H. and J. A. Moody. 2010. Causes for the Decline of Suspended-Sediment Discharge in the Mississippi River System, 1940–2007. Hydrological Processes 24:35-49.

Mendelssohn, I. A. and K. L. McKee. 1988. Spartina Alterniflora Die-Back in Louisiana: Time-Course Investigation of Soil Waterlogging Effects. The Journal of Ecology 76:509-521.

Nyman, J. A., M. Carloss, R. D. DeLaune, and W. H. P. Jr. 1994. Erosion Rather Than Plant Dieback as the Mechanism of Marsh Loss in an Estuarine Marsh. Earth Surface Processes and Landforms 19:69-84.

O'Neil, T. 1949. The Muskrat in the Louisiana Coastal Marshes. Louisiana Wildlife and Fisheries Commission, New Orleans, Louisiana. 152 p.

Raymond, P. A., N. H. Oh, R. E. Turner, and W. Broussard. 2008. Anthropogenically Enhanced Fluxes of Water and Carbon from the Mississippi River. Nature 451:449-452.

Reed, D. J. 2002. Understanding Tidal Marsh Sedimentation in the Sacramento-San Joaquin Delta, California. Journal of Coastal Research SI 36:605-611.

Roberts, H. H. 1997. Dynamic Changes of the Holocene Mississippi River Delta Plain: The Delta Cycle. Journal of Coastal Research 13:605-627.

Simenstad, C., J. Toft, H. Higgins, J. Cordell, M. Orr, P. Williams, L. Grimaldo, Z. Hymanson, and D. Reed. 2000. Sacramento/San Joaquin Delta Breached Levee Wetland Study (Breach). Preliminary report. Seattle (WA): Wetland Ecosystem Team, University of Washington, School of Fisheries. 46 p.

SONRIS. 2012. Petroleum Production Data to 1977. Louisiana Office of Conservation. Baton Rouge, Louisiana.

Stanley, D. J. and A. G. Warne. 1994. Worldwide Initiation of Holocene Marine Deltas by Deceleration of Sea-Level Rise. Science 265:228-231.

Stevenson, J. C., L. G. Ward, and M. S. Kearney. 1988. Sediment Transport and Trapping in Marsh Systems: Implications of Tidal Flux Studies. Marine Geology 80: 37-59.

Swenson, E. M. and R. E. Turner. 1987. Spoil Banks: Effects on a Coastal Marsh Water-Level Regime. Estuarine, Coastal and Shelf Science 24:599-609.

Turner, R., E. Swenson, and C. Milan. 2002. Organic and Inorganic Contributions to Vertical Accretion in Salt Marsh Sediments. M. P. Weinstein and D. A. Kreeger, eds. Concepts and Controversies in Tidal Marsh Ecology. Kluwer Publishers. p. 583-595.

Turner, R. E. 1990. Landscape Development and Coastal Wetland Losses in the Northern Gulf of Mexico. American Zoologist 30:89-105.

Turner, R. E. 1997. Wetland Loss in the Northern Gulf of Mexico: Multiple Working Hypotheses. Estuaries and Coasts 20:1-13.

Turner, R. E., J. J. Baustian, E. M. Swenson, and J. S. Spicer. 2006. Wetland Sedimentation from Hurricanes Katrina and Rita. Science 314:449-452.

Turner, R. E. and N. N. Rabalais. 1994. Coastal Eutrophication near the Mississippi River Delta. Nature 368:619-621.

Turner, R. E., E. M. Swenson, C. S. Milan, and J. M. Lee. 2007. Hurricane Signals in Salt Marsh Sediments: Inorganic Sources and Soil Volume. Limnology and Oceanography 52:1231-1238.

Tweel, A. W. and R. E. Turner. 2012. Landscape-Scale Analysis of Wetland Sediment Deposition from Four Tropical Cyclone Events. PloS ONE 7:e50528.

Tweel, A. W. and R. E. Turner. 2012. Watershed Land Use and River Engineering Drive Wetland Formation and Loss in the Mississippi River Birdfoot Delta. Limnology and Oceanography 57:18-28.

Wells, J. T. and J. M. Coleman. 1987. Wetland Loss and the Subdelta Life Cycle. Estuarine, Coastal and Shelf Science 25:111-125.

CHAPTER 2
WATERSHED LAND USE AND RIVER ENGINEERING DRIVE WETLAND FORMATION AND LOSS IN THE MISSISSIPPI RIVER BIRDFOOT DELTA[1]

Introduction

Intensive agricultural practices are typically associated with increased soil erosion (Walling 1999, Dearing and Jones 2003) that can result in riverine suspended sediment concentrations increasing up to an order of magnitude (Meade 1969, Douglas 1997). This increased sediment flux has muddied rivers, shoaled ports, and accelerated delta progradation from Greco-Roman and Medieval times to 19th century America (Figure 2.1). The Mediterranean's easily erodible soils and low tidal energy made ports especially vulnerable to siltation from rivers carrying eroded soils from the deforested and farmed lands of the ancient Greeks and Romans (Brückner 1986, Hughes 1996). Centuries later, as intensive agriculture spread westward, crops such as tobacco gave birth to a booming export industry in Chesapeake Bay settlements, but heavy soil erosion from those fields often formed new wetlands and shoals, rendering the ports inaccessible (Gottschalk 1945, Hillgartner and Brush 2006). The Plum Island estuary in Massachusetts also experienced rapid marsh formation in the 18th and 19th centuries as a consequence of increased sediment delivery following land clearing and agricultural development (Kirwan et al. 2011).

The effect of intensive cultivation on erosion and subsequent suspended sediment transport is more readily observed in smaller watersheds, because much of the increased sediment load accumulates locally (Trimble 1999). By contrast, much of the soil eroded in large, continental watersheds is re-deposited before reaching the main stem, dampening the downstream effects of increased erosion upstream (Costa 1975, Walling 1999). Variations in the

[1]Published as Tweel and Turner 2012. Limnology and Oceanography 57(1):18-28

suspended sediment load of large, sediment-laden rivers, such as the Yellow River in China, however, have been attributed to changes in agricultural land use (hereafter land use) over many centuries, if not millennia (Xu 1998, Wang et al. 2010).

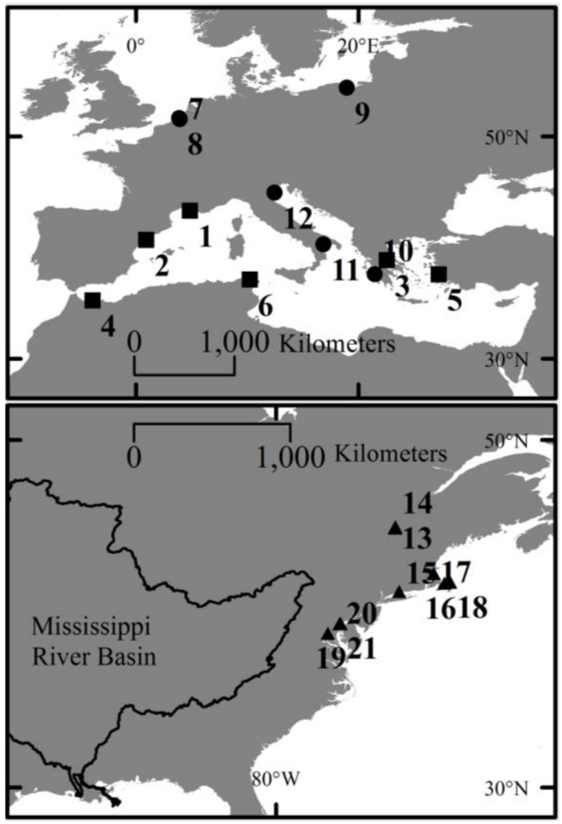

Figure 2.1 Select examples of increased sedimentation attributed to land use change. The Mississippi River basin is outlined in black. Symbol shapes indicate approximate timing of earliest anthropogenic sedimentation for Greco-Roman (square), Medieval (circle), and colonial American (triangle) periods. Numbers are indexed in Table 2.1.

The Mississippi River basin (MRB, Figure 2.2) is unique among the world's large watersheds in that agriculture was introduced more recently and at an unprecedented scale and intensity than other rivers of comparable discharge. Severe erosion was commonplace as intensive European-style agriculture expanded into the MRB, and was significant enough to necessitate the formation of the Soil Conservation Service in 1935 (Turner and Rabalais 2003). Increasingly intensive river engineering, especially reservoir construction, greatly reduced sediment transport within the basin beginning in the early 20th century (Meade and Moody

2010). Other factors that may have also altered 19th century sediment transport include bank clearing and channel dredging, as well as engineering to regulate flow near the delta mouth (Winkley 1977, Wells and Coleman 1987, Kesel 1988), but changes in land use are considered to be the greatest effect, at least until reservoir construction (Keown et al. 1981, Dardeau and Causey 1990, Saucier 1994).

Table 2.1 Legend for points in Figure 2.1.

Point	Delta/Estuary	Reference
1	Rhone	Vella et al. 2005
2	Ebro	Sanchez-Arcilla and Jiminez 1997
3	Spercheios	Hughes 1996
4	Al Hocemia	Brückner 1986
5	Maeander	Hughes 1996
6	Medjerda	Brückner 1986
7, 8	Rhine/Zwin	Hoffman 1996
9	Vistula	Hoffman 1996
10	Olympia	Brückner 1986
11	Basilicata Province	Brückner 1986
12	Po	Cencini 1998
13	Winooski	Bierman et al. 1997
15-18	New Haven, Barnstable, Boston, Nauset	Cronon 1983
19	Potomac	Montgomery 2007
20	Joppa Towne	Gottschalk 1945
21	Otter Point	Hilgartner and Brush 2006

The earliest maps of the Mississippi River birdfoot delta (MRBD) depict channels bounded by marshes slightly wider than the channels. Later surveys documented a period of rapid subdeltaic land formation that began in the mid-1800s, resulting in 560 km^2 of new land (>3 × the area of Washington, DC) in less than 100 years (Wells and Coleman 1987). These areas of rapid land formation resulted from breaches in the river's natural levees, referred to as crevasses, which allowed direct sediment input into coastal bays, eventually filling them in. Maps of the 1930s delta depict this enlarged wetland landscape, much of which has since eroded.

This recent erosion accounted for 10.1% of all Louisiana coastal land lost between 1932 and 1990, and accounted for the two highest rates of land loss between 1932 and 1958 (West and East Delta 15-minute quadrangles) (Dunbar et al. 1992). The growth and retreat of these four subdeltas of the Mississippi River birdfoot delta over the past two centuries has provided a framework for understanding the subdelta life cycle and has also served as a smaller-scale model of the six delta lobes formed by the Mississippi River over the past several millennia (Fisk et al. 1954, Coleman and Gagliano 1964, Wells and Coleman 1987). The re-creation of these subdelta processes has been incorporated into restoration plans for one of the largest ecosystem restoration efforts in history (LDNR 1998, CLEAR 2008).

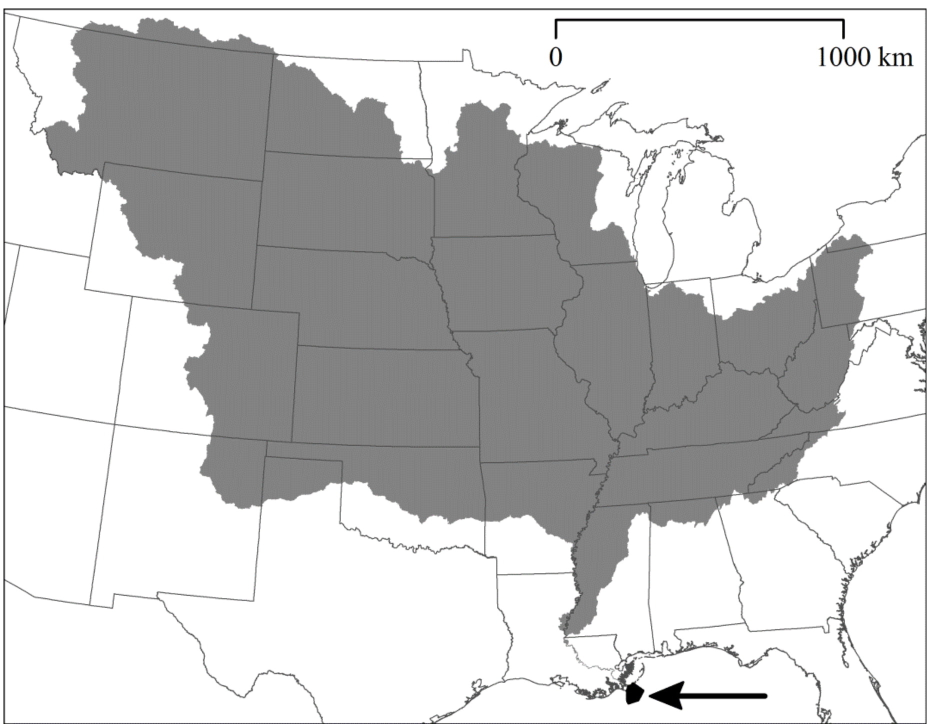

Figure 2.2 The MRB (gray) and the study area used for delta land area analysis (black) indicated by arrow.

Here I quantify the relationship between soil erosion in the MRB, Mississippi River suspended sediment concentrations, and variations in land area in the MRBD. I test the hypothesis that the timing and amount of land gain and loss in the MRBD is proportional to

changes in the suspended sediment load carried by the river. I analyzed ten maps from 1778 to 2002 and compiled suspended sediment records from 1838 to 2002. Additionally, I compared these records to a model designed to assess pre-disturbance sediment load and evaluated the results in the context of land use, population growth, and surrogates of land disturbance.

<u>Methods</u>

Spatial data compilation and accuracy

I collected maps and spatial data for the MRBD for 1778 to 2002 from the Louisiana State University Cartographic Information Center and various public data servers. I only used maps with a published survey date for the entire study area. Privately published maps from before the 1800s were typically stylized, copied from earlier maps or, in some cases, not updated from survey data for several decades. National Oceanic and Atmospheric Administration (NOAA) nautical charts were not suitable for this analysis because they are produced for navigational purposes and do not necessarily contain uniformly updated topographic information.

George Gauld compiled several surveys of the Louisiana coast that included depth soundings and published them in a 1778 map entitled '*A Plan of the coast of part of West Florida and Louisiana: Including the River Yazous*.' This map was based on surveys from 1764-1771 conducted for the Admiralty in Florida, and its accuracy and background have been previously discussed (Gauld 1969, Morgan 1973). I did not consider this map entirely suitable for quantitative analysis because of the surveying technology used, although I referred to it as the most accurate depiction of the delta from that period (Morgan 1955).

The first reliable surveys of the region are the topographic sheets (T-sheets) produced by A. Talcott for the United States Coast and Geodetic Survey (USC and GS) in 1838. An 1890

Mississippi River Commission map of West Bay, based on surveys completed between 1839 and 1845, complements a missing portion of the 1838 survey (Morgan 1973). Subsequent surveys for individual subdeltas were performed between 1859 and 1887 by the USC and GS and combined into one dataset for the overall analysis, but were kept separate for interpreting changes in the individual subdeltas. The first photographic surveys were carried out in 1922 by the Naval Air Service, and were compiled as T-sheets by the USC and GS. A follow-up survey was completed in 1932, yielding an entirely new set of T-sheets.

I obtained six of the ten data layers used for this analysis in a usable digital format. The remaining data were digitized using the same procedure used to develop the layers created by NOAA. Five datasets were obtained digitally in vector format from NOAA (1870s, 1932, and 1959) and the Louisiana Oil Spill Coordinator's Office (1992 and 2002). The 1978 data were acquired digitally as a bi-level raster from the United States Geological Survey who developed it from United States Fish and Wildlife Service data (Barras et al. 2004). Data from 1838, 1922, and 1971 were obtained from maps that were scanned and geo-referenced to a minimum of four control points and had a maximum root mean square error of 0.002 degrees. Specific map projection information was not available for digitization of the 1778 survey, and so I used the Bonne projection- a popular projection for surveys prior to 1853 (Daniels and Huxford 2001). Area measurements from Airy, Bessel, and Bonne projections were compared to account for possible errors caused by using a different projection, and only negligible differences in area were observed. The 1838 and 1922 surveys were on-screen digitized at an average scale of 1:7500. The 1971 USGS maps, originally printed as photographic quadrangles, were scanned and converted to a bi-level image in Adobe Photoshop before being vectorized using ArcScan, which is an extension of ArcGIS software (Environmental Systems Research Institute). All data were re-projected in ArcGIS to the North American Datum 1983 Universal Transverse Mercator

zone 16-north to measure land area. All polygons smaller than 0.02 km^2 were omitted to compensate for potential differences in mapping scale. The change in total area resulting from this filtering was recorded for each map, and calculated as a percent loss due to processing. This loss was generally less than 1%, but was up to 6% in maps surveyed during periods of marsh breakup, and was considered inconsequential to my goal of identifying periods of increasing, maximum, decreasing, and stable land area.

The study area included all land downstream of a line drawn between Bay Tambour and Grand Coquille Bay, approximately equal to all land downstream of St. Phillips Bend in the Mississippi River located 32 km above Head of Passes. All polygons were clipped to the study area, and their areas were re-calculated in the final projection. Initially, the study area was divided into smaller hydrologic units, but I determined that changes in one area were not independent of changes in another unit. For example, if river discharge increases in one area, it comes at the expense of river discharge to another area. The study area was, therefore, examined as a single system changing with time.

I also compared wetland soil type in the MRBD to other areas of the coast. The percent mineral matter for the top 24 centimeters of soil at Coastwide Reference Monitoring System (www.ocpr.louisiana.gov/crm/coastres/monitoring.asp) sites was analyzed in ArcGIS. The data were highly spatially autocorrelated (n = 716, Moran's I: 0.96) and were, therefore, appropriate for kriging to interpolate between sites. The final output was clipped to National Wetlands Inventory data (www.fws.gov/wetlands/Data/DataDownload.html).

Suspended sediments

Suspended sediment concentration data for the Mississippi River at New Orleans were compiled from a variety of sources dating back to 1838; portions of this data set have been

discussed previously (Turner and Rabalais 2003, Thorne 2008). Data before 1877 are sparse, and there were various methods used in their collection (Humphreys and Abbot 1876, Vogel 1930, Keown et al. 1981). Two full years of suspended sediment data were collected at Carrollton, Louisiana, starting in February 1851, and ending February 1853 (Humphreys and Abbot 1876). The first year of these data was comprised of daily mass ratio observations (except Sunday) at three depths, and three distances from the riverbank, and the second year consisted of only surface readings, under the assumption that the relationship between first year depths could be used to estimate the mass ratios in the second year. One additional full year of concentration data exists for 1850 (Vogel 1930), but was collected at Fulton, Tennessee. The Fulton station location was about 275 river kilometers below Cairo, Illinois (Winkley 1977), and downstream from both the largest sediment and water inputs to the river (Keown et al. 1981). To test for differences between sampling location or methods, overlapping monthly data from 1879 and 1880 were compared to observations from Carrollton, Port Eads, and Fulton. These were also used to establish a ratio that was used to estimate the sediment concentration at Carrollton, using the Fulton data. Mean monthly sediment concentrations at Fulton were more dampened than at Carrollton, and tended to be higher during low discharge flows, but were lower in high flow months, and averaged 7% greater than the concentrations measured at Carrollton.

Suspended sediment concentrations in 1838 and 1846 were estimated based on sampling during the three and four spring months, respectively, thus capturing the period of the highest and most variable sediment discharge (Keown et al. 1981). The concentration data for 1838 were collected at South Pass by A. Talcott for the Army Corps of Engineers and included surface and subsurface samples. The 1846 sediment concentration data were derived from surface water collected at New Orleans by Professor Riddell, Tulane University (Humphreys and Abbot 1876). The mean annual suspended sediment concentrations for 1838 and 1846 were estimated by

prorating the missing monthly values using observations for 1851-1853 and forming a sediment concentration ratio for each month. These estimated concentrations are probably the least accurate of all of the data used, but their variation and discharge to concentration ratios were comparable to that of the two consecutive years of data collected at Carrollton. Five other sampling occasions between 1838 and 1867 consisted of insufficient records or sampling information to include in this analysis. The Army Corps of Engineers maintained a continuous record of suspended sediments between 1877 and 1895 at Port Eads (Turtle 1884, Quinn 1894, Quinn 1896), and the New Orleans Water and Sewerage Board has the longest continuous record of suspended sediment concentrations, which began in 1910. Suspended sediment data were calculated as a three-year moving average because of my objective of summarizing long-term trends in the data.

I compared annual loads and mean annual suspended sediment concentrations for the 33 years ranging from 1851 to 1988 when detailed discharge data were available. A simple linear regression of suspended sediment concentration and discharge confirmed the suitability of using mean annual suspended sediment concentration as a proxy for annual load (mg $L^{-1} = 0.0439 \times Q_s + 107.73$, $r^2 = 0.85$, $F_{(1,31)} = 169.08$, $p < 0.0001$ [Q_s = annual sediment load in kg s^{-1}]). I also estimated annual load based on annual discharge (Poore et al. 2001), but since detailed discharge data were not available before 1933, I could not pair daily sediment observations to discharge data. I kept this calculation consistent throughout the study period.

I used the Area Relief Temperature (ART) model to estimate the suspended sediment concentrations before the 1800s (Syvitski et al. 2003). The ART model was calibrated using a database of 340 watersheds worldwide. This model is based on the physical characteristics of the basin at four latitude divisions, with specific constants for each division, and estimates the pre-disturbance annual load (Q_s in kg s^{-1}) using this equation: $Q_s = \alpha_3 A^{\alpha 4} R^{\alpha 5} e^{kT}$. I used constants

specific to temperate northern hemisphere river basins ($\alpha_3 = 6.1 \times 10^{-5}$, $\alpha_4 = 0.55$, $\alpha_5 = 1.12$, k = 0.07) and three input parameters specific to the Mississippi River Basin (*A:* basin area = 3.22×10^6 km^2, *R:* maximum basin relief = 4402 m, and *T:* average basin temperature = 9.77°C). The average temperature was based on a 29-year record from the NOAA Earth System Research Laboratory (www.esrl.noaa.gov/psd/data/usclimate/tmp.state.19712000.climo), and was weighted for the area of each state that lies within the watershed, assuming equal temperatures inside and outside. The annual suspended sediment load was converted to a mean annual concentration using the linear regression of annual load against the sediment concentration noted above. Most of the uncertainty in the ART model output arises from rivers with smaller sediment loads, or watersheds that are greatly affected by reservoir construction (Syvitski et al. 2003). The ART model predicts sediment load within a factor of 2 for 75% of the 340 rivers included, but error is less than a factor of 2 for all of the 15 largest loads reported, and the model may underpredict for the largest basins (Syvitski et al. 2003). While there is inherently no observed sediment load to test the model estimate for the period before European settlement, I examined the results in the context of other indicators of disturbance as well as sediment observations collected at various points during watershed development.

I investigated the relationship between suspended sediment concentration and the percent of the Mississippi River watershed under cultivation to see how well the ART model estimate (zero cultivation) compared. The United States Census Bureau collected data on the area of land improved for agriculture starting in 1850 (Historical Census Data Browser, mapserver.lib.virginia.edu). I prorated these data for the percent of each state that lies in the watershed, assuming a homogenous distribution of farmland inside and outside the watershed for each state. Population data are available for the period beginning in 1790 and were prorated amongst the watershed boundaries as was done for the agricultural data. To estimate land

improvements prior to the 1850 census, the percent of improved land for the years 1850 to 1920 was linearly regressed against population size ($r^2 = 0.99$, $F_{(1,6)} = 721.6$, $p < 0.0001$) to estimate land use for the period between 1790 and 1850. I compared watershed land use to the observed suspended sediment concentrations and to the pre-disturbance estimate from the ART model. I also included MRBD subdelta volume (Wells and Coleman 1987) in this analysis.

Bed load, the component of sediment transport that travels along the bottom of a river, is not included in this analysis. A recent estimate of bed load in the Mississippi River is 2.5% of the total sediment load (Nittrouer et al. 2008). I did not correct for Mississippi River discharge entering the Atchafalaya River, which was about 10% in 1900 and increased to 30% by the 1960s (Turner et al. 2007).

Data analysis

I conducted a simple linear regression analysis of land area vs. ten-year means of suspended sediment concentration. Data from the rapid land building period (1838 to 1867) were excluded because of the delay between subaqueous land building and when subaerial land appears (Wells and Coleman 1987). I also examined how the relationship between sediment concentration and various 5 to 20 year lags in land area changed for when suspended sediment concentrations were rising, declining or stable (PROC REG, Statistical Analysis System 9.1; SAS Institute). I expected to find threshold effects for wetland colonization and loss at different stages of development that were dependent on the net sediment accretion, hence elevation (McKee and Patrick 1988).

Results

Land area in the MRBD closely followed the changes in suspended sediment concentrations, with a longer response lag after periods of suspended sediment increase than

when the suspended load was in decline (Figure 2.3). Both land area and suspended sediment concentrations increased to a maximum, declined rapidly, then stabilized and remained relatively stable with only minor fluctuations since 1971. The peak in land area (692 km^2 in 1932, compared to 314 km^2 in 1838; Figure 2.4A, page 26) occurred about 47 years following the peak in suspended sediments, but the relative stabilization of land area (358 ± 13 km^2; $\mu \pm 1$ standard error [SE] for the four datasets from 1971 to 2002) occurred 5 years after the suspended sediment concentrations stabilized at a level that was much lower than the peak in the 1890. Land area closely followed sediment concentration at uniform lags ranging from 0 to 15 years (Figure 2.5, $p < 0.05$, $n = 6$). The relationship between annual load and land area was similarly significant, and the intercepts for the two regressions averaged 226 km^2.

The suspended sediment concentrations averaged 563 ± 79 mg L^{-1} (338 ± 23 × 10^9 kg yr^{-1}, $\mu \pm 1$ SE) for the three full years of sampling that started in 1850 (Figure 2.3B). If the estimated concentrations for the earliest two sampling periods are included, then the mean concentration for 1838 to 1853 is 611 ± 53 mg L^{-1} (324 ± 15 × 10^9 kg yr^{-1}). The peak suspended sediment concentrations occurred between the 1870s and 1890s, averaging 675 ± 38 mg L^{-1} (348 ± 27 × 10^9 kg yr^{-1}) for 19 years. The decline in suspended sediments began gradually, but accelerated until significant reductions occurred around 1955. Following another sharp drop in the early 1960s, the suspended sediment concentrations at Carrollton, Louisiana, remained fairly stable at 157 ± 7 mg L^{-1} (91 ± 7 × 10^9 kg yr^{-1}). Overlapping suspended sediment concentrations for 1880 at Carrollton and Fulton were within the error of suspended sediment concentration for samples collected at Port Eads (Figure 2.3B). The relationship between mean annual suspended sediment concentration and annual load was constant throughout the study period, but periods of increasing, peak, and diminished sediment loads are distinct from one another (Figure 2.6).

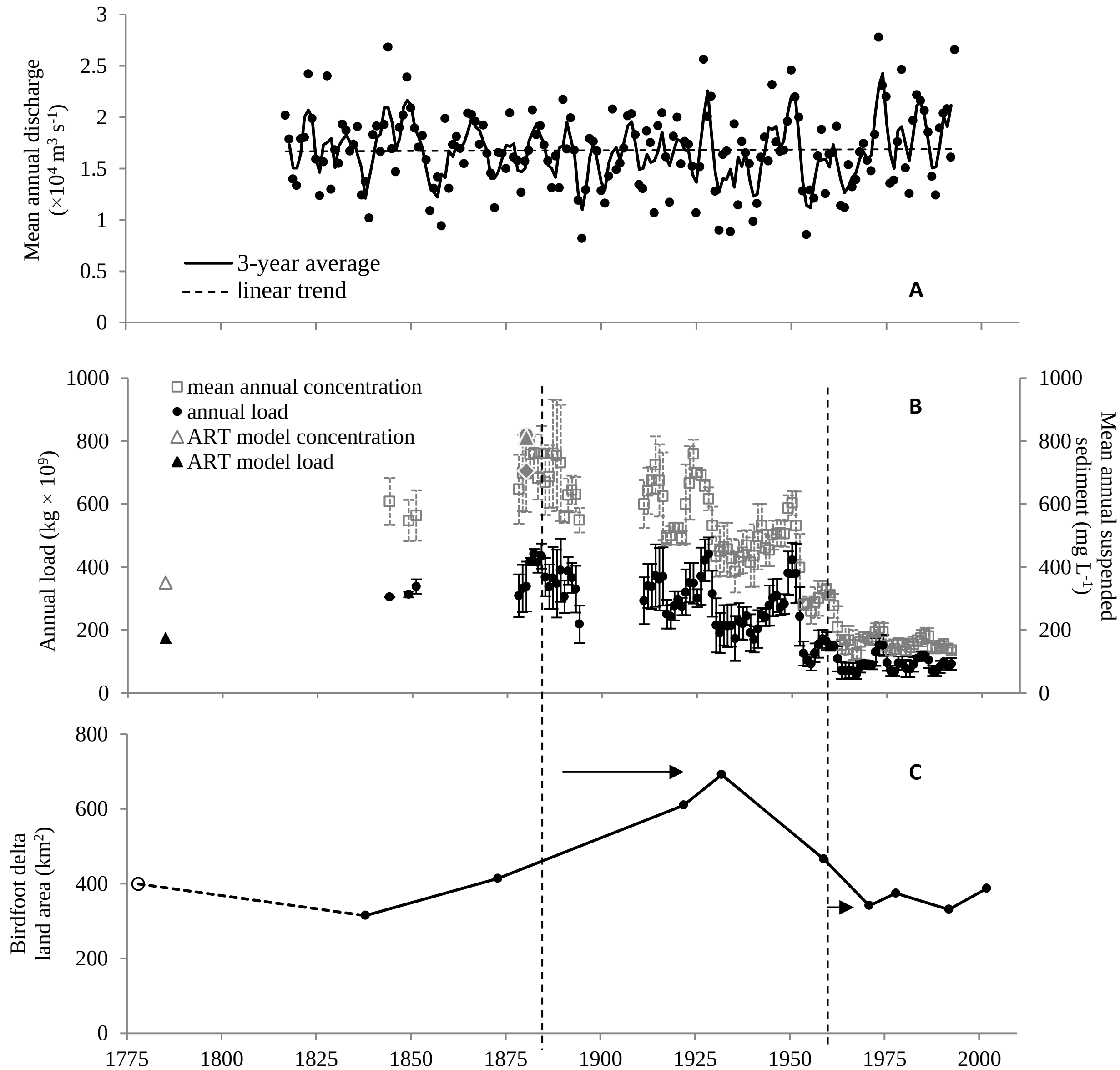

Figure 2.3 Changes in suspended sediment concentrations in the lower river (principally New Orleans) and land area of the birdfoot delta. **A**. Mean annual discharge at Vicksburg, Mississippi, and three-year moving average (Poore et al. 2001). **B**.Three-year averages of mean annual suspended sediment concentration (gray) and annual load (black) at New Orleans ($\mu \pm 1$ SE). Triangles show the predicted pre-disturbance suspended sediment concentration (open triangle) and annual load (solid triangle) determined using the ART model (Syvitski et al. 2003). Also plotted are 1880 observations from Carrollton (gray diamond), Fulton (gray triangle), and Port Eads (gray circle, partly obscured by Fulton). **C**. The area of subaerial land in the Mississippi River birdfoot delta. The solid lines link accurate surveys, and the dashed line connects data from a 1778 survey.

There is no overall trend in discharge for the study period (Figure 2.3A). The high discharge during the 1927, 1949-1951, and 1973-1974 flood years, however, corresponds to spikes in sediment concentration, and the abnormally low discharge years are co-related to lows in sediment concentration around 1895 and 1954. Despite this relationship, however, the mean discharge for the five years around 1850 was 5% greater than between 1870 and 1890, even though the sediment concentration was 10% lower. Additionally, the drastic sediment reductions after 1962 do not correspond to a reduction in discharge. These differences indicate that there is a changing relationship between sediment concentration and discharge throughout the study period that is independent of the variations in discharge.

Agricultural land use increased in a sigmoidal fashion between 1800 and 1920, and has remained relatively stable, at around 40% of the basin, until today (Figure 2.7, Raymond et al. 2008). The period of most rapid land use change was between 1870 and 1900 for both the whole basin and also for only the sub-basin states of Kansas, Missouri, Iowa, and Nebraska, which contain the highly erosive Missouri River basin soils (up to 2×10^6 kg km^{-2} yr^{-1} with modern land use, Keown et al. 1981). The reservoir volume in the Missouri River basin increased in two large increments. Nineteen percent of the total 1979 reservoir volume was constructed between 1935 and 1937, and an additional 55% was constructed between 1952 and 1958. Reservoir construction between 1958 and 1979 was 12% of the 1979 capacity. The decline in sediment concentration was coincidental with the increase in reservoir volume (Figure 2.7).

The ART model estimate of the pre-disturbance annual sediment load for the Mississippi River was 174×10^9 kg yr^{-1}, equal to an estimated mean concentration of 350 ± 37 mg L^{-1} ($\mu \pm$ 95% CI for the regression of suspended sediment concentration and load).

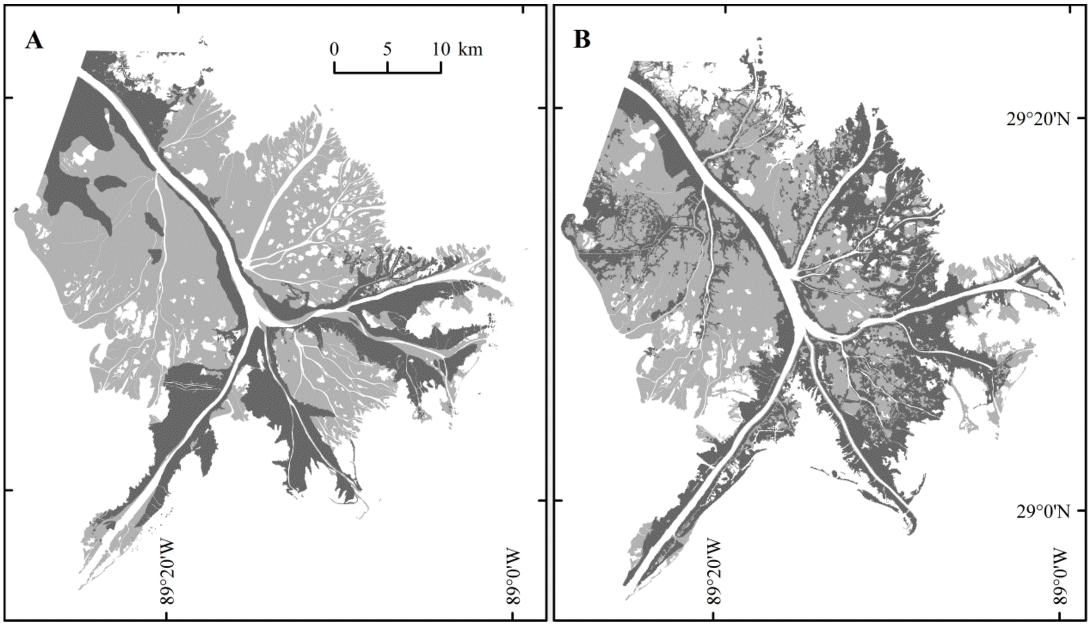

Figure 2.4 The study area. **A.** Mississippi River birdfoot delta in 1838 (dark) and near its maximum size in 1932 (light) showing areas of wetland formation. **B**. Mississippi River birdfoot delta in 2002 (dark) and near its maximum size in 1932 (light), showing areas of wetland loss.

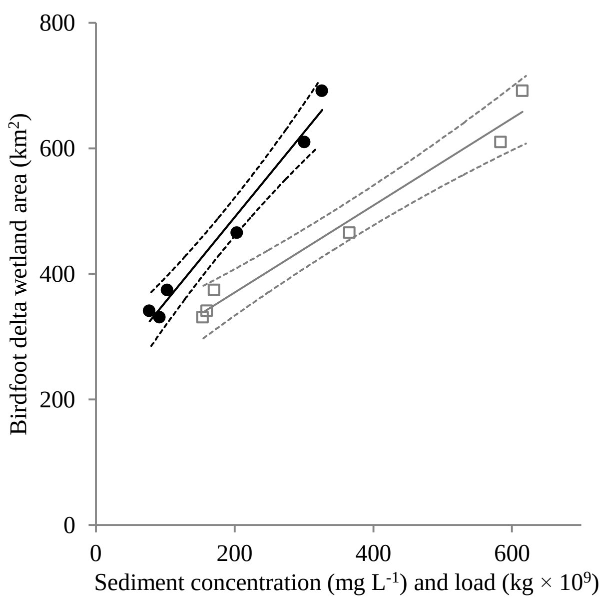

Figure 2.5 Ten-year mean suspended sediment concentrations (gray) and annual loads (black) vs. land area of the Mississippi River birdfoot delta since 1922 (Concentration: $r^2 = 0.98$, $F_{(1,4)} = 155.22$, $p < 0.001$, Load: $r^2 = 0.98$, $F_{(1,4)} = 160.67$, $p < 0.001$). The linear regression is significant for response intervals from 0 (shown) to 15 years; earlier points are omitted due to a lag between bay infilling and wetland formation (see text for explanation). The dotted lines show the 95% confidence intervals.

The land area of the MRBD grew at an average rate of 4.1 km^2 yr^{-1} from 1838 (315 km^2) to its peak in 1932 (692 km^2), when it was 220% of the area present in 1838 (Figure 2.3C). Land loss following this peak was rapid, and occurred at an average rate of 9.0 km^2 yr^{-1} between 1932 and 1971. The size of the MRBD in 1971 (341 km^2) was 110% its size in 1838, although the distribution of wetlands following subdelta decay was much more fragmented and covered a larger area (Figure 2.4). There were relatively small gains and losses of land after 1971, and in 2002 the land area (387 km^2) was 120% the area present in 1838.

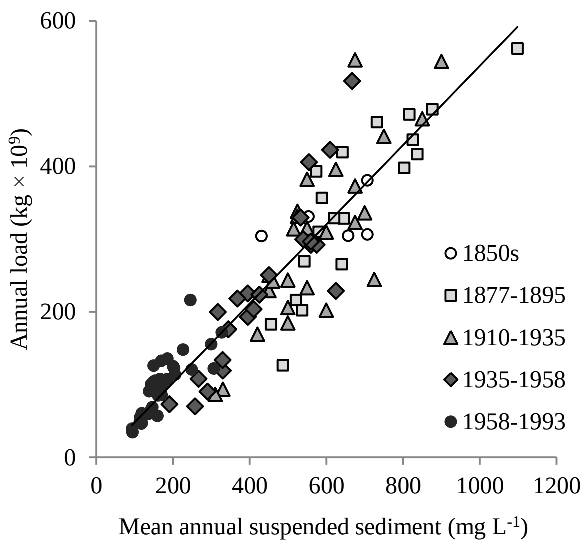

Figure 2.6 Mean annual suspended sediment concentration vs. annual load at the following time intervals: increasing sediment transport (1850s), peak sediment transport (1880s), early reservoir construction (1910-1935), rapid reservoir construction (1935-1958), and decreased reservoir construction (after 1958).

Wetland soil inorganic content varied widely, ranging from 97.1% in the MRBD to as low as 8.3% in the upper reaches of Barataria and Terrebonne basins (Figure 2.8). Mean inorganic content for the whole coast was 58.3 ± 19.1 % ($\mu \pm 1\ \sigma$).

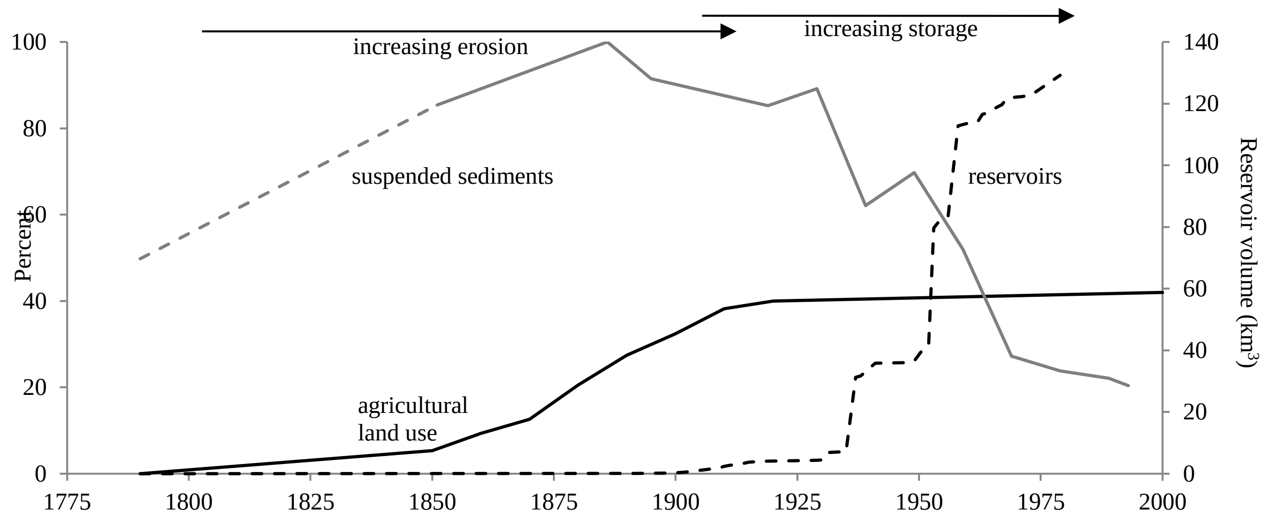

Figure 2.7 Comparison of watershed agricultural land use (solid), cumulative reservoir volume (dashed), and ten-year means of suspended sediment concentration (gray). Land use is presented as the percent of the whole basin area, reservoir volume is km^3 of storage within the Missouri River basin (Keown et al. 1981), and sediments are the percent of maximum observed for the interval. Other factors that may have influenced sediment transport are not shown (Kesel 1988).

Discussion

The conversion of prairie and forest to an agricultural landscape following European settlement in the Mississippi River watershed is mirrored in several large-scale changes in the river system, including the timing and rate of enlargement of the MRBD. Additional changes that were synchronous with 19th century land use change in the MRB include increases in offshore nutrient concentrations (Turner and Rabalais 1994), suspended sediment and nutrient deposition along the Upper Mississippi River (Engstrom et al. 2009), and overbank sedimentation in the Upper Mississippi Valley (Knox 1987). These analyses confirm that the change in land use had consequences extending well beyond the area of direct erosion effects, and are consistent with the results from the ART sediment load model that identifies a pre-disturbance load lower than the peak concentrations observed in the late 19th century. Because of the direct connection of the MRBD wetlands to fluvial input, which differs from the rest of the

Louisiana coast, wetland area in the MRBD would be expected to vary with sediment input (Blum and Roberts 2009).

The rapid increase in Mississippi River birdfoot delta size between 1838 and 1932 is consistent with similar observations of land building resulting from changes in land use, including at least nine Mediterranean deltas and ports (Brückner 1986, Hughes 1996, Vella et al. 2005), two northern European river deltas (Hoffman 1996), and eight deltas and upper estuaries in eastern North America (Cronon 1983, Bierman et al. 1997, Hilgartner and Brush 2006). This example at the mouth of the Mississippi River represents the largest and most recently developed watershed where this link has been quantified.

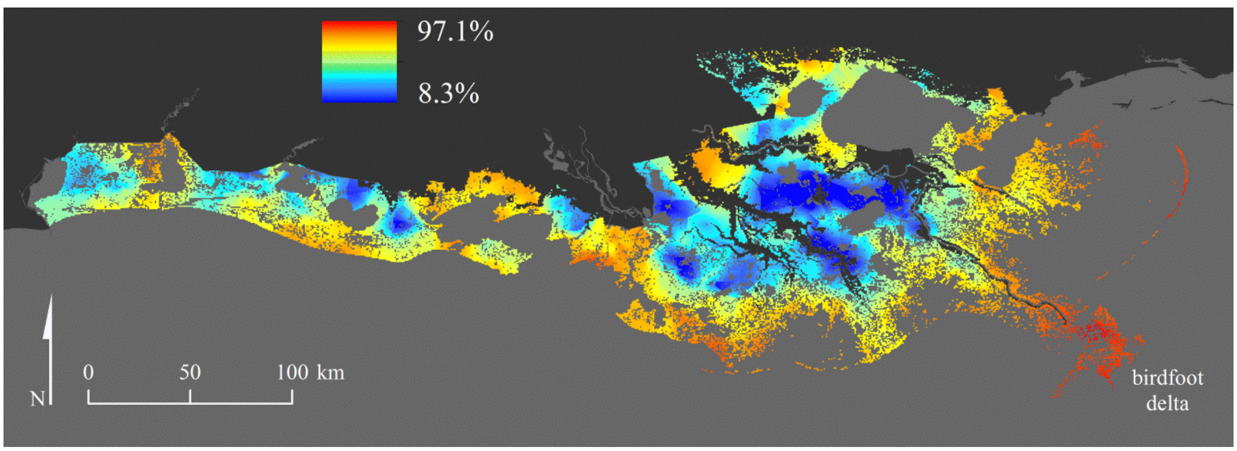

Figure 2.8 The percent soil inorganic matter (0-24 cm) across the Louisiana coast. There is highly inorganic soil in the birdfoot delta compared to more organic soil in the deltaic plain. The dark gray denotes upland areas and non-coastal zone wetlands.

Wetland formation lagged 47 years behind the peak in sediment discharge, whereas the reversion back to open water lagged 5 years following the decline in sediment loading, indicating a hysteretic relationship between sediment loading and wetland area. The difference in lag times between growth and decline is expected because sediments filled shallow bays ranging from 2 to 9 meters deep before wetlands ‘capped’ the sediment accumulation in the final stages of land building. Wetland loss, however, is much more sensitive to changes in elevation, because plants

are adapted to a narrow range (a few centimeters) of tidal variation on this coast (McKee and Patrick 1988). The area of all four of the subdeltas peaked around 1930, even though these subdeltas were initiated over a span of 50 years, indicating that the land formation and loss were influenced by a process operating at a larger scale than the growth and decay of a single subdelta. The areal decline in the Baptiste Collette subdelta was slightly more delayed than the other three subdeltas, possibly because deltaic subsidence rates decline with distance from the continental shelf (Roberts et al. 1994). The increasing proportion of Mississippi River discharge entering the Atchafalaya River starting around 1900 likely exacerbated this land loss.

The total volume of sediments in the four MRBD subdeltas increased by 0.15 km^3 yr^{-1} between 1875 and 1895, which is twice the rate of increase for the whole growth period (0.07 km^3 yr^{-1}, Wells and Coleman 1987). The rate of land use change was also greatest during this period for the both the whole basin and the states containing the highly erosive soils of the Missouri River basin (up to 2×10^6 kg km^{-2} yr^{-1} after land use change), and increases in MRBD volume and land use both slowed in the early 20th century (Keown et al. 1981). Changes in Missouri River reservoir capacity and suspended sediments followed similar trends, and the rapid increases in reservoir capacity correspond to sediment concentration reductions. Reservoir construction slowed after 1958, and was mirrored by a decline of suspended sediment concentrations (Figure 2.7).

There may have been several periods of subdelta lobe growth and decay before the 19th century growth period (Coleman 1981). An earlier study (Coleman and Gagliano 1964) surmised that there was an intermediate delta north of the modern delta and south of the Plaquemine delta below present-day New Orleans. The marsh fragments interpreted as indicators of previous subdelta cycles (Coleman 1981) could be remnants of this intermediate delta, or portions of the modern delta as it prograded away from the former Plaquemine delta.

Knowing the number of subdelta cycles, however, does not inform us about the areal extent or timing of processes for the entire MRBD. Additionally, the complex relationship between the two processes of changing sediment supply and land area serves as a reminder that such land change processes are rarely a consequence of purely geological or purely anthropogenic processes, but rather a result of the interaction between the two (Brookfield 1999).

The difference between the ART model estimate of annual sediment loads, peak loads (1890s), and for the earliest records (1850s) is proportional to changes in the MRB occurring then, which included land use and perhaps bank clearing and channel dredging (Winkley 1977), and is similar to changes observed in other watersheds. The ART model parameters are based on physical features of the basin (bottom-up), and the comparison to agricultural development represents a different approach (top-down), yet both analyses support a pre-disturbance sediment concentration that is lower than the maximum observed (late 19th century) mean annual suspended sediment concentrations in the Mississippi River. This pre-disturbance value also falls within the range of historical background to maximum disturbance concentration ratios previously reported (Dearing and Jones 2003), of up to 1:3 for a basin of this size. Although this estimate may be improved by future research, it represents my best estimate based on all available data and models.

The present-day sediment load of 115×10^9 kg yr^{-1} (1987-2006) reaching the MRBD is 66% of the pre-disturbance load estimated by the ART model (Meade and Moody 2010). The estimated current sediment load for the whole river system, including discharge into the Atchafalaya River, is 83% of the ART model estimate of pre-disturbance sediment load. I report a lower post-dam sediment load than Meade and Moody (2010) that may be an artifact of different sampling procedures or deposition between the Tarbert Landing and Carrollton stations (Winkley 1977, Kesel 1988). While this analysis confirms that there has been a significant

reduction in Mississippi River sediment transport since the 1890s, the pre-disturbance estimate by Meade and Moody (2010) is based on data collected after basin-wide changes had already occurred, and does not account for effects from changing land use or river dredging that could favor sediment transport. Sediment transport analyses for the Mississippi River basin have concluded that changes in land use had a significant, if not the greatest, historical effect on sediment transport (Keown et al. 1981, Dardeau and Causey 1990, Saucier 1994).

The two highest historical land loss rates on this coast occurred between the 1930s and the 1950s and were in the 15-minute quadrangles covering the MRBD. The beginning, peak and reduction of wetland loss rates in other coastal areas are not synchronous with the changes observed in the MRBD (Dunbar et al. 1992) and are not correlated with the changing suspended sediment concentration or load in the river. The highly inorganic wetland soils of the MRBD are distinct from the highly organic wetlands that occupy most of the deltaic plain (Figure 2.8, page 29). These differences in soil type and wetland loss rates indicate that processes regulating wetland loss and gain in the MRBD are distinct from the deltaic plain. The MRBD, therefore, may not be a suitable archetype for most of this coast.

The results from this study are consistent with the hypothesis that the growth, decline, and stabilization of mineral-rich wetland area in the MRBD are driven by the fluctuations in suspended sediment load. These observations are consistent with the anticipated consequences of land use changes in the MRB and elsewhere in the world. Anthropogenic reductions in sediment transport have become the dominant factor determining whether relative sea level rise is positive or negative in many areas (Syvitski and Kettner 2011). The MRBD is one of the most dramatic of such deltas and an indicator of what may occur in other developing watersheds around the world. Because of the positive relationship between suspended sediments and land area in the MRBD, future variation in suspended sediments delivered to the mouth of the river,

higher or lower, would likely lead to proportional land area changes in the MRBD, but not necessarily in the more organic soils of the deltaic plain.

References

Barras, J., S. Beville, D. Britsch, S. Hartley, S. Hawes, J. Johnston, P. Kemp, Q. Kinler, A. Martucci, and J. Porthouse. 2004. Historical and Projected Coastal Louisiana Land Changes: 1978-2050. USGS Open File Report:03-334.

Bierman, P., A. Lini, P. Zehfuss, A. Church, P. T. Davis, J. Southon, and L. Baldwin. 1997. Postglacial Ponds and Alluvial Fans: Recorders of Holocene Landscape History. GSA TODAY 7:1-8.

Blum, M. D. and H. H. Roberts. 2009. Drowning of the Mississippi Delta Due to Insufficient Sediment Supply and Global Sea-Level Rise. Nature Geoscience 2:488-491.

Brookfield, H. 1999. Environmental Damage: Distinguishing Human from Geophysical Causes. Global Environmental Change B: Environmental Hazards 1:3-11.

Brückner, H. 1986. Man's Impact on the Evolution of the Physical Environment in the Mediterranean Region in Historical Times. GeoJournal 13:7-17.

Cencini, C. 1998. Physical Processes and Human Activities in the Evolution of the Po Delta, Italy. Journal of Coastal Research 14:775-793.

CLEAR. 2008. Coastal Louisiana Ecosystem Assessment and Restoration (Clear) Program. Volume 4. Final Report to Department of Natural Resources, Coastal Restoration Division. Baton Rouge, Louisiana. www.clear.lsu.edu

Coleman, J. M. 1981. Deltas: Processes of Deposition & Models for Exploration. Burgess Publishing, Minneapolis, Minnesota. 124 p.

Coleman, J. M. and S. M. Gagliano. 1964. Cyclic Sedimentation in the Mississippi River Deltaic Plain. Transactions of the Gulf Coast Association of Geological Societies 14:67-80.

Costa, J. E. 1975. Effects of Agriculture on Erosion and Sedimentation in the Piedmont Province, Maryland. Bulletin of the Geological Society of America 86:1281-1286.

Cronon, W. 1983. Changes in the Land: Indians, Colonists, and the Ecology of New England. 257 p.

Daniels, R. C. and R. H. Huxford. 2001. An Error Assessment of Vector Data Derived from Scanned National Ocean Service Topographic Sheets. Journal of Coastal Research 17:611-619.

Dardeau, E. A. and E. M. Causey. 1990. Downward Trend in Mississippi River Sediment Loads. Potamology Program (P-1) Report 5, Environmental Laboratory. US Army Engineer Waterways Experiment Station, Vicksburg, Mississippi.

Dearing, J. A. and R. T. Jones. 2003. Coupling Temporal and Spatial Dimensions of Global Sediment Flux through Lake and Marine Sediment Records. Global and Planetary Change 39:147-168.

Douglas, I. 1997. Sediment Transfer and Siltation. B. L. Turner, Clark, W.C., Kates, R.W., Richards, J.F., Mathews, J.T., Meyer, W.B., eds. The Earth as Transformed by Human Action. Cambridge University Press, New York. p. 215-234.

Dunbar, J. B., L. Britsch, and E. Kemp. 1992. Land Loss Rates: Louisiana Coastal Plain. US Army Engineer Waterways Experiment Station, Vicksburg, Mississippi. Report GO-90-2, Part 3.

Engstrom, D. R., J. E. Almendinger, and J. A. Wolin. 2009. Historical Changes in Sediment and Phosphorus Loading to the Upper Mississippi River: Mass-Balance Reconstructions from the Sediments of Lake Pepin. Journal of Paleolimnology 41:563-588.

Fisk, H. N., C. R. Kolb, E. McFarlan, and L. J. Wilbert. 1954. Sedimentary Framework of the Modern Mississippi Delta. Journal of Sedimentary Petrology 24:76-99.

Gauld, C. A. 1969. A Scottish View of West Florida in 1769. Tequesta 29:61-66.

Gottschalk, L. C. 1945. Effects of Soil Erosion on Navigation in Upper Chesapeake Bay. Geographical Review 35:219-238.

Hilgartner, W. B. and G. S. Brush. 2006. Prehistoric Habitat Stability and Post-Settlement Habitat Change in a Chesapeake Bay Freshwater Tidal Wetland, USA. The Holocene 16:479-494.

Hoffmann, R. C. 1996. Economic Development and Aquatic Ecosystems in Medieval Europe. The American Historical Review 101:631-669.

Hughes, J. D. 1996. Pan's Travail: Environmental Problems of the Ancient Greeks and Romans. Johns Hopkins University Press. 288 p.

Humphreys, A. A. and H. L. Abbot. 1876. Report Upon the Physics and Hydraulics of the Mississippi River; Upon the Protection of the Alluvial Region against Overflow; and Upon the Deepening of the Mouths. US Government Printing Office, Washington DC.

Keown, M. P., E. A. Dardeau Jr, and E. M. Causey. 1981. Characterization of the Suspended Sediment Regime and Bed-Material Gradation of the Mississippi River Basin. US Army Engineer Waterways Experiment Station, Vicksburg, Mississippi.

Kesel, R. H. 1988. The Decline in the Suspended Load of the Lower Mississippi River and Its Influence on Adjacent Wetlands. Environmental Geology 11:271-281.

Kirwan, M. L., A. B. Murray, J. P. Donnelly, and D. R. Corbett. 2011. Rapid Wetland Expansion During European Settlement and Its Implication for Marsh Survival under Modern Sediment Delivery Rates. Geology 39:507-510.

Knox, J. C. 1987. Historical Valley Floor Sedimentation in the Upper Mississippi Valley. Annals of the Association of American Geographers 77:224-244.

LDNR. 1998. Louisiana Department of Natural Resources, Coast 2050. Baton Rouge, Louisiana. 161 p.

McKee, K. L. and W. H. Patrick. 1988. The Relationship of Smooth Cordgrass (Spartina Alterniflora) to Tidal Datums: A Review. Estuaries and Coasts 11:143-151.

Meade, R. H. 1969. Errors in Using Modern Stream-Load Data to Estimate Natural Rates of Denudation. Geological Society of America Bulletin 80:1265.

Meade, R. H. and J. A. Moody. 2010. Causes for the Decline of Suspended-Sediment Discharge in the Mississippi River System, 1940-2007. Hydrological Processes 24:35-49.

Montgomery, D. R. 2007. Dirt: the Erosion of Civilizations. University of California Press. 295 p.

Morgan, D. J. 1973. The Mississippi River Delta- Legal Geomorphic Evaluation of Shoreline Changes. M.S. Thesis. Louisiana State University.

Morgan, J. P. 1955. A Geographical and Geological Study of the Louisiana Coast. Coastal Studies Institute, Louisiana State University. Baton Rouge, Louisiana.

Nittrouer, J. A., M. A. Allison, and R. Campanella. 2008. Bedform Transport Rates for the Lowermost Mississippi River. Journal of Geophysical Research 113:F03004.

Poore, R. Z., J. Darling, H. J. Dowsett, and L. Wright. 2001. Variations in River Flow to the Gulf of Mexico: Implications for Paleoenvironmental Studies of Gulf of Mexico Marine Sediments. US Geological Survey Bulletin 2187.

Quinn, J. B. 1894. Report of the Chief of Engineers. House of Representatives Executive Documents. 53rd Congress 3rd session, V 2 Pt 2.

Quinn, J. B. 1896. Report of the Chief of Engineers. House of Representatives Executive Documents. 54th Congress 2nd session, V 2 Pt 4.

Raymond, P. A., N. H. Oh, R. E. Turner, and W. Broussard. 2008. Anthropogenically Enhanced Fluxes of Water and Carbon from the Mississippi River. Nature 451:449-452.

Roberts, H. H., A. Bailey, and G. J. Kuecher. 1994. Subsidence in the Mississippi River Delta; Important Influences of Valley Filling by Cyclic Deposition, Primary Consolidation Phenomena, and Early Diagenesis. Transactions of the Gulf Coast Association of Geological Societies 44:619-629.

Sanchez-Arcilla A. and J. A. Jimenez. 1997. Physical Impacts of Climatic Change on Deltaic Coastal Systems (I): An Approach. Climatic Change 35:71-93.

Saucier, R. T. 1994. Geomorphology and Quarternary Geologic History of the Lower Mississippi Valley. Volume 2. US Army Corps of Engineers. Waterways Experiment Station. Vicksburg, Mississippi.

Syvitski, J. P. and A. Kettner. 2011. Sediment Flux and the Anthropocene. Philosophical Transactions of the Royal Society A 369:957-975.

Syvitski, J. P. M., S. D. Peckham, R. Hilberman, and T. Mulder. 2003. Predicting the Terrestrial Flux of Sediment to the Global Ocean: A Planetary Perspective. Sedimentary Geology 162:5-24.

Thorne, C., O. Harmar, N. Clifford, R. Measures, C. Watson, and D. Biedenham. 2008. Current and Historical Sediment Loads in the Lower Mississippi River. US Army European Research Office. 146 p.

Trimble, S. W. 1999. Decreased Rates of Alluvial Sediment Storage in the Coon Creek Basin, Wisconsin, 1975-93. Science 285:1244-1246.

Turner, R. E. and N. N. Rabalais. 1994. Coastal Eutrophication near the Mississippi River Delta. Nature 368:619-621.

Turner, R. E. and N. N. Rabalais. 2003. Linking Landscape and Water Quality in the Mississippi River Basin for 200 Years. BioScience 53:563-572.

Turner, R. E., E. M. Swenson, C. S. Milan, and J. M. Lee. 2007. Hurricane Signals in Salt Marsh Sediments: Inorganic Sources and Soil Volume. Limnology and oceanography 52:1231-1238.

Turtle, T. 1884. Report of the Chief of Engineers. House of Representatives Executive Documents. 48th Congress 2nd session, V 2 Pt 2.

Vella, C., T. J. Fleury, G. Raccasi, M. Provansal, F. Sabatier, and M. Bourcier. 2005. Evolution of the Rhone Delta Plain in the Holocene. Marine Geology 222:235-265.

Vogel, H. D. 1930. Sediment Investigations on the Lower Mississippi River and Its Tributaries Prior to 1930.US Army Corps of Engineers. Waterways Experiment Station. Vicksburg, Mississippi.

Walling, D. E. 1999. Linking Land Use, Erosion and Sediment Yields in River Basins. Hydrobiologia 410:223-240.

Wang, H., N. Bi, Y. Saito, Y. Wang, X. Sun, J. Zhang, and Z. Yang. Recent Changes in Sediment Delivery by the Huanghe (Yellow River) to the Sea: Causes and Environmental Implications in Its Estuary. Journal of Hydrology 391:302-313.

Wells, J. T. and J. M. Coleman. 1987. Wetland Loss and the Subdelta Life Cycle. Estuarine, Coastal and Shelf Science 25:111-125.

Winkley, B. R. 1977. Man-Made Cutoffs on the Lower Mississippi River, Conception, Construction, and River Response. US Army Engineer District. Vicksburg, Mississippi.

Xu, J. 1998. Naturally and Anthropogenically Accelerated Sedimentation in the Lower Yellow River, China, over the Past 13,000 Years. Geografiska Annaler. Series A, Physical Geography 80:67-78.

CHAPTER 3
LANDSCAPE-SCALE ANALYSIS OF WETLAND SEDIMENT DEPOSITION FROM FOUR TROPICAL CYCLONE EVENTS[1]

Introduction

Recent hurricanes caused significant damage to coastal communities, and brought increased attention to the role of coastal wetlands in buffering storm surge (Costanza et al. 2008, Gedan et al. 2011). This buffering capacity is due to the reduction in wave energy as the incoming storm surge moves across wetlands and shallow coastal waters (Dietrich et al. 2010, Shepard et al. 2011). Sediments are transported across the coastal landscape as the potential for sediments to become suspended rises with storm energy and declines as wave energy is reduced. The amount of re-distributed sediment can be huge - up to 10^8 t (metric tons) deposited across hundreds of km^2 of wetlands - and dense (Turner et al. 2006). Up to 68 g cm^{-2} of sediment, for example, were deposited on Louisiana's coastal wetlands during Hurricane Katrina (Turner et al. 2006). The average deposition reported for this same study was 2.2 g cm^{-2}.

These newly-deposited sediments may have been transported from as far offshore as the continental slope. The infrequent, but intense, storm surge events regularly punctuating the microtidal Louisiana coastal zone can reach heights exceeding normal tidal cycles by several orders of magnitude. Data from offshore buoys during Hurricane Katrina, for example, show that the maximum wave height 100 km east of the hurricane path was about 17 meters, with a wave period exceeding 14 seconds (NOAA 2012). The shear stress produced by such waves is capable of suspending grains at least as large as coarse sand (1 mm) at water depths greater than 140 m (Madsen 1994, Miller et al. 1977). The sea floor depth in this area is also around 140

---

[1]Published as Tweel and Turner 2012. PLoS ONE 7(11): e50528

meters, which is the approximate depth where the continental shelf transitions to deeper water along the Gulf Coast (Figure 3.1A). Therefore, Louisiana continental shelf sediments, much of which once flowed down the Mississippi River, may be available for transport by waves associated with tropical cyclone events.

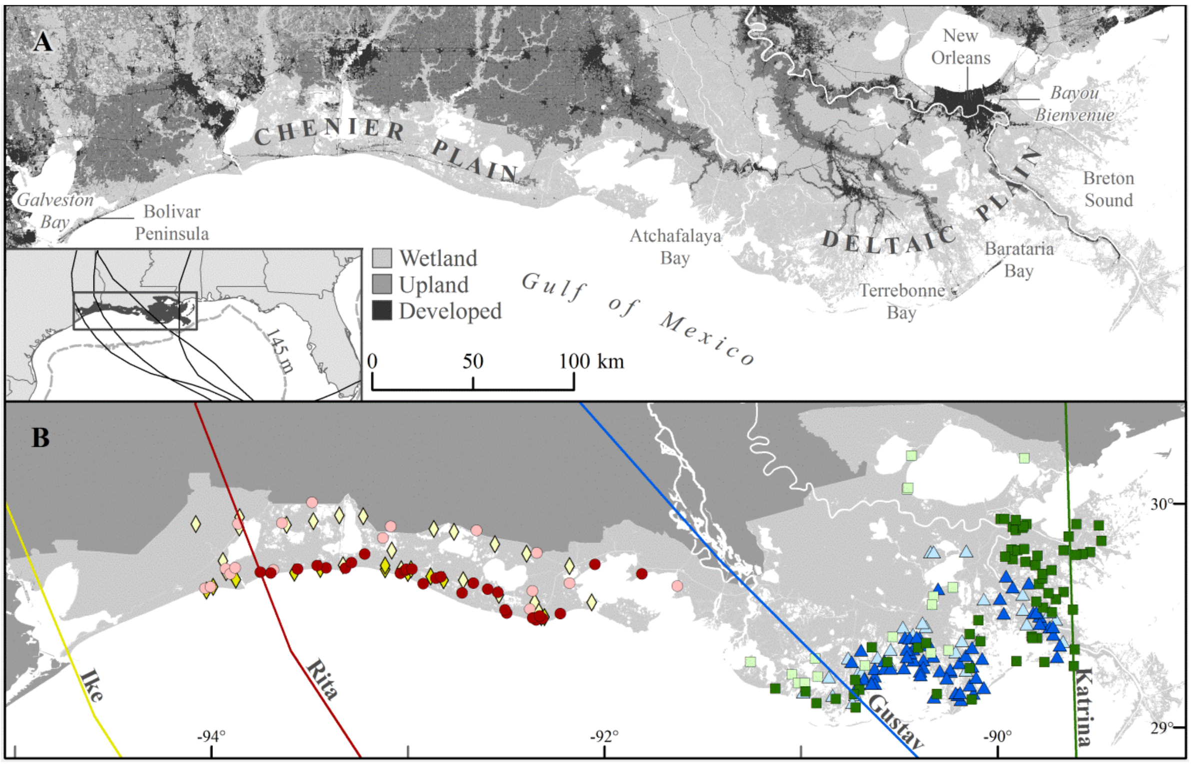

Figure 3.1 A. Map showing locations of geographic names used in text. Inset shows general location of study area, hurricane paths (black lines), and 145 m isobath (dotted line). **B**. Sampling locations and storm paths for Hurricanes Katrina (green square), Rita (red circle), Gustav (blue triangle), and Ike (yellow diamond). The dark colored symbols mark observed deposition and light colored symbols mark observation of no hurricane sedimentation. Sampling for Hurricane Ike did not include Texas, although considerable deposition occurred (Williams 2012).

The suspended sediment is carried in waves whose fate depends on the bathymetry encountered as they propagate shoreward. Massive hurricane depositional events have been observed offshore of coastal Louisiana. Following hurricanes Katrina and Rita, the deposition on the inner continental shelf was estimated to be 1160 MMT (million metric tons) - 10 times the

average annual deposition rate for that area (Goñi et al. 2007). Similar depositional events were observed following Hurricane Lili in 2002 (Allison et al. 2005), and Hurricane Ivan in 2004 (Allison et al. 2010). The characteristics of these newly deposited sediments did not appear to be from inshore sources such as wetlands or ponds (Goñi et al. 2007). East of the Mississippi River, at depths of 4 to 10 meters, sediment cores revealed the preservation of event layers that corresponded to large storm events up to 50 years prior (Keen et al. 2004).

Sediment deposition in inshore waters has also been reported following hurricane events. Sediment accumulations up to 2 m thick were found in tidal creeks of the Florida Everglades following Hurricane Andrew in 1992 (Risi et al. 1995). The storm surge associated with Hurricane Andrew's Louisiana landfall also deposited several centimeters of mud in coastal Louisiana marsh ponds located 5 km northwest of Terrebonne Bay and 45 km east of the storm path (Parsons 1998). More recently, sediment deposition of up to 10 cm was observed in Sister Lake, located 5 km inland from the Gulf of Mexico, following Hurricanes Rita (200 km to the west of Sister Lake) and Katrina (130 km to the east) (Freeman and Roberts 2012). These sediments contained up to 42% sand, and were considered to be indicative of high-energy transport and deposition. The results of isotopic analysis of these sediments revealed high ^{234}Th activity, which was interpreted to indicate an offshore sediment origin (Freeman and Roberts 2012).

Sediment deposition on the wetland platform has been more widely studied than subaqueous deposition, possibly because it is more readily distinguished from the existing soil surface. Early reports noted storm surge deposition on wetlands as far back as Hurricane Audrey in 1957 (Morgan et al. 1958), and later studies analyzed sediment deposition following Hurricane Andrew (Nyman et al. 1995, Guntenspergen et al. 1995). While mostly observed in

Louisiana due to its broad coastal wetland landscape, wetland sedimentation has also been described in Florida after Hurricanes Andrew in 1992 (Risi et al. 1995), Irene in 1999 (Davis et al. 2004), and Wilma in 2005 (Castañeda-Moya et al. 2010). Wetland sediment deposition was also observed from Texas to the Mississippi and Alabama coasts following the 2005 hurricane season (Williams 2012, Horton et al. 2009).

The deposition of these sediments is influenced by a variety of factors related to various physical and biological conditions, but there is little understanding about the spatial distribution of the sediment deposited, and how it varies from storm to storm. The focus of this analysis is to investigate the spatial distribution of sediments on coastal wetlands following hurricanes at an event or coast-wide scale. I conducted a large-scale spatial analysis, and incorporated an analysis of smaller scale variations by examining the residuals within a landscape-scale model. The objective of this research is to determine how the quality and quantity of sediments deposited during 4 hurricanes in the last 10 years varies spatially within a Louisiana coastal landscape.

Methods

Sediments that were deposited following Hurricanes Katrina (2005), Rita (2005), Gustav (2008) and Ike (2008) were sampled within four months of landfall (Figure 3.1B). These data were compiled into a spatial database that was used to estimate where and how much sediment was deposited in each event.

Field sampling and laboratory analysis

The field sampling was designed to encompass the entire depositional area following Hurricanes Katrina, Rita, Gustav, and Ike. The entire Louisiana depositional areas were sampled (Figure 3.1), but the depositional area of Hurricane Ike was not completely sampled because of

the logistical impediments to accessing wash-over areas from the Texas border to Bolivar Peninsula. I distinguished sedimentation from storms that occurred the same season by identifying gaps between the sampled areas where one event layer tapered to no deposition before the other began (Figure 3.1). Samples were collected by accessing the sites by outboard boat, car, helicopter or airboat at increasing distance from the coast and storm path with the objective of enclosing the sample area with observations of zero deposition on all sides. Sampling was done as quickly as possible following the events, but was not completed until as late as four months after landfall because of the time required to sample such a large area and storm damage to roads and social/economic infrastructure.

Each observation consisted of measuring sediment thickness, percent mineral content, and bulk density. In order to accurately quantify sediment deposition, several preliminary samples were taken before the final sample was collected using the method discussed by Turner and others (Turner et al. 2006). The depth of deposition was measured using a ruler. Sediment was collected from the vegetated areas only, and away from the wetland edge, using a modified syringe to take a small core, and therefore a known volume, from which bulk density could be determined. Hurricane-deposited sediment was clearly distinguishable from pre-existing sediment where green blades of marsh grasses were preserved below the new layer, thus indicating very recent deposition. Deposition less than 0.5 cm was difficult to accurately separate from existing detritus, and was considered zero for this analysis. The depositional areas and total amount deposited are, therefore, conservative estimates.

Sediment characteristics

Sediment samples were dried and analyzed for inorganic content by loss on ignition. Mineral accretion was used to model sediment deposition, and derived by multiplying deposition

depth by sample bulk density and percent mineral content to yield mineral accretion in g cm^{-2}. Bulk density and mineral content were compared at increasing distances from storm path and the coastline.

I used a subsample from 24 locations impacted by Hurricane Gustav to investigate grain size distributions within the event. The subsample was drawn from an area 30 km east of the track at the head of Terrebonne Bay, where sampling density was greatest, and included a gradient of inorganic sediment from 6.6 g cm^{-2} near the bay to 0.6 g cm^{-2} 19 km inland. Samples were prepared for analysis using standard procedures (Carver 1971). Rehydrated sediment was passed through a 250 μm sieve to remove large particles, if any. Organic material was assumed to be hydrodynamically equivalent, and was oxidized with a solution of 30% H_2O_2. The sediment samples were then dispersed with 0.05% sodium hexametaphosphate. Sediment grain size distributions were determined using a laser diffraction particle size analyzer (Beckman Coulter LS 13 320).

Spatial analysis

All spatial analyses were conducted using ArcInfo 10.0 (ESRI, Redlands, CA, USA). Two distinct interpolation methods were tested to estimate depositional patterns on a coastwide scale. A kriging analysis was not a suitable method when observed deposition lacked significant spatial autocorrelation, as was the case in several locations within the sampling areas. Inverse distance weighting (IDW), which does not assume input data are spatially autocorrelated, was applied to these datasets and provided the most statistically viable results. Inverse distance weighting is considered an exact interpolator, in that the output surface passes through each observation. The areas between sampled locations are estimated based on nearby samples, and are weighted to favor closer samples over more distant observations. I selected model

parameters for neighborhood and power that minimized interpolation error. I could only estimate the Louisiana portion of the deposition during Hurricane Ike because the depositional area in Texas was not sampled.

The method used to bound the depositional area was imperfect because the observed areas with zero deposition did not always completely encircle the areas with deposition. Based on decay relationships within areas that were more densely sampled, I applied a 20 kilometer buffer to each sample area, and assumed that no deposition occurred beyond this boundary. This served as the outer bound of spatial interpolation. To analyze Hurricanes Katrina and Gustav I divided the study areas east and west of the Mississippi River, and recombined them following interpolation. All data were processed in North American Datum 1983 Universal Transverse Mercator zone 15 north and a pixel size of 1 km^2. About 15% of the study area is in Universal Transverse Mercator zone 16-north, but the difference in area computed in its native zone compared to zone 15-north at this latitude was 0.1% in one area tested.

I used United States Fish and Wildlife Service National Wetlands Inventory data to calculate wetland areas because it is consistent in coverage and source data throughout the study area. The mean pixel value (mineral sediment deposition per cm^2) for each event was multiplied by the area of wetlands in each area to produce an estimate of total deposition. These estimates were formulated for all Louisiana coastal wetlands, and all Texas coastal wetlands to Galveston Bay. The root mean square error, also in units of mineral sediment deposition per cm^2, from each interpolation was used to calculate interpolation error terms for each estimate.

To estimate the total depositional area from Hurricane Ike, I combined my estimate with that of a previously published estimate that covered the area that was inaccessible (Williams

2012). I subtracted the overlapping areas from my model, and then combined the two figures to estimate the total wetland deposition following Hurricane Ike.

Spatial distribution

In addition to the total sediment deposited per event, I also analyzed the spatial distribution of sediment within each depositional area. I measured the amount of total deposition that occurred within 10 km increments from the storm track and also from open water. Based on preliminary observations that sediment distribution was highest near the open water of the Gulf of Mexico and also large inshore water bodies, I defined the open water buffer as beginning 5 km from land along inshore areas (e.g., Breton Sound, Barataria Bay) and directly along marshes that extend to the Gulf. Land-to-water ratios within each area were also calculated to test if the results reflected differing wetland coverage rather than deposition.

Results

Total deposition

The storm surges of Hurricanes Katrina, Rita, and Gustav deposited 67.8 ± 8.6, 48.2 ± 8.3, and 20.6 ± 3.9 (estimate ± root mean square error) million metric tons (MMT) of inorganic sediment on coastal wetlands, respectively, when calculated using the IDW method (Figure 3.2, Table 3.1). Hurricane Ike deposited an estimated 32.8 ± 10.9 MMT on Louisiana wetlands alone, but the sampling density was less than the other events and resulted in a greater percent error. The results from the kriging analysis were within 2% of the results from the IDW model for Katrina and Gustav, and 6% for Rita, but some sample areas did not meet the model assumption of spatial autocorrelation. The use of the IDW method tended to reduce data variability, and observations of high deposition were tempered because the final estimate pixel values represent the mean of the observation as well as estimated values possibly driven down by

neighboring points. For this reason, the total deposition estimates may be conservative figures because half of the total deposition is estimated to occur in these high deposition areas (Figure 3.3).

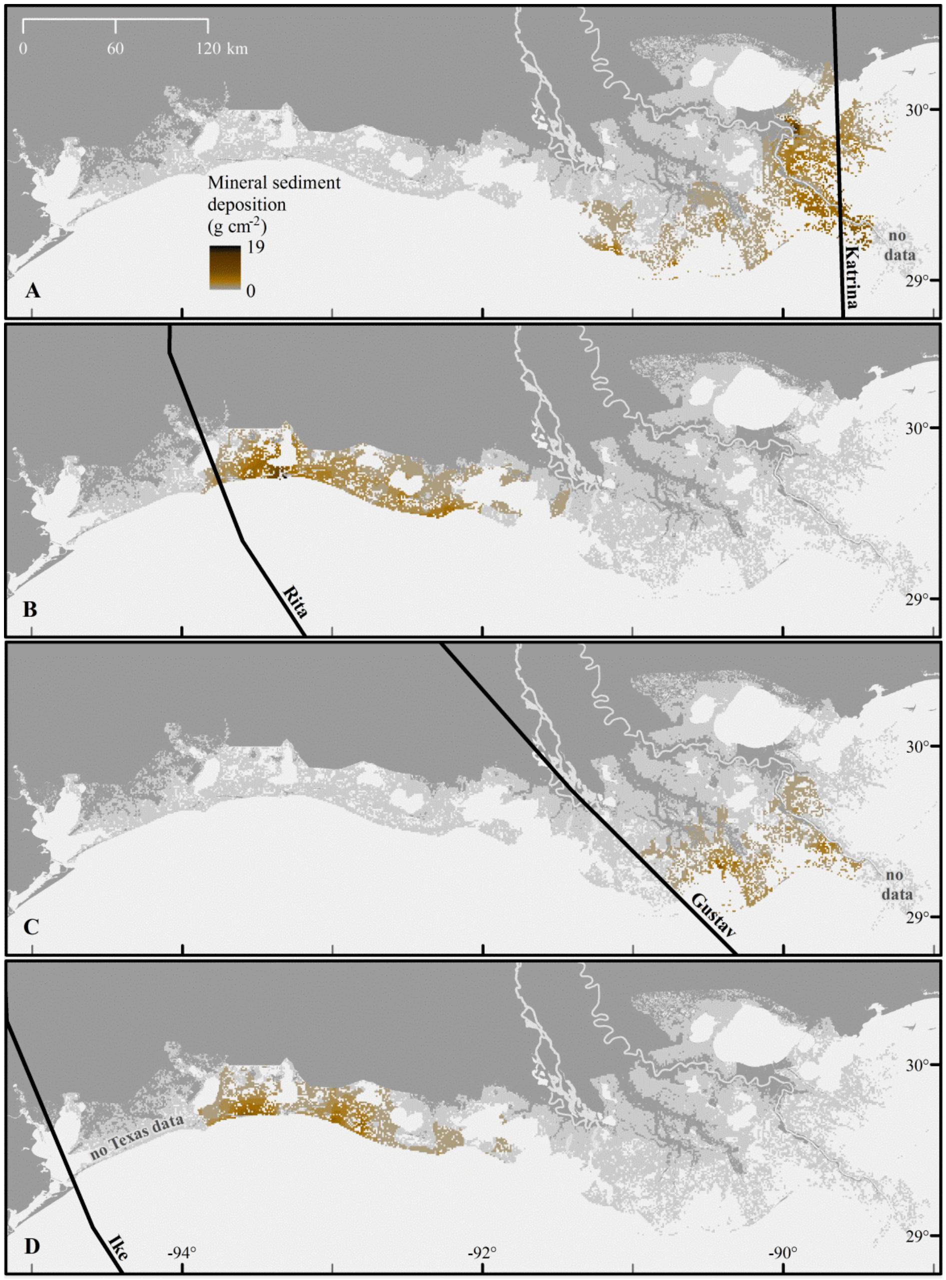

Figure 3.2 Mineral sediment deposition (g cm^{-2}) from Hurricanes Katrina (**A**), Rita (**B**), Gustav (**C**), and the Louisiana portion of Ike (**D**) interpolated using inverse distance weighting at 1 km^2 resolution.

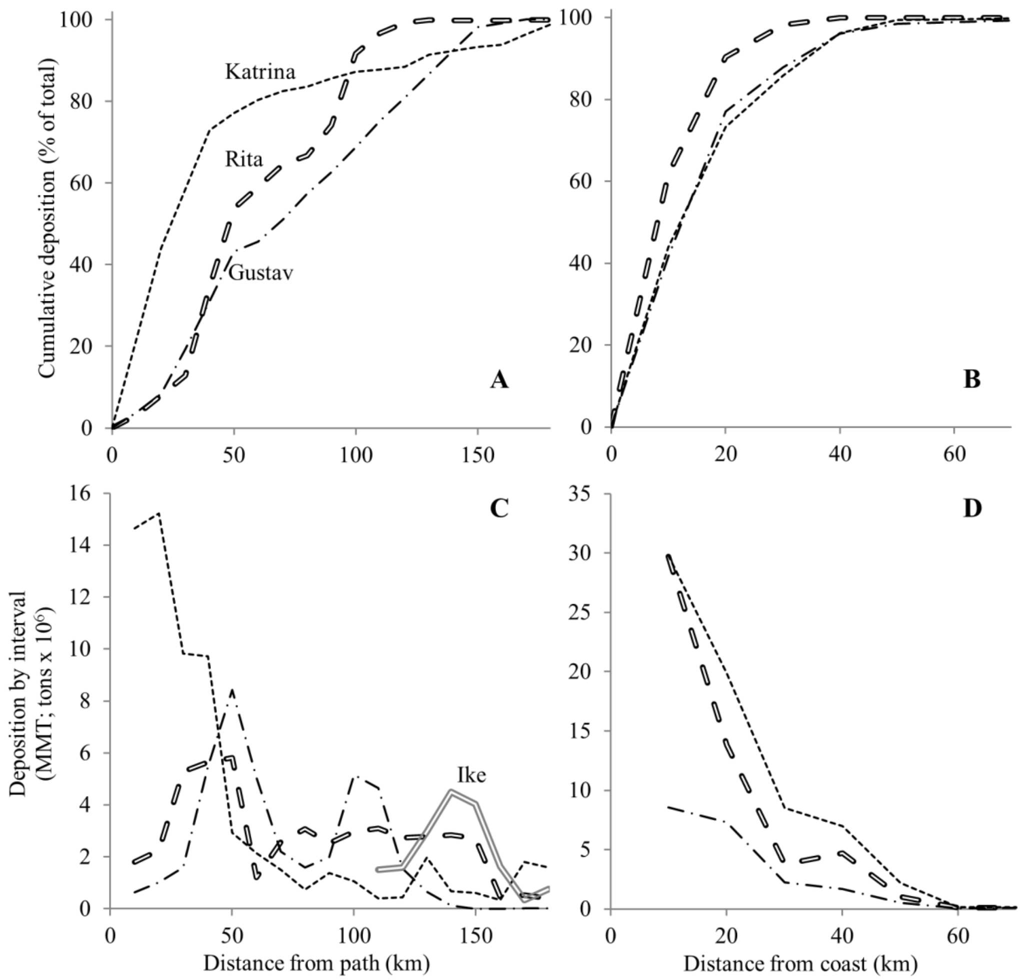

Figure 3.3 The top panels (**A**, **B**) show cumulative deposition and bottom panels (**C**, **D**) show deposition within each 10 km interval, plotted at the midpoint. The panels at left (**A**, **C**) show distance from path and the panels at right (**B**, **D**) show distance from coast. Deposition is based on spatially interpolated sediment distribution measured at 10 km increments. Deposition is measured east of the storm path for Gustav, Rita, and Ike, and on both sides for Katrina because of the distinct distribution of sediment. The data for Hurricane Ike in panel **C** is for the Louisiana portion of the deposition footprint; Texas is excluded.

Spatial distribution

The storm surge from Hurricane Ike resulted in sedimentation farthest from the storm path (214 km) when compared to the other three storms (Table 3.1). Sedimentation from Hurricane Katrina reached the farthest inland, however. The observed inland limit of sedimentation was also greater in the two deltaic plain events than those in the chenier plain.

The percent water within the study areas was similar, but chenier plain study areas contained less open water (Table 3.1).

Table 3.1 Mineral sediment deposition estimates and model results for Hurricanes Katrina, Rita, Gustav, and Ike. [1]Texas deposition not sampled. [2]IDW: Inverse distance weighting, the method used to estimate total deposition. [3]RMSE: Root mean square error.

		Wetland deposition			IDW statistics[2]			Most distant observed sedimentation			
	Gulf Coast landfall	Total (MMT)		Model error (MMT)	RMSE[3] (g cm^{-2})	Mean error (g cm^{-2})	*n*	(km from track)	(km from coast)	Maximum accretion (g cm^{-2})	Percent land in depositional area
Katrina	8/29/2005	67.8	±	8.6	2.4	0.09	77	148	43	20.81	52.19
Rita	9/24/2005	48.2	±	8.3	3.25	0.11	45	166	12	19.95	64.29
Gustav	9/1/2008	20.6	±	3.9	1.19	0.04	110	100	40	7.46	55.40
Ike[1]	9/13/2008	32.8	±	10.9	1.85	0.17	37	214	7	16.73	65.54
Total		169.4	±	31.7							

Hurricane Katrina deposited 80% of the total amount within 60 km of the hurricane track, which is more than from Hurricanes Rita or Gustav, (Figure 3.3A). By comparison, Hurricanes Rita and Gustav deposited 46% and 59%, respectively, within the same distance. All three of these events deposited over 90% of the total mineral sediment within 140 km of the path. In contrast to Hurricane Katrina, Hurricanes Rita and Gustav deposited the most sediment between 20 and 50 km from the path, with less sediment being deposited closer to the path (Figure 3.3C). The peak sedimentation from Hurricane Katrina occurred nearest the track.

The patterns of deposition relative to distance from the coast were more consistent than distance from storm track, and nearly identical for the two deltaic plain events, Katrina and Gustav, as a percent of their total deposition (Figure 3.3B). The inland distribution from Hurricane Rita was similar, but the decrease along an inland trend, as a percent of total, occurred more quickly (Figure 3.3B). Hurricanes Katrina and Rita both resulted in the deposition of 27

MMT within the first 10 km inland, which was the highest quantity observed in any 10 km interval for the 4 events in this study (Figure 3.3D). The total sedimentation from Gustav within this same interval was nearly an order of magnitude lower than Hurricanes Katrina and Rita. At least 80% of the total sedimentation occurred within the first 30 km inland.

Sediment characteristics

The sediment deposited in wetlands near Bayou Bienvenue, the area bounded by the Mississippi River on the west and the Mississippi River Gulf Outlet on the east, was distinct from that of the surrounding areas following Hurricane Katrina. The maximum observed mineral accretion in this area was 20.81 g cm^{-2}, 28 km from the storm path and 5 km from Lake Borgne, while the maximum for the remainder of the study area was 9.92 g cm^{-2}, 8 km from the path and 3 km from Breton Sound. The percent mineral sediment in this area was as much as 98%, which was much greater than the 66% observed in wetlands 10 km south of this area. This high mineral content was more similar to that of areas 0 to 15 km from the storm path (μ = 93%). In contrast to Hurricane Katrina, the maximum sedimentation in the other storm events occurred nearest coastal bays and the Gulf of Mexico, and decreased inland.

There were significant trends in organic content and bulk density with distance from the coast, but the relationships were noisy (Figure 3.4). There was a significant decreasing inland trend of mineral content for all four hurricanes, with the Chenier Plain events being more tightly clustered towards higher mineral content and shorter distances. The sediment bulk density was more variable than mineral content, but decreased along a coastline-to-inland gradient for all events studied. The mean inorganic content within the first 5 km from coast was 92.0% ± 0.8 SE (86.2 % ± 0.8 for all sites) and the mean bulk density within the same distance was 0.63 g cm^{-3} ± 0.04 SE (0.48 g cm^{-3} ± 0.02 for all sites).

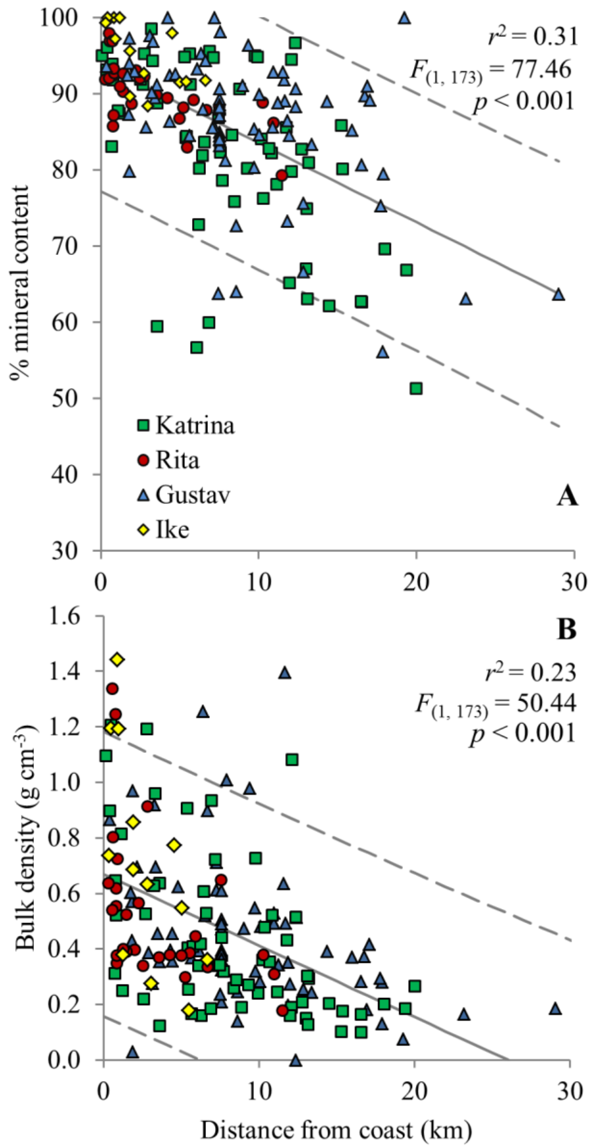

Figure 3.4 Percent mineral content (**A**) and bulk density (**B**) with distance from coastline for sediment deposited from Hurricanes Katrina (squares), Rita (circles), Gustav (triangles), and Ike (diamonds). Note that the Y-axis for Figure **A** begins at 30%. Dashed lines show 95% prediction intervals.

These results demonstrated that sediment characteristics with respect to distance from the storm track were more variable between depositional events. For this reason, each event was analyzed separately. With increasing distance from track, sediments deposited following Hurricane Rita decreased in mineral content ($r^2 = 0.35$, $F_{(1, 26)} = 13.68$, $p = 0.001$) and bulk density ($r^2 = 0.18$, $F_{(1, 26)} = 5.86$, $p = 0.023$). The peak bulk density was observed 31 km east of

the storm path, which is also where the greatest deposition occurred. The bulk density of Hurricane Katrina sediment samples decreased until 100 km from the hurricane track, and then there was a sharp increase, with the maximum bulk density observed at 148 km from the track. The mineral content of samples collected immediately after Hurricane Gustav decreased slightly with increasing distance from the hurricane track ($r^2 = 0.06$, $F_{(1, 72)} = 4.44$, $p = 0.039$), but there was no significant relationship between bulk density and distance from the hurricane track, which initially increased with distance, but then decreased in samples closer to Mississippi River levees. The peak bulk density from Hurricane Gustav was observed 35 km to the east of the hurricane track. Hurricane Ike sediments exhibited similar patterns to the other chenier plain event, Rita. Sediment mineral content ($r^2 = 0.49$, $F_{(1, 11)} = 10.74$, $p = 0.007$) and bulk density ($r^2 = 0.42$, $F_{(1, 11)} = 7.89$, $p = 0.017$) both decreased significantly with distance from the storm track, but there were fewer samples than the other events, and no samples closer than 75 km from the storm track.

The mode grain size within the subsampled area of Hurricane Gustav decreased with increasing distance from shoreline ($r^2 = 0.25$, $F_{(1, 22)} = 7.19$, $p = 0.013$; Figure 3.5). Sediment was more poorly sorted further inland along the same gradient, as determined by increasing coefficients of variation ($r^2 = 0.26$, $F_{(1, 22)} = 7.88$, $p = 0.010$). Overall, the mean grain size was 34.8 µm, which is classified as silt. However, 17.3% of the total sample volume was comprised of grains larger than very fine sand (63.4 µm), and the range extended to fine sand (256.9 µm).

Discussion

The quantity of sediment left on the marsh surface following tropical cyclone events can exceed 10^8 t yr^{-1} (100 MMT yr^{-1}), but the spatial and temporal distribution of these events can vary widely. The amount of sediment deposited on coastal wetlands ranged considerably

between the hurricanes, with Hurricane Katrina depositing nearly three times the total sediment of Hurricane Gustav. Hurricane Rita deposited about 70% of the amount left by Hurricane Katrina. My combined estimate of 116 MMT for Hurricanes Katrina and Rita is 89% of the 131 MMT reported by Turner and others using the same dataset (Turner et al. 2006), but different analysis methods. This equates to 80% of the modern annual sediment discharge from the Mississippi River being deposited on wetlands alone (Meade and Moody 2010). Subaqueous deposition, if prorated for inshore waters, increases the total deposition to as high as 135, 67, and 38 MMT for Hurricanes Katrina, Rita, and Gustav, respectively.

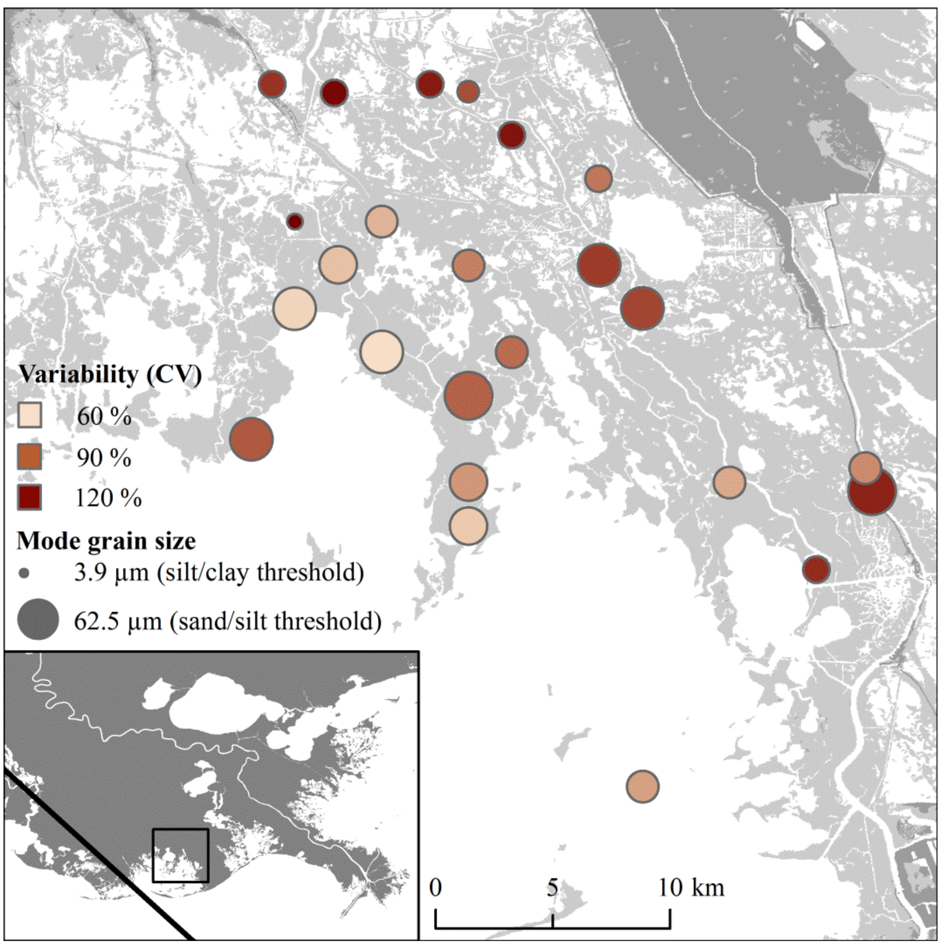

Figure 3.5 The grain sizes decrease (symbol size) and are more poorly sorted (symbol color) with distance from open water. Variability is calculated as the coefficient of variation (CV). Inset shows sample area and track of Hurricane Gustav.

A previously published estimate of the total deposition from Hurricane Ike is 16.2 MMT, but the sampling did not include the entire area impacted by the storm (Williams 2012). My estimate of 32.8 MMT in Louisiana for Hurricane Ike reflects differences in sampling methodology and areal coverage, because my sampling design included thinner deposits observed farther inland. The portion of my estimate beyond that sampled in the previous study is 26.8 MMT. I estimate the combined total from both studies at 43 MMT, making Hurricane Ike most similar to Hurricane Rita in terms of total deposition, although this estimate has a larger margin of uncertainty because it combines two sampling and analysis methods.

Sediment deposition tended to be greatest just east of the storm path, and nearer the coastline, for the two storms making landfall west of the Mississippi River. The areas of high deposition generally coincided with the highest storm surges in previously reported models, but modeled surges covered a broader area (Dietrich et al. 2010, Dietrich et al. 2011). The distribution of sediment in Louisiana wetlands following Hurricane Katrina was mostly west of the path, due to the strong easterly winds that preceded the storm and drove the storm surge into the east-oriented estuary. This effect is demonstrated by previous storm surge events (USACE 1972) and simulated events (Dietrich et al. 2010).

The majority of sedimentation (80% ± 5 SE) occurred within the first 20 km inland, and declined exponentially. With distance from the storm track, about half (48% ± 10 SE) of the total occurred within the first 50 km, but the distribution was more variable. Comparing between the three events, there are remarkably consistent depositional patterns along a shoreline-to-inland gradient. These patterns were more variable with distance from the path, because the high sedimentation during Hurricane Katrina was closest to its storm track, whereas the other two events peaked 50 km east of the storm tracks. A similar relationship with distance from landfall

was reported for Hurricane Ike, where deposition was greatest about 40 km east of landfall, and then decreased with distance (Williams 2012). The most distant sedimentation averaged 157 km from the storm track (Table 3.1), which compares well to the 130 km maximum observed after Hurricane Andrew (Cahoon et al. 1995). The chenier plain events spread sediment farther along the coast than the deltaic plain landfalls, but this could also result from characteristics of the storms rather than landfall location.

The high deposition I observed in the Bayou Bienvenue area following Hurricane Katrina was anomalous compared to nearby sample locations and the otherwise decreasing inland trend, but is consistent with high storm surge energy reported for that area (Mashriqui et al. 2006, Ebersole et al. 2010). The spatial distribution of wetland sedimentation for Hurricane Rita, which was up to 8.7 cm thick 0.3 km from the coast and diminishing to 0.1 cm 12 km inland, is consistent with the reported ranges of 7.6 to 188 cm on and directly behind ridges that led to increased over-wash (Faulkner et al. 2005). This wetland sedimentation from Hurricane Rita was described as two distinct sequences: an underlying thin layer comprised of fine sand and mud overlain by a coarser, thicker layer comprised mainly of sand, but with a more limited areal extent (Williams 2009). The finer sediment layer was rich in foraminiferal remains, suggesting a more offshore origin, whereas the higher sand content of the coarser layer resembled beach and dune overwash.

The reduction in storm surge as it propagates shoreward is reflected in observations of deposition ranging from offshore to inshore ponds and wetlands. Offshore deposition in 2005 was at least 10 times greater than my estimate for wetlands (Goñi et al. 2007). This offshore deposition may remain as in-tact event horizons for decades (Keen et al. 2004). Inshore deposition following hurricanes can also be significant (Risi et al. 1995, Parsons 1998, Freeman

and Roberts 2012), but the spatial extent and how well it compares to deposition in surrounding wetlands remains unclear. Although these estimates were within range of observations of wetland deposition for Hurricanes Andrew and also Rita/Katrina, local bathymetry and channel morphology can play a major role in determining whether erosion or deposition will occur (Miner et al. 2009).

Landscape-scale wetland sedimentation events have been observed in other areas following tropical cyclones, such as the Florida coast. In southwest Florida following Hurricane Andrew in 1992, an average deposition of 7 cm (range: 0-20 cm) across an area of 110 km^2 was observed (Risi et al. 1995). The mean organic content of these sediments was 8% (range: 4-22%). I observed a greater organic content in Louisiana of 14% (range: 2-49%) for all three hurricanes, which is consistent with the contrast between bottom sediments in coastal Louisiana and Florida Bay.

The areas of highest mineral content and bulk density were near the coast, which is where storm surge energies were greatest, and decreased inland. Similar trends in organic content and bulk density were observed following Hurricane Andrew in Louisiana (Guntenspergen et al. 1995). In this same location studied during Hurricane Andrew, I observed anomalously high bulk density and mineral content that strayed from the overall distance-from-track trends following the 2005 hurricanes. This area was 148 km from the nearest storm path, but near Atchafalaya Bay, and may have been the result of overlapping influences of both 2005 hurricanes as well as the nearby Atchafalaya River acting as a sand source.

Although grain size measurements were more spatially limited, an inland trend of decreasing grain size was also observed in Florida following Hurricane Andrew, but the Florida sediments were predominantly carbonate-rich sand (Risi et al. 1995). There was a sharper

decline in sediment grain size for Hurricane Andrew in Florida than I observed for Gustav in Louisiana, which was attributed to the relatively short storm surge duration resulting from Andrew's small eye and rapid speed. The overall decreasing inland trends in bulk density, mineral content, and grain size are indicative of storm energy attenuation by marshes and shallow inshore waters, whereby the heavier materials are dropped from suspension closer to the Gulf. Some variability in bulk density, however, may reflect consolidation that occurred following their initial deposition, because sampling did not occur for several months for some samples. The residual variability in organic content, bulk density, and grain size, despite being statistically significant with distance from the coast, likely results from smaller scale factors that also affect sediment distribution such as vegetation and local geomorphology. Sediment deposition may also vary on a more local scale because of variations in local bathymetry or channel morphology (Miner et al. 2009, Otvos 2011), or on an even smaller scale such as differing vegetation types or stem densities (Nyman et al. 1995, Rejmànek et al. 1998). From a coast-wide perspective, however, these effects appear to be overshadowed by variations in storm energy.

Some of the sediment deposited during storms from inshore sources may include newly eroded wetland soils. The amounts of this lateral erosion of coastal wetlands during tropical cyclones can vary widely; some effects recover within months, while others may remain for decades (Morton and Barras 2011). Following Hurricanes Katrina and Rita in 2005, 525 km^2 of new water area was observed, but a portion of this may be due to the removal of floating aquatic vegetation rather than wetland (Morton and Barras 2011). Many areas lost whole blocks of marsh peat, forming linear scars parallel to the wind direction, accordion-like features, and rolled up vegetation mats. Although large areas of open water appeared after the 2005 and 2008

hurricane seasons, some recovery occurred within a couple years, but the long-term trend of land loss continued in many areas (Couvillion et al. 2011). Much of the land loss from the 2005 hurricane season occurred in areas where the wetland substrate had been weakened due to the introduction of Mississippi River water, which led to changes in vegetation composition (Howes et al. 2010) as well as increased soil decomposition and decreased root biomass (Kearney et al. 2011).

The contribution of these powerful, but infrequent, events to the long-term sedimentary record of wetlands may vary widely (Cahoon 2006), and be significant (Turner et al. 2007). McKee and Cherry (2009) examined what happened in wetlands that had sediments deposited during the 2005 hurricane season. They observed that, compared to a control site receiving less sediment, that the wetlands under the strong influence of the hurricanes had a lower soil elevation loss. Sediment deposited in wetlands of the chenier plain from Hurricane Rita in 2005 had been incorporated into the soil profile when re-examined in 2007, and the authors concluded that these types of events contributed one to two thirds of the sediment in the soil profile (Williams and Flanagan 2009). In a study covering a longer time scale, Turner and others (2007) reported peaks in mineral content of salt marsh soils as early as 1880 that coincided with periods of increased hurricane frequency. A similar study also noted peaks in sand content of wetland soils in New England that were correlated with known storm events (Boldt et al. 2010). Peaks in sand content beyond the historical record were observed as early as 1450, indicating that, although storm-deposited sediment may become reworked by physical or biological processes, some of this sediment is incorporated into the long term sediment record. Variations in inorganic sedimentation rates in a North Sea salt marsh were found to be driven by storm frequency and

intensity, with periods of intense storm tides corresponding to high sedimentation for the 70-year period studied (Schuerch et al. 2012).

Tropical cyclone events represent both potential agents of land loss, but also a significant input of sediment to the wetland soil profile. In a deltaic system with rates of isostatic sea level rise approaching one cm yr^{-1} (Gonzàlez and Tornqvist 2006), storm-driven inputs of sediment from nearshore or offshore may be an important, if not dominant, component of coastal wetland inorganic accretion (Turner et al. 2007). The Mississippi River is the ultimate source of most of this sediment, via the continental shelf, but its transport from offshore to inshore during infrequent, but intense, events represents an important component of coastal sedimentation, and may represent the greatest allogenic source of sediment for coastal wetlands in abandoned delta lobes. Although I have described massive sedimentation following these four events, further research is needed to identify how these types of events contribute to the long-term sediment budget for coastal Louisiana wetlands. A more complete understanding of the factors driving sedimentation events for coastal wetlands will lead to the implementation of more efficient and effective coastal restoration actions.

References

Allison, M. A., T. M. Dellapenna, E. S. Gordon, S. Mitra, and S. T. Petsch. 2010. Impact of Hurricane Katrina (2005) on Shelf Organic Carbon Burial and Deltaic Evolution. Geophysical Research Letters 37:L21605.

Allison, M. A., A. Sheremet, and G. W. Stone. 2005. Storm Layer Deposition on the Mississippi-Atchafalaya Subaqueous Delta Generated by Hurricane Lili in 2002. Continental Shelf Research 25:2213-2232.

Boldt, K. V., P. Lane, J. D. Woodruff, and J. P. Donnelly. 2010. Calibrating a Sedimentary Record of Overwash from Southeastern New England Using Modeled Historic Hurricane Surges. Marine Geology 275:127-139.

Cahoon, D. R. 2006. A Review of Major Storm Impacts on Coastal Wetland Elevations. Estuaries and Coasts 29:889-898.

Cahoon, D. R., D. J. Reed, J. W. Day Jr, G. D. Steyer, R. M. Boumans, J. C. Lynch, D. McNally, and N. Latif. 1995. The Influence of Hurricane Andrew on Sediment Distribution in Louisiana Coastal Marshes. Journal of Coastal Research SI 21:280-294.

Carver, R. 1971. Procedures in Sedimentary Petrography. New York: Wiley. 653 p.

Castañeda-Moya, E., R. R. Twilley, V. H. Rivera-Monroy, K. Zhang, S. E. Davis, and M. Ross. 2010. Sediment and Nutrient Deposition Associated with Hurricane Wilma in Mangroves of the Florida Coastal Everglades. Estuaries and Coasts 33:45-58.

Costanza, R., O. Perez-Maqueo, M. L. Martinez, P. Sutton, S. J. Anderson, and K. Mulder. 2008. The Value of Coastal Wetlands for Hurricane Protection. Ambio 37:241-248.

Couvillion, B. R., J. A. Barras, G. D. Steyer, W. Sleavin, M. Fischer, H. Beck, N. Trahan, B. Griffin, and D. Heckman. 2011. Land Area Change in Coastal Louisiana (1932 to 2010). US Geological Survey, National Wetlands Research Center. 12 p.

Davis III, S. E., J. E. Cable, D. L. Childers, C. Coronado-Molina, J. W. Day Jr, C. D. Hittle, C. J. Madden, E. Reyes, D. Rudnick, and F. Sklar. 2004. Importance of Storm Events in Controlling Ecosystem Structure and Function in a Florida Gulf Coast Estuary. Journal of Coastal Research 20:1198-1208.

Dietrich, J., S. Bunya, J. Westerink, B. Ebersole, J. Smith, J. Atkinson, R. Jensen, D. Resio, R. Luettich, and C. Dawson. 2010. A High-Resolution Coupled Riverine Flow, Tide, Wind, Wind Wave, and Storm Surge Model for Southern Louisiana and Mississippi. Part II: Synoptic Description and Analysis of Hurricanes Katrina and Rita. Monthly Weather Review 138:378-404.

Dietrich, J., J. Westerink, A. Kennedy, J. Smith, R. Jensen, M. Zijlema, L. Holthuijsen, C. Dawson, R. Luettich Jr, and M. Powell. 2011. Hurricane Gustav (2008) Waves and Storm Surge: Hindcast, Synoptic Analysis and Validation in Southern Louisiana. Monthly Weather Review 139:2488-2522.

Ebersole, B., J. Westerink, S. Bunya, J. Dietrich, and M. Cialone. 2010. Development of Storm Surge Which Led to Flooding in St. Bernard Polder During Hurricane Katrina. Ocean Engineering 37:91-103.

Faulkner, S., W. Barrow, T. Doyle, M. Baldwin, T. Michot, C. Wells, C. Jeske, G. Farris, G. Smith, and M. Crane. 2005. Sediment Deposition from Hurricane Rita on Hackberry Beach Chenier in Southwestern Louisiana. GS Farris, GJ Smith, MP Crane, CR Demas, LL Robbins and DL Lavois, eds. Science and the storms: the USGS response to the hurricanes of 2005. p. 157-162.

Freeman, A. M. and H. H. Roberts. 2012. Storm Layer Deposition on a Coastal Louisiana Lake Bed. Journal of Coastal Research 29:31-42.

Gedan, K. B., M. L. Kirwan, E. Wolanski, E. B. Barbier, and B. R. Silliman. 2011. The Present and Future Role of Coastal Wetland Vegetation in Protecting Shorelines: Answering Recent Challenges to the Paradigm. Climatic Change 106:7-29.

Goñi, M. A., Y. Alleau, R. Corbett, J. P. Walsh, D. Mallinson, M. Allison, E. Gordon, S. Petsch, and T. M. Dellapenna. 2007. The Effects of Hurricanes Katrina and Rita on the Seabed of the Louisiana Shelf. Sedimentary Record 5:4-9.

González, J. L. and T. E. Tornqvist. 2006. Coastal Louisiana in Crisis: Subsidence or Sea Level Rise? Eos Trans. AGU 87:493-498.

Guntenspergen, G., D. Cahoon, J. Grace, G. Steyer, S. Fournet, M. Townson, and A. Foote. 1995. Disturbance and Recovery of the Louisiana Coastal Marsh Landscape from the Impacts of Hurricane Andrew. Journal of Coastal Research SI 21:324-339.

Horton, B. P., V. Rossi, and A. D. Hawkes. 2009. The Sedimentary Record of the 2005 Hurricane Season from the Mississippi and Alabama Coastlines. Quaternary International 195:15-30.

Howes, N. C., D. M. FitzGerald, Z. J. Hughes, I. Y. Georgiou, M. A. Kulp, M. D. Miner, J. M. Smith, and J. A. Barras. 2010. Hurricane-Induced Failure of Low Salinity Wetlands. Proceedings of the National Academy of Sciences 107:14014-14019.

Kearney, M. S., J. C. A. Riter, and R. E. Turner. 2011. Freshwater River Diversions for Marsh Restoration in Louisiana: Twenty-Six Years of Changing Vegetative Cover and Marsh Area. Geophysical Research Letters 38:L16405.

Keen, T. R., S. J. Bentley, W. Chad Vaughan, and C. A. Blain. 2004. The Generation and Preservation of Multiple Hurricane Beds in the Northern Gulf of Mexico. Marine Geology 210:79-105.

Madsen, O. S. 1994. Spectral Wave-Current Bottom Boundary Layer Flows. Coastal Engineering 94:384-397.

Mashriqui, H. S., G. P. Kemp, I. van Heerden, Y. Xu, and V. Singh. 2006. Experimental Storm Surge Simulations for Hurricane Katrina. YJ Xu and VP Singh, eds. Coastal Environment and Water Quality. Highlands Publications. p. 481-490.

McKee, K. L. and J. A. Cherry. 2009. Hurricane Katrina Sediment Slowed Elevation Loss in Subsiding Brackish Marshes of the Mississippi River Delta. Wetlands 29:2-15.

Meade, R. H. and J. A. Moody. 2010. Causes for the Decline of Suspended-Sediment Discharge in the Mississippi River System, 1940–2007. Hydrological Processes 24:35-49.

Miller, M. C., I. McCave, and P. Komar. 1977. Threshold of Sediment Motion under Unidirectional Currents. Sedimentology 24:507-527.

Miner, M. D., M. A. Kulp, D. M. FitzGerald, and I. Y. Georgiou. 2009. Hurricane-Associated Ebb-Tidal Delta Sediment Dynamics. Geology 37:851-854.

Morgan, J. P., L. G. Nichols, and M. Wright. 1958. Morphological Effects of Hurricane Audrey on the Louisiana Coast. Louisiana State University, Coastal Studies Institute Technical Report 10.

Morton, R. A. and J. A. Barras. 2011. Hurricane Impacts on Coastal Wetlands: A Half-Century Record of Storm-Generated Features from Southern Louisiana. Journal of Coastal Research 27:27-43.

NOAA. 2012. National Oceanic and Atmospheric Administration, National Data Buoy Center, Station 42040. www.ndbc.noaa.gov.

Nyman, J. A., C. R. Crozier, and R. D. DeLaune. 1995. Roles and Patterns of Hurricane Sedimentation in an Estuarine Marsh Landscape. Estuarine, Coastal and Shelf Science 40:665-679.

Otvos, E. G. 2011. Hurricane Signatures and Landforms—toward Improved Interpretations and Global Storm Climate Chronology. Sedimentary Geology 239:10-22.

Parsons, M. L. 1998. Salt Marsh Sedimentary Record of the Landfall of Hurricane Andrew on the Louisiana Coast: Diatoms and Other Paleoindicators. Journal of Coastal Research 14:939-950.

Rejmánek, M., C. E. Sasser, and G. W. Peterson. 1988. Hurricane-Induced Sediment Deposition in a Gulf Coast Marsh. Estuarine, Coastal and Shelf Science 27:217-222.

Risi, J. A., H. R. Wanless, L. P. Tedesco, and S. Gelsanliter. 1995. Catastrophic Sedimentation from Hurricane Andrew Along the Southwest Florida Coast. Journal of Coastal Research 31:83-102.

Schuerch, M., J. Rapaglia, V. Liebetrau, A. Vafeidis, and K. Reise. 2012. Salt Marsh Accretion and Storm Tide Variation: An Example from a Barrier Island in the North Sea. Estuaries and Coasts 35:486-500.

Shepard, C. C., C. M. Crain, and M. W. Beck. 2011. The Protective Role of Coastal Marshes: A Systematic Review and Meta-Analysis. PloS ONE 6:e27374.

Turner, R. E., J. J. Baustian, E. M. Swenson, and J. S. Spicer. 2006. Wetland Sedimentation from Hurricanes Katrina and Rita. Science 314:449-452.

Turner, R. E., E. M. Swenson, C. S. Milan, and J. M. Lee. 2007. Hurricane Signals in Salt Marsh Sediments: Inorganic Sources and Soil Volume. Limnology and Oceanography 52:1231-1238.

USACE. 1972. History of Hurricane Occurrences Along Coastal Louisiana. US Army Corps of Engineers. New Orleans. 66 p.

Williams, H. F. L. 2009. Stratigraphy, Sedimentology, and Microfossil Content of Hurricane Rita Storm Surge Deposits in Southwest Louisiana. Journal of Coastal Research 25:1041-1051.

Williams, H. F. L. 2012. Magnitude of Hurricane Ike Storm Surge Sedimentation: Implications for Coastal Marsh Aggradation. Earth Surface Processes and Landforms 37:901-906.

Williams, H. F. L. and W. M. Flanagan. 2009. Contribution of Hurricane Rita Storm Surge Deposition to Long-Term Sedimentation in Louisiana Coastal Woodlands and Marshes. Journal of Coastal Research SI 56:1671-1675.

CHAPTER 4
CONTRIBUTION OF TROPICAL CYCLONES TO THE SEDIMENT BUDGET FOR COASTAL LOUISIANA WETLANDS

Introduction

Coastal wetlands provide storm protection for coastal communities (Barbier et al. 2008, Costanza et al. 2008, Gedan et al. 2008, Shepard et al. 2011). The protection and restoration of coastal areas is projected to cost $50 billion in Louisiana alone, and is largely centered on the delivery of sediment to coastal wetlands (CPRA 2012). It is widely acknowledged that intense, but infrequent, storm surge events, such as those resulting from tropical cyclones and tsunamis, can result in the deposition of inorganic sediments which may get incorporated into the soil profile (Turner et al. 2006, Tweel and Turner 2012a, Stone et al. 1997, Schuerch et al. 2012, Boldt et al. 2010, Nanayama et al. 2007). These sediments can increase wetland elevation, slow wetland subsidence, and affect habitat quality (McKee and Cherry 2009). However, the frequency, magnitude, and spatial distribution of this sedimentation are not well understood for Louisiana or other coastal systems.

About 80% of the total wetland sedimentation from a given hurricane striking Louisiana occurs within 20 km inland from the Gulf of Mexico, and 58% occurs within 50 km of the landfall location (Tweel and Turner 2012a). A 160-year history of Louisiana hurricane landfalls suggests, however, that hurricane landfall location, timing, and intensity have varied widely across the coast (McAdie et al. 2009).

The long-term and coast-wide effect of these events on the distribution of inorganic sediment has been difficult to quantify because of the irregular and infrequent occurrence of the storms, and the logistical challenges of sampling in a timely manner after each storm. Here I investigate the long-term contribution of tropical cyclone events to soil inorganic matter content

in Louisiana coastal wetlands. I use a long-term and spatially explicit statistical model that includes historical records dating to 1851 and examine the results within the context of two independent, but complimentary, analyses of inorganic sediment distributions for coastal Louisiana. One dataset describes the inorganic content of the top 24 cm of wetland soil across the coast (Tweel and Turner 2012b), and the other examines temporal fluctuations in mineral sediment deposition in deltaic plain salt marshes since 1910 (Turner et al. 2007).

Methods

Study area and model scope

The study area includes wetlands within the coastal zone from the Louisiana/Mississippi border west to Galveston Bay (Figure 4.1). I excluded developed and upland areas from the analysis. Although I was primarily interested in wetland sedimentation within the deltaic and chenier plains of Louisiana, I included coastal wetlands west to Galveston Bay because tropical cyclone effects can extend hundreds of kilometers from landfall (Tweel and Turner 2012a, Cahoon et al. 1995). Hurricane Ike, for instance, made landfall at the western edge of the study area, but produced significant sedimentation in the Louisiana chenier plain (Williams 2012).

Review of tropical cyclones in Louisiana

I used NOAA's HURDAT database to isolate tropical cyclones entering the study area between 1851 and 2008 (http://www.aoml.noaa.gov/hrd/hurdat/Data_Storm.html). This database contains the geographic location, wind speed, barometric pressure, and Saffir-Simpson Category for all known tropical cyclone events in the Atlantic Basin at six-hour intervals. I assumed that the event characteristics preceding landfall were most representative of those at landfall. Additional events may have resulted in sedimentation within the study area, such as tropical cyclones passing near coastal Louisiana but not making landfall, or larger hurricanes passing

near the boundaries of the study area. However, on a per-event basis, over 90% of sedimentation occurs within 150 km of landfall (Tweel and Turner 2012a).

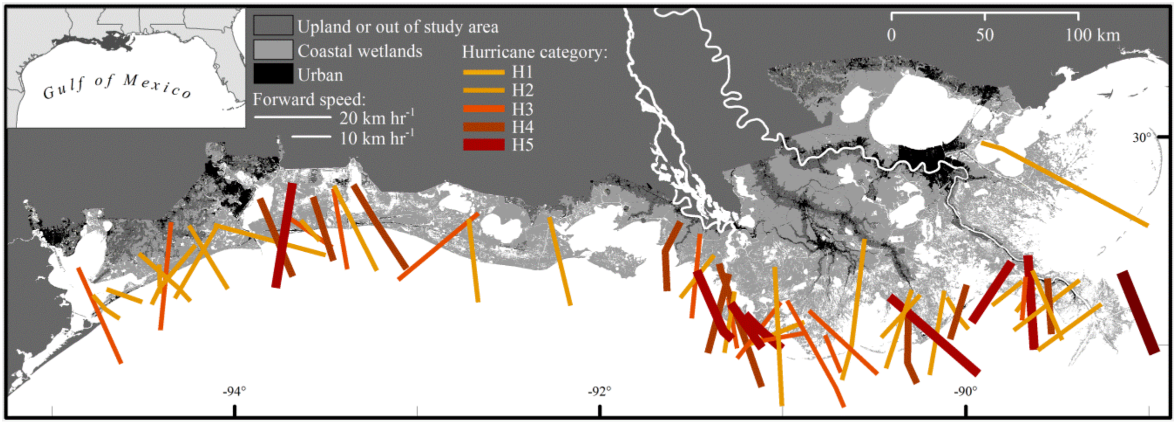

Figure 4.1. Hurricane landfalls in Louisiana and Texas west to Galveston Bay from 1851 to 2008. Bar lengths show hurricane forward speed, and line thickness corresponds to storm strength. The inset shows the general location of study area (black). Hurricane strength (H) is defined by the Saffir-Simpson hurricane intensity scale, where H5 is the strongest storm.

Model parameterization

I investigated the quantity and distribution of sedimentation following three recent sedimentation events: Hurricanes Katrina (2005), Rita (2005), and Gustav (2008). With regard to historical landfalls, the characteristics of these storms were representative of the database, with their parameters falling within range of common landfall speeds and approach angles (Figure 4.2). These hurricanes resulted in the deposition of 68, 48 and 21 × 10^6 t, respectively, of inorganic sediment on the marsh surface (Tweel and Turner 2012a). This deposition, whether on only wetlands or extrapolated to include inshore waters, was proportional to wind speed at landfall and inversely proportional to barometric pressure at landfall (Figure 4.3A). I used this relationship as the basis for modeling the total wetland sedimentation and wetland plus inshore deposition from historical events as a function of pressure (Table 4.1). When pressure data were

not available, especially before 1960, I estimated pressure based on its relationship to wind speed ($p < 0.0001$, Figure 4.4). I used a square-root transformation for the dependent variable to meet parametric assumptions, and compared estimates derived from this regression to those derived using non-transformed data.

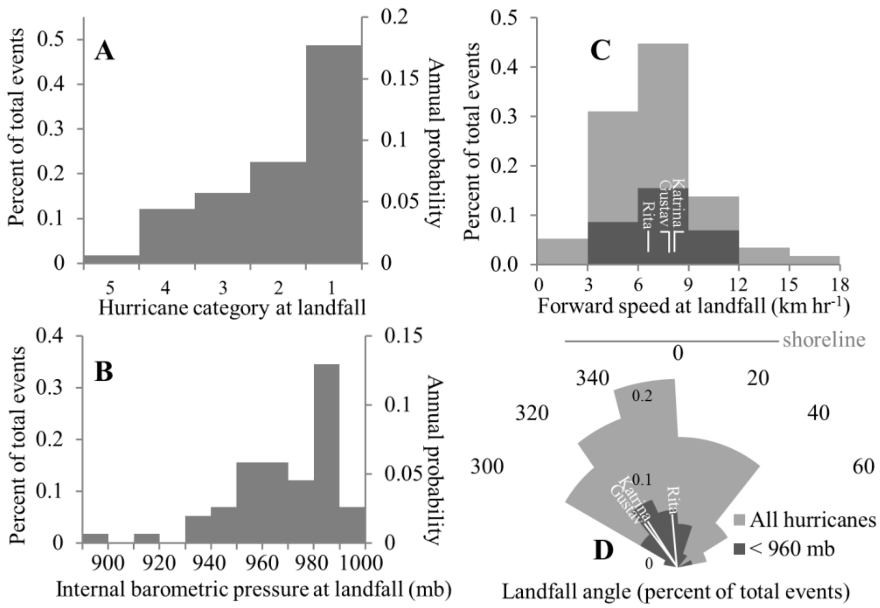

Figure 4.2 Probability distributions for hurricane landfalls in the study area, based on data from 1851 to 2008. **A.** Saffir-Simpson hurricane intensity scale, **B.** internal pressure (mb) at landfall, **C.** forward speed at landfall (km hr^{-1}) for all hurricanes (light gray) and hurricanes with landfall pressure below 960 mb, and, **D.** direction of hurricane travel at landfall relative to 2 m isobath for all hurricanes (light gray) and hurricanes with landfall pressure below 960 mb.

I previously observed that sediment deposition within each storm event decayed with distance from storm track and distance from shoreline (Tweel and Turner 2012a), and used this as a starting point to model sediment deposition within a given event. Because the wetland sedimentation estimates include variability due to differing land-to-water ratios within the depositional area, I used combined estimates for wetland and inshore subaqueous sedimentation. Estimates of wetland-only sedimentation were then obtained by multiplying the deposition rate for each pixel by the area of wetlands in that pixel.

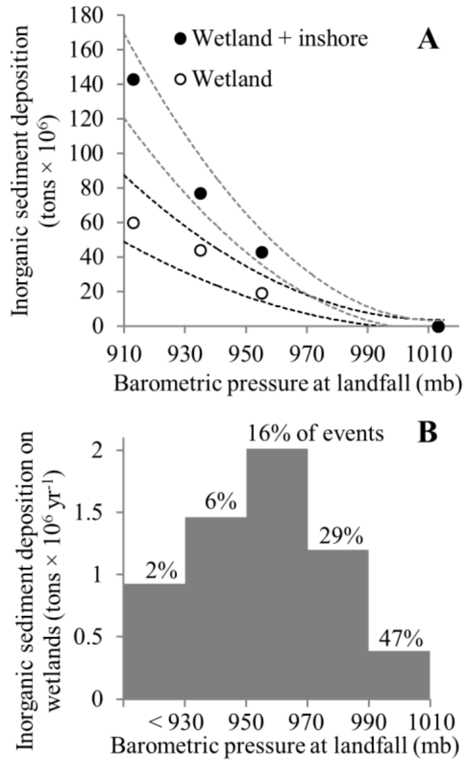

Figure 4.3 Relationship between pressure at landfall and total wetland deposition (± 95% CI, open circles) and wetland plus extrapolated inshore subaqueous deposition (solid circles), and **B.** distribution of sediment deposition by landfall barometric pressure.

I used a pixel size of 10 km^2, which balanced the precision of my sedimentation estimates with the uncertainties of the HURDAT storm tracks (McAdie et al. 2009), as well as the objective of producing a landscape-scale model. The deposition data modeled here were the inverse distance weighted interpolations reported earlier (Tweel and Turner 2012a). The total sample size was 263 pixels, with an average percent wetland of 51.3 ± 1.3 % (μ ± S.E.). Because the spatial distribution of sedimentation resulting from Hurricane Katrina was different than that of Rita and Gustav, I fit two separate spatial distribution models: the first was for events occurring west of the Mississippi River (W Model), and the second for events occurring east, or crossing north or east over the Mississippi River (E Model, Table 4.1). This distinction follows differences in previously reported storm surge heights and modeled storm surges between the east-facing Breton Sound Basin and south-facing coast west of the Mississippi River (USACE

1972, Dietrich et al. 2010). I excluded nine pixels in the Mississippi River birdfoot delta and Biloxi Marsh where no sediment sampling occurred. I also excluded one observation of anomalously high sedimentation from the same location where altered storm surge dynamics have been attributed to anthropogenic landscape modifications in the upper Breton Sound Basin (Mashriqui et al. 2006, Ebersole et al. 2010).

Table 4.1 Statistics and parameters used to estimate the total inorganic sediment deposition per event, and the spatial distribution of sedimentation within events. Distances are measured in km and pressure is measured in mb, see text for explanation of equations. Inputs of W Model distances are square-root transformed. Inputs of E Model distance from track are square-root transformed.

Model	Variable	Coefficient	F	p	Adj. R^2	n
Total deposition (tons × 10^6)						
Wetland + inshore	$= (b_0 + b_1P)^2$		718.37	0.0014	0.99	4
	intercept	b_0: 119.15696		0.0012		
	pressure (P)	b_1: -0.11775		0.0014		
Wetland only	$= (b_0 + b_1P)^2$		246.60	0.0040	0.99	4
	intercept	b_0: 80.42468		0.0036		
	pressure (P)	b_1: -0.07939		0.0040		
Spatial distribution (% of total)						
W Model	$= (b_1T^2 + b_2T + b_3C + b_4C \times T + b_5T \times P + b_0)^2$		77.27	<0.0001	0.73	143
	track (T^2)	b_1: -0.00201		<0.0001		
	track (T)	b_2: 0.14523		<0.0001		
	coast (C)	b_3: -0.04347		<0.0001		
	coast × track ($C \times T$)	b_4: 0.00301		<0.0001		
	track × pressure ($T \times P$)	b_5: -0.00014		<0.0001		
	intercept	b_0: 0.21407		<0.0001		
E Model	$= (b_1T^2 + b_2T + b_3C + b_0)^2$		109.74	<0.0001	0.75	110
	track (T^2)	b_1: 0.00001		<0.0001		
	track (T)	b_2: -0.00181		<0.0001		
	coast (C)	b_3: -0.00112		<0.0001		
	intercept	b_0: 0.16253		<0.0001		

I used a backward-selection multiple polynomial regression to fit the most appropriate models (PROC REG, SAS Institute, Cary, NC), and selected variables based on curve shapes observed earlier (Tweel and Turner 2012a). The independent variables were distances to coastline and storm track in km, and, in the case of the W Model, barometric pressure at landfall. I used percent of total, as opposed to absolute deposition in grams per square centimeter, to allow

for scaling of the output according to storm intensity. For this analysis, I defined the coastline as the landward extent of the large (20 km) coastal bays (e.g., Barataria, Terrebonne, Breton Sound). I started with third-order polynomial functions, and also tested linear interactions between the independent variables. These additional terms allowed the depositional surface to vary throughout the study area. The decay relationship away from the storm, for example, might be different than nearer the storm. Variables that were not significant regression parameters were removed, and the regressions were reanalyzed. I used partial residuals and the PRESS statistic to ensure that the dependent variable was adequately modeled and that the most appropriate models were selected. I restricted the depositional area to within 150 km from the storm track in both models, and also to the area east of the track for the W Model. The latter decision was based on observations of the distribution of mineral sediment on the marsh surface during four prior events (Tweel and Turner 2012a). My final model results are presented in grams inorganic matter per square centimeter, rather than total sedimentation per pixel, and so potential differences between sedimentation on the marsh platform and subaqueous sedimentation are not a factor.

Model application

I estimated the total inorganic wetland deposition and spatial distribution for each event between 1851 and 2008 that was categorized as Category 1 or higher on the Saffir-Simpson scale for a 10 km^2 grid of coastal Louisiana. I then combined these estimates to determine the cumulative deposition in coastal wetlands, and divided by the number of years in the study period to determine a long-term average annual rate of inorganic sediment deposition resulting from hurricane events. These results were then compared to both planar and stratigraphic

distributions of mineral sediment for coastal Louisiana wetland soils (Tweel and Turner 2012b, Turner et al. 2007).

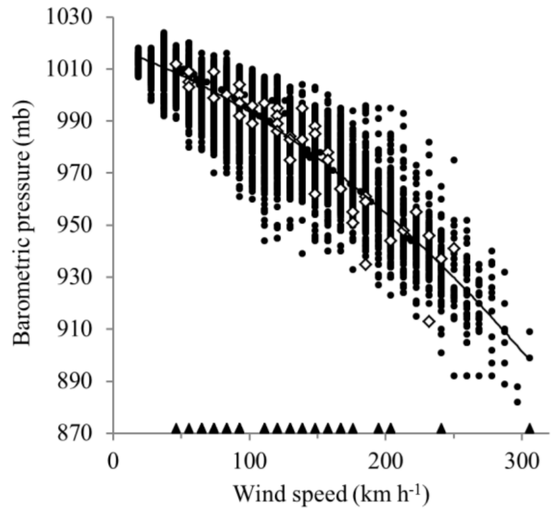

Figure 4.4 Relationship between wind speed and internal barometric pressure at landfall for Louisiana (white diamonds) and all other Atlantic observations (black dots) from 1851 to 2008. The wind speed observations where pressure was estimated are shown at bottom (black triangles).

Model limitations

This model is a landscape-scale or 'event-scale' model of sedimentation resulting from tropical cyclones in Louisiana. Sedimentation from these events may also vary on a more local scale (10^3 m) due to local bathymetry or channel morphology (Otvos 2011, Miner et al. 2009) or even smaller scales ($\leq 10^0$ m) such as vegetative cover (Rejmànek et al. 1988). The model is calibrated, therefore, for the mean wetland sedimentation in a given pixel, and may be locally higher or lower within that pixel. This result is consistent with my objective of identifying long-term patterns in sediment distribution on this coast, whereby smaller variations, although locally significant, would be of less consequence to the long-term and large-scale trends. Because the model is based on geographic characteristics of sedimentation events in Louisiana's gently-sloping coastal plain, I expect that the model parameters vary for other geographic locations. I

also assume that wind speed and internal atmospheric pressure at landfall are the dominant factors determining sedimentation, as identified by the three study events, although additional factors such as approach angle, storm size, and forward speed may also be factors (Irish et al. 2011). Future research on tropical cyclone sedimentation events should identify if and how these factors may also affect the distribution and magnitude of wetland sedimentation.

Results

Between 1851 and 2008 coastal Louisiana and the adjacent Texas coast (Galveston Bay to the Louisiana border) were traversed by 58 hurricanes ranked as Category 1 or greater on the Saffir-Simpson scale, and 55 smaller tropical cyclones (Figure 4.1, page 65). The annual probability of tropical cyclone landfall decreases with increasing storm intensities (Figure 4.2, page 66), and spatial and meteorological parameters of these events were applied to my sedimentation model ($p < 0.01$, Figure 4.5 and Table 4.1). The cumulative effect of all storms would be equivalent to an annual inorganic sediment deposition in wetlands of 5.99×10^6 t for the whole study area, with approximately 94% (5.62×10^6 t) occurring in the Louisiana portion. However, the amount of sediment for the Texas portion is probably underestimated as storm surges and waves from storms tracking south of Galveston Bay would have also brought sediment to the area.

Wetlands in the deltaic plain receive 64% of the total hurricane deposition for Louisiana, and those in the chenier plain receive 26%. I estimate that 60% of the total deposition from hurricanes and tropical storms results from events with landfall barometric pressure below 960 mb (approximately Category 3 or greater; 16% of cyclone events), with 92% resulting from events ranked as Category 1 or greater (51% of events, Figure 4.3B). Additionally, 79% of the total estimated long-term hurricane sedimentation occurs within the first 20 km inland from the

coastline (7400 km^2 wetlands) and 50% occurs in the first 10 km inland, which is similar to the observations from discrete events studied previously (Tweel and Turner 2012a).

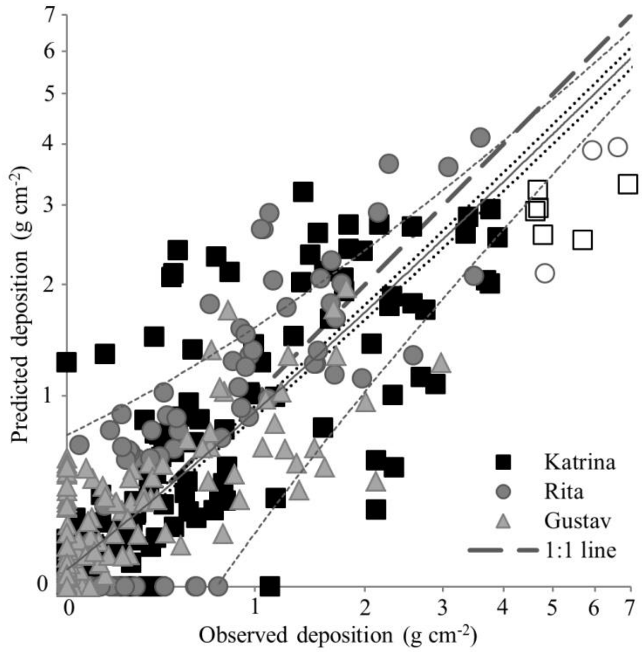

Figure 4.5 Prediction plot showing model performance for Hurricanes Katrina, Rita, and Gustav. The outer bands mark the 95% prediction interval, the inner bands mark the 95% confidence interval, and the open shapes indicate under-predicted values. The axes are scaled logarithmically to increase resolution at lower values.

The average hurricane deposition is 0.047 g cm^{-2} yr^{-1} for all Louisiana coastal wetlands, but the spatial distribution is highly variable (σ = 0.031). The greatest sedimentation appears to occur in the marshes flanking Terrebonne and Barataria Bays, where up to 0.16 g cm^{-2} yr^{-1} of inorganic sediment is deposited. By comparison, the results indicate that inorganic sediment deposition in the upper reaches of Barataria Basin from tropical cyclones is less than 0.001 g cm^{-2} yr^{-1} (Figure 4.6).

The spatial distribution of hurricane landfalls varied throughout the study area. The greatest landfall density was in the 60 km stretch of coastline between Point Chevreuil and Sister (Caillou) Lake. This area was traversed by 15 Category 1 or greater events during the study

period, while the nearby 60 km stretch from Marsh Island to Tigre Point received only 1 landfall. These differences are apparent in the spatial distribution of long-term tropical cyclone sedimentation rates (Figure 4.6).

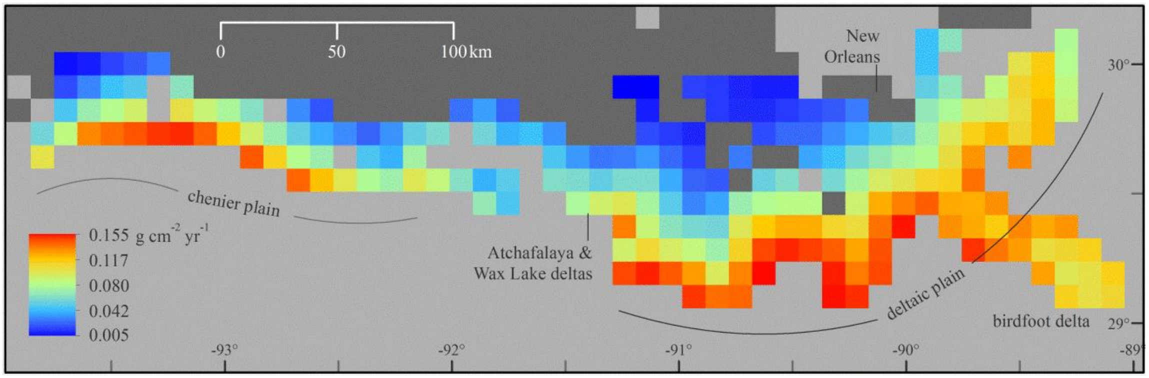

Figure 4.6 Spatial distribution of mean annual tropical cyclone sedimentation for coastal Louisiana wetlands. The data are based on estimated deposition from Category One and greater events from 1851 to 2008.

The results I present for tropical cyclone driven sedimentation on wetlands, I believe, are as accurate as existing data allow. All parameters for total deposition model are statistically significant (Table 4.1, $p < 0.01$), as are all parameters for the spatial distribution model ($p < 0.0001$). Though the full model is accurate for the broad range of observations ($R^2 = 0.72$, $F_{(1, 777)} = 1952$, $p < 0.001$), it tends to under-predict at the largest values and over-predict at the smallest values. The largest 9 observations have high leverage on the validation line, and the slope increases from 0.70 to 0.82 for the remaining 98.8% of the data ($R^2 = 0.69$, $F_{(1, 768)} = 1731$, $p < 0.001$; Figure 4.5). This prediction plot incorporates the variability introduced by estimating the total deposition as well as the spatial distribution. The deposition values below 0.01 g cm^{-2} are over-predicted, but there are few (< 10) observations this small. I estimate that the bottom 1.3% of data is over-predicted by nearly 50%, and that the top 1.2% (> 6.9 g cm^{-2}) is under-predicted by 43%. The 95% prediction interval contains 93% of the data.

Discussion

The annual deposition of sediment on the marsh surface from hurricanes is estimated to be 5.6×10^6 t of inorganic sediment for Louisiana coastal wetlands, which equates to 3.8% of the modern annual Mississippi River load (Meade and Moody 2010) and 3.2% of the estimated pre-disturbance load (Tweel and Turner 2012b). The spatial distribution, however, varies along the coast with landfall location and with distance inland as storm surge intensity, and thus sediment transport capacity, is reduced. If the deposition rate in open water during storms is equal to what it is on the wetlands, then the total deposition in wetlands and open water would be about twice what occurs on the wetlands alone. There are limited measurements of storm deposition in ponds and bays, however, and so I recommend this as a future research objective.

The magnitude and chronology of sedimentation events developed from this analysis compares well to the inorganic content of 51 deltaic plain salt marsh cores dated using ^{210}Pb and ^{137}Cs (Turner et al. 2007). While discrete event laminae are typically not recognizable in centuries-old peat, periods of high tropical cyclone activity correspond to peaks in mineral content relative to soils formed in the absence of hurricanes. The largest spike for the periods of overlap occurs around 1970 for both datasets (Figure 4.7). The period from 1964 to 1974 marks the period of greatest historical hurricane frequency for Louisiana, during which it was struck by four hurricanes ranking Category 3 or greater, as well as one Category 2 event. The core data show a smoothed peak in mineral sediment content, rather than discrete events, indicating that as sediments are consolidated, some of this sediment may be redistributed vertically. Peaks in hurricane activity and intensity also correspond to peaks in soil mineral content around 1915 (2 unnamed Category 3 events) and 1992 (Hurricane Andrew).

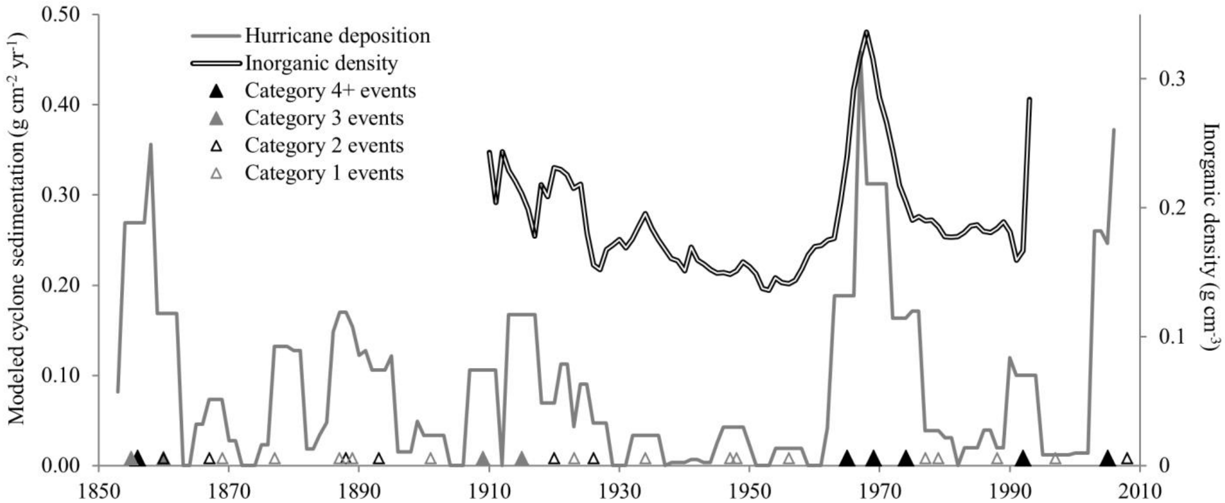

Figure 4.7 Temporal distribution of estimated tropical cyclone sedimentation for deltaic plain salt marshes, shown as five-year averages. Data are compared to the inorganic sediment content of deltaic plain salt marsh soils presented in Turner and others (2007). Deltaic plain hurricane landfalls are marked by triangles at the bottom.

Our model of long-term tropical cyclone sedimentation is consistent with the spatial distribution of wetland soil types along the Louisiana coast. Wetland soils where inorganic content in the top 24 cm comprises about 60% by mass are found in two main areas along this coast: active deltas and salt marshes. Figure 4.8 shows that there are two distinct clusters that do not fit the general trend: the Mississippi River birdfoot delta and the Atchafalaya/Wax Lake deltas, through which almost all of the Mississippi River discharge passes. The dominant inorganic sediment source for these wetland soils is from the deposition of suspended sediments directly from the river rather than the resuspension of sediments by storm-associated waves (Tweel and Turner 2012b).

The marine-dominated sediment budget for inactive delta portions of the Louisiana coast compares well with observations from other coastal wetlands. The Ganges-Brahmaputra delta in Bangladesh, for instance, exhibits similarities to the Mississippi River delta (Allison and Kepple 2001). Using grain size-normalized ^{137}Cs inventories, it was reported that between 7-13% of the annual Ganges-Brahmaputra sediment load is delivered to the Sunderbans delta plain during

cyclonic and monsoonal events, which is within range of the estimate for this study. They also report a decreasing inland trend of sediment accretion that is comparable to the trend I observe for the Louisiana deltaic plain. Similarly, accretion rates in a German salt marsh are driven primarily by periods of high storm activity and storm surge events (Schuerch et al. 2012). Consistent sediment input from historic and pre-historic storm events has also been observed in New England (Boldt et al. 2010) and mid-Atlantic salt marshes (Stumpf 1983).

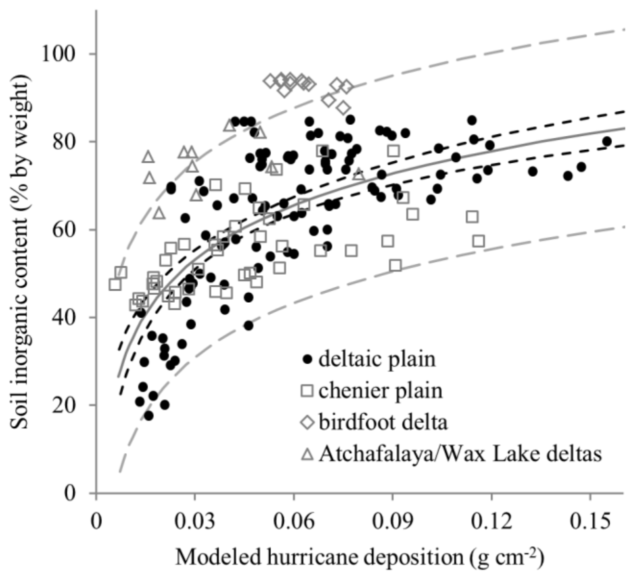

Figure 4.8 Comparison of modeled hurricane deposition and soil type for Louisiana coastal marshes. The curve is logarithmically fit to data for deltaic plain and chenier plain marshes. Soil data from the Atchafalaya/Wax Lake deltas and birdfoot delta are clustered above most points from the coastal plains. The outer bands mark the 95% prediction interval and the inner bands mark the 95% confidence interval.

The differing storm strengths in this analysis provide an opportunity to investigate their relationship to sediment deposition. However, the three hurricanes studied made landfalls in different locations, with different approach angles and forward speeds. In this regard, the high correlation (R^2 = 0.99) between sediment deposition and barometric pressure should be expected to co-vary with additional storm characteristics. Reliable evidence (Irish et al. 2011) nonetheless suggests that the characteristics of storm intensity have a greater influence than forward speed or

approach angle. Therefore, I have no reason to reject this model based on currently available data. More data are needed to improve these estimates and better understand the relationship between storm characteristics and the spatial distribution of sediment deposition.

Tropical cyclone storm surge sedimentation events are likely the dominant source of inorganic sediment for the 90% of the Louisiana coast that comprises abandoned delta lobes and the chenier plain. I estimate that, by comparison to sedimentation rates from coast-wide soil core studies (Piazza et al. 2011), 65% of the inorganic sediment in soils of the deltaic plain, and 80% for the chenier plain, could directly result from hurricanes making landfall in the study area. This is a conservative estimate, because additional sedimentation may result from tropical storms and from hurricanes passing near the study area but not making landfall. This reworking of deltaic sediment follows the widely used delta cycle model for overwash processes that regulate barrier island development (Penland et al. 1988, Coleman et al. 1998), albeit at a larger scale - hundreds of kilometers from source to sink. In the absence of anthropogenic landscape modification, marine-dominated coastal wetlands can persist for thousands of years, with vertical accretion driven largely by organic accretionary processes (Turner et al. 2002, McKee et al. 2007), but supplemented by tropical cyclones and more local sedimentation events. The Biloxi Marsh, in the abandoned St. Bernard Delta of the Mississippi River (4000-2000 BP), is an example of this, as wetlands in this area persist with one of the lowest land loss rates along the Louisiana coast (Couvillion et al. 2011). Future changes in storm frequency or intensity, coupled with both isostatic and eustatic sea level rise, would result in changes to the distribution and magnitude of these sedimentation events.

References

Allison, M. and E. Kepple. 2001. Modern Sediment Supply to the Lower Delta Plain of the Ganges-Brahmaputra River in Bangladesh. Geo-Marine Letters 21:66-74.

Barbier, E. B., E. W. Koch, B. R. Silliman, S. D. Hacker, E. Wolanski, J. Primavera, E. F. Granek, S. Polasky, S. Aswani, and L. A. Cramer. 2008. Coastal Ecosystem-Based Management with Nonlinear Ecological Functions and Values. Science 319:321-323.

Boldt, K. V., P. Lane, J. D. Woodruff, and J. P. Donnelly. 2010. Calibrating a Sedimentary Record of Overwash from Southeastern New England Using Modeled Historic Hurricane Surges. Marine Geology 275:127-139.

Cahoon, D. R., D. J. Reed, J. W. Day Jr, G. D. Steyer, R. M. Boumans, J. C. Lynch, D. McNally, and N. Latif. 1995. The Influence of Hurricane Andrew on Sediment Distribution in Louisiana Coastal Marshes. Journal of Coastal Research SI 21:280-294.

Coleman, J. M., H. H. Roberts, and G. W. Stone. 1998. Mississippi River Delta: An Overview. Journal of Coastal Research 14:699-716.

Costanza, R., O. Perez-Maqueo, M. L. Martinez, P. Sutton, S. J. Anderson, and K. Mulder. 2008. The Value of Coastal Wetlands for Hurricane Protection. Ambio 37:241-248.

Couvillion, B. R., J. A. Barras, G. D. Steyer, W. Sleavin, M. Fischer, H. Beck, N. Trahan, B. Griffin, and D. Heckman. 2011. Land Area Change in Coastal Louisiana (1932 to 2010). US Geological Survey, National Wetlands Research Center. 12 p.

Dietrich, J., S. Bunya, J. Westerink, B. Ebersole, J. Smith, J. Atkinson, R. Jensen, D. Resio, R. Luettich, and C. Dawson. 2010. A High-Resolution Coupled Riverine Flow, Tide, Wind, Wind Wave, and Storm Surge Model for Southern Louisiana and Mississippi. Part Ii: Synoptic Description and Analysis of Hurricanes Katrina and Rita. Monthly Weather Review 138:378-404.

Ebersole, B., J. Westerink, S. Bunya, J. Dietrich, and M. Cialone. 2010. Development of Storm Surge Which Led to Flooding in St. Bernard Polder During Hurricane Katrina. Ocean Engineering 37:91-103.

USACE 1972. History of Hurricane Occurrences Along Coastal Louisiana. US Army Corps of Engineers. New Orleans. 66 p.

Gedan, K. B., M. L. Kirwan, E. Wolanski, E. B. Barbier, and B. R. Silliman. 2011. The Present and Future Role of Coastal Wetland Vegetation in Protecting Shorelines: Answering Recent Challenges to the Paradigm. Climatic Change 106:7-29.

Irish, J. L., D. T. Resio, and D. Divoky. 2011. Statistical Properties of Hurricane Surge Along a Coast. Journal of Geophysical Research 116:C10007.

Mashriqui, H. S., G. P. Kemp, I. van Heerden, Y. Xu, and V. Singh. 2006. Experimental Storm Surge Simulations for Hurricane Katrina. Y. J. Xu and V. P. Singh, eds. Coastal Environment and Water Quality. Highlands Publications. p. 481-490.

McAdie, C. J., C. W. Landsea, C. J. Neuman, J. E. David, E. Blake, and G. R. Hamner. 2009. Tropical Cyclones of the North Atlantic Ocean, 1851-2006. National Hurricane Center, Miami, Florida. 243 p.

McKee, K. L., D. R. Cahoon, and I. C. Feller. 2007. Caribbean Mangroves Adjust to Rising Sea Level through Biotic Controls on Change in Soil Elevation. Global Ecology and Biogeography 16:545-556.

McKee, K. L. and J. A. Cherry. 2009. Hurricane Katrina Sediment Slowed Elevation Loss in Subsiding Brackish Marshes of the Mississippi River Delta. Wetlands 29:2-15.

Meade, R. H. and J. A. Moody. 2010. Causes for the Decline of Suspended-Sediment Discharge in the Mississippi River System, 1940–2007. Hydrological Processes 24:35-49.

Miner, M. D., M. A. Kulp, D. M. FitzGerald, J. G. Flocks, and H. D. Weathers. 2009. Delta Lobe Degradation and Hurricane Impacts Governing Large-Scale Coastal Behavior, South-Central Louisiana, USA. Geo-Marine Letters 29:441-453.

Nanayama, F., R. Furukawa, K. Shigeno, A. Makino, Y. Soeda, and Y. Igarashi. 2007. Nine Unusually Large Tsunami Deposits from the Past 4000 Years at Kiritappu Marsh Along the Southern Kuril Trench. Sedimentary Geology 200:275-294.

Otvos, E. G. 2011. Hurricane Signatures and Landforms—toward Improved Interpretations and Global Storm Climate Chronology. Sedimentary Geology 239:10-22.

Penland, S., R. Boyd, and J. R. Suter. 1988. Transgressive Depositional Systems of the Mississippi Delta Plain: A Model for Barrier Shoreline and Shelf Sand Development. Journal of Sedimentary Research 58:932-949.

Piazza, S. C., G. D. Steyer, K. F. Cretini, C. E. Sasser, J. M. Visser, G. O. Holm, L. A. Sharp, D. E. Evers, and J. R. Meriwether. 2011. Geomorphic and Ecological Effects of Hurricanes Katrina and Rita on Coastal Louisiana Marsh Communities. U. S. Geological Survey. 139 p.

Rejmanek, M., C. E. Sasser, and G. W. Peterson. 1988. Hurricane-Induced Sediment Deposition in a Gulf Coast Marsh. Estuarine, Coastal and Shelf Science 27:217-222.

Schuerch, M., J. Rapaglia, V. Liebetrau, A. Vafeidis, and K. Reise. 2012. Salt Marsh Accretion and Storm Tide Variation: An Example from a Barrier Island in the North Sea. Estuaries and Coasts 35:486-500.

Shepard, C. C., C. M. Crain, and M. W. Beck. 2011. The Protective Role of Coastal Marshes: A Systematic Review and Meta-Analysis. PloS ONE 6:e27374.

Stone, G. W., J. M. Grymes III, J. R. Dingler, and D. A. Pepper. 1997. Overview and Significance of Hurricanes on the Louisiana Coast, USA. Journal of Coastal Research 13:656-669.

Stumpf, R. P. 1983. The Process of Sedimentation on the Surface of a Salt Marsh. Estuarine, Coastal and Shelf Science 17:495-508.

Turner, R., E. Swenson, and C. Milan. 2002. Organic and Inorganic Contributions to Vertical Accretion in Salt Marsh Sediments. M. P. Weinstein and D. A. Kreeger, eds. Concepts and Controversies in Tidal Marsh Ecology. Kluwer Publishers. p. 583-595.

Turner, R. E., J. J. Baustian, E. M. Swenson, and J. S. Spicer. 2006. Wetland Sedimentation from Hurricanes Katrina and Rita. Science 314:449-452.

Turner, R. E., E. M. Swenson, C. S. Milan, and J. M. Lee. 2007. Hurricane Signals in Salt Marsh Sediments: Inorganic Sources and Soil Volume. Limnology and Oceanography 52:1231-1238.

Tweel, A. W. and R. E. Turner. 2012a. Landscape-Scale Analysis of Wetland Sediment Deposition from Four Tropical Cyclone Events. PloS ONE 7:e50528.

Tweel, A. W. and R. E. Turner. 2012b. Watershed Land Use and River Engineering Drive Wetland Formation and Loss in the Mississippi River Birdfoot Delta. Limnology and Oceanography 57:18-28.

Williams, H. F. L. 2012. Magnitude of Hurricane Ike Storm Surge Sedimentation: Implications for Coastal Marsh Aggradation. Earth Surface Processes and Landforms 37:901-906.

CHAPTER 5
CAUSES OF WETLAND LOSS IN COASTAL LOUISIANA: A NEW ANALYTICAL APPROACH TO UNDERSTAND AN OLD PROBLEM

Introduction

Wetland gain and loss in Louisiana's deltaic plain has been an ongoing process throughout its 7,000 y history of net gain (Walker et al. 1987). The coastal landscape sitting atop of the mostly mineral accumulations include cypress-tupelo swamps, fresh, brackish and salt marshes pocked with ponds, ridges, and tidal creeks. It is this biogenic layer that has been reduced by 22% in the last 80 years (Couvillion et al. 2010). Despite decades of research, there are still many uncertainties about why wetland loss rates increased in the 1930s (Gagliano et al. 1981), accelerated quickly (Dunbar et al. 1992), and now decline (Couvillon 2010), especially on a coast-wide scale.

Much of this uncertainty likely arises from the natural complexity of Louisiana's coastal systems and its history of human interventions. On a geologic time-scale, the coastal landscape is shaped by the shifting Mississippi River, and remnant former deltas provide the platform for wetland peats to flourish (Kolb and Van Lopik 1966, Kosters 1989). On shorter time scales, coastal wetlands are exposed to storm surge and riverine flooding events, subsurface faulting, drought, eustatic sea level rise and deltaic subsidence (isostatic).

Humans began to modify the coastal landscape as early as the 18th century, beginning with small levees and trappers' canals, and then expanding to large-scale river engineering, marsh water level management, polders, cypress harvest, and an extensive network of canals used in oil and gas production (Davis 1973). There were, as of 2007, over 21,000 oil and gas wells in wetlands in the Louisiana coastal zone and an additional 32,000 in coastal zone waters (SONRIS 2010). The coastal area is also subject to varying nutrient and sediment inputs from

intensive land use in the Mississippi River watershed (Turner and Rabalais 1994, Raymond et al. 2008) and locally. Large-scale “eat-outs” by waterfowl and invasive rodents may also lead to plant stress and eventual wetland loss in some areas (O’Neil 1949).

The mechanisms of wetland loss are varied, but can be grouped into three main categories: edge erosion, submergence, and direct human loss (Craig et al. 1979). However, these are not necessarily isolated processes- one type of loss may make surrounding wetlands more vulnerable to additional losses. For instance, direct loss via canal construction is spatially related to the indirect loss of wetlands (Turner 1997), and is attributed to subsequent changes in hydrology via increased frequency of flooding and drying events (Swenson and Turner 1987) that can cause plant stress (Mendelssohn and McKee 1988). Berms and spoil banks that impound wetlands can also trap or block storm surge and retain salinity or high water levels for months (Barras 2007). These barriers can also lead to reduced sediment deposition as storm surge is blocked or diminished (Day et al. 2012). The wetland loss that initially begins by submergence can reach an alternative equilibrium as open water (Simenstad et al. 2000) that can cause further loss via edge erosion (Fearnley et al. 2009, Nyman et al. 1994). Fluid withdrawal may lead to increased subsidence (Morton et al. 2005), and storm surges may be more damaging near the coast before wave attenuation increases as they travel inland.

Large-scale multivariate analyses can help identify which factors drive wetland loss in various areas, and provide a framework for further research of specific processes or areas. Several studies have used different spatial scales and input variables. Deegan et al. (1984), for example, used stepwise regression to model the effects of various factors on land loss in 139 7.5’ quadrangles (approximately 12.5 km per side). They found that 25 to 39% of wetland loss was related to canal construction, and that 10 to 13% was correlated to urban and agricultural

development. Cowan and Turner (1988) used multiple regression and cluster analyses to investigate patterns of land loss at the 7.5' scale. The results of their cluster analysis revealed three main groups of land loss patterns: (1) moderate wetland loss resulting from high canal dredging that is buffered by moderate subsurface sediment thickness near the Mississippi River and Biloxi Marsh, (2) high wetland loss due to moderate canal dredging that is exacerbated by thicker deltaic sediments in Barataria and Terrebonne basins, and (3) low wetland loss due to thin underlying sediments in the chenier plain. Turner (1997) used regression analysis of data from 15' quadrangles (approximately 25 km per side) to test different hypotheses about coastal Louisiana wetland loss, and reported that there was a direct correlation between canal dredging and indirect land loss. His analysis also suggested that canals closer to the Gulf of Mexico could cause more indirect loss than canals in the upper (northern) estuary. Day et al. (2000) tested the effects of canals at a smaller scale of 4100 ha (6.4 km), and observed a weaker relationship than Turner (1997). Their study area, however, was not coast-wide, and the sampling scale may have been too small to incorporate both direct and indirect losses in the same pixel (Turner 2001). Too small of a pixel size could return a false negative if cause and effect are classified in different pixels (type II error), yet too large of a pixel size will reduce sample size and decrease statistical power (Figure 5.1). The variability in results from these previous analyses demonstrates that the choice of sampling scale and experimental design can have direct consequences for data reliability and interpretation.

An underlying assumption of regression analysis is that the variables have stationarity, i.e., that they have an equal influence on the dependent variable across space and time. A scientific assessment of Louisiana's coastal system suggests that this is unlikely. A more accurate model should allow for the possibility that patterns of land loss exhibit spatial non-

stationarity, i.e., that wetlands may be more sensitive to a forcing factor in one area than another (Figure 5.2). For instance, different marsh soil types may respond differently to changes in hydrology, older delta deposits may be more vulnerable to certain stressors than younger deposits, and thicker Holocene deposits may consolidate at lower rates than younger deposits.

Figure 5.1 Example of how pixel size could bias data analysis. Pixels that are too small risk the classification of independent and dependent variables into different pixels. Pixels that are too large sacrifice sample size and statistical power.

New geographic analysis methods that address spatially varying relationships could yield a more powerful analysis. I applied a geographically weighted regression (GWR) analysis to investigate non-stationarity in patterns of land loss in coastal Louisiana wetlands. I also investigated the effect of sampling scale on the model results. To study these patterns, I distinguished interior wetland loss from total wetland loss, because interior loss involves the submergence of marsh platform, whereas edge land loss is related to wave processes. Interior land loss accounts for the majority of land loss in Barataria Basin. High rates of wetland edge

loss could also be exacerbated by human actions, but should be analyzed separately. I investigated the relationship between various potential drivers, both natural and anthropogenic, of interior wetland loss in coastal Louisiana by means of a multivariate analysis. I use Barataria Basin as a study area, because it contains a wide variety of coastal habitats, and is also comprised of areas that have experienced both low and high land loss.

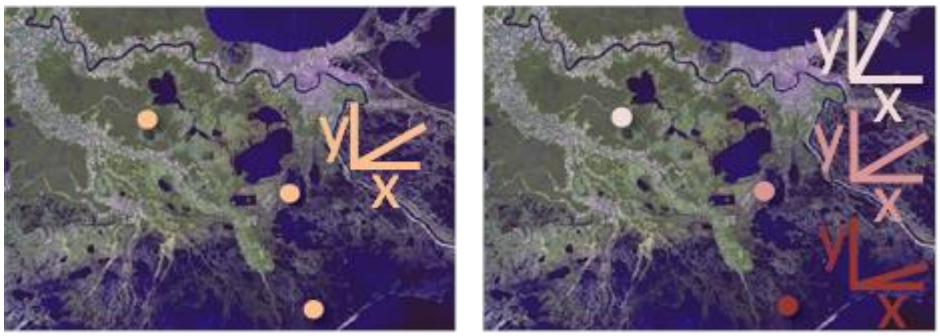

Figure 5.2 Example of data stationarity (left) and non-stationarity (right). Traditional regression analysis assumes that the relationships between variables are constant across the study area. Geographically weighted regression analysis allows variable relationships to differ spatially.

Methods

Development of spatial data layers

1. Land loss

This dataset was developed from Britsch and Dunbar (2006). This dataset that contains land loss data at six years: 1932, 1958, 1974, 1983, 1990, and 2001 (Figure 5.3). Coastal swamps were omitted from this analysis because decreases in habitat quality occur over a different timescale via reduced tree recruitment, rather than the comparatively faster marsh loss. The original digital files were converted to a grayscale tagged image format (TIF) in Adobe Photoshop at 500 DPI, which preserved all original data by being converted at a finer scale than the original maps that were digitized at a scale of 1:62,500. The seven coast-wide maps were georeferenced based on the coordinates of their corners (quadrangle intersections). The data

were geo-referenced to North American Datum 1927, Universal Transverse Mercator (UTM) zone 15N to maintain consistency with the original data, and to provide a more accurate projection. The far eastern edge of the data lies in UTM zone 16N, and was georeferenced to a corresponding grid that was re-projected to zone 15N. The measured difference in area between the original zone and the projected zone was 0.1% in a sample area that was tested. Georeferencing accuracy was increased by georeferencing to additional imagery. The total root mean square error was between 4 and 66 meters. The difference in land area between the original published data and final dataset was less than 5% of the total area, which is at least partly due to the use of more accurately projected data rather than the original geographic coordinate data.

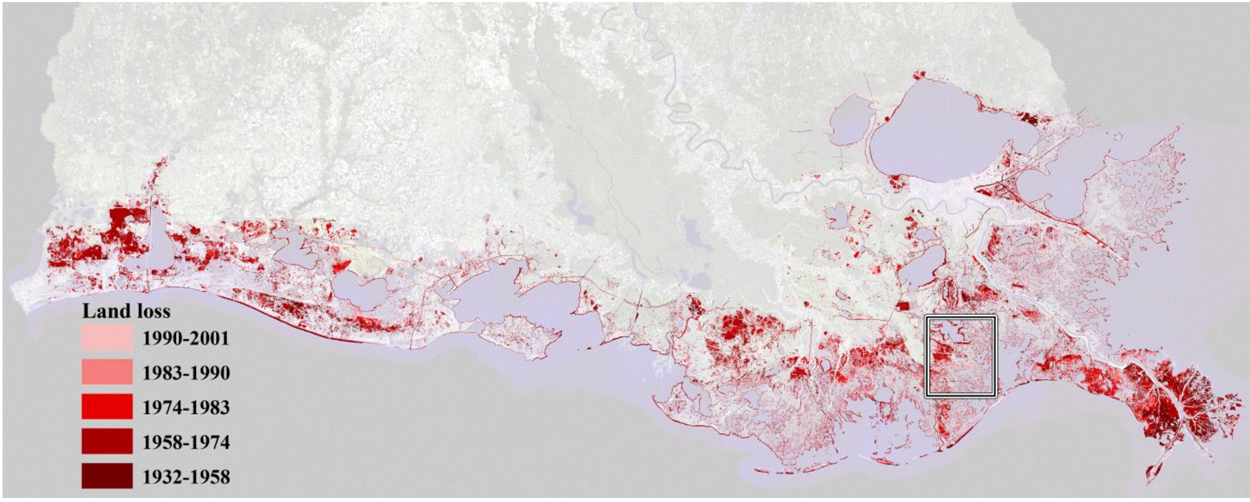

Figure 5.3 Land loss in coastal Louisiana from 1932 to 2001, based on land loss data from Britch and Dunbar (2005).

Once georeferenced, the seven layers were combined to a single coast-wide raster data set. The raster data were passed through a series of reclassifications to isolate each desired time interval based on its pixel value. The result was six separate layers that depicted the amount of land at each interval. Once isolated, the land loss data were combined into a new raster at a 10 × 10 m pixel size, which is finer than the original resolution. These rasters were vectorized in

ArcScan (ArcEditor 9.3; ESRI, Redlands, CA), without smoothing, which ensured topology between year layers.

The next step was to isolate land loss. This was accomplished by taking the union of the first two years, and selecting polygons with a value of -1, which corresponded to areas of land loss. This new set of polygons was copied to a new shapefile. Because the rasters were vectorized as a single color, the data could be stored as a single polygon. The Multipart to Singlepart tool was used to convert islands to their own polygons.

Once each time interval had been digitized, the next process was to categorize land loss into five different types: edge loss, interior loss, canal loss, canal edge loss, and agricultural loss. The principal interest of this study was interior loss and canal loss. All six time intervals were pooled into a single file that represented land changes between 1932 and 2001. Canal loss was categorized manually, based on the unnatural shape of dredged canals, comparison to earlier canal maps (Lee and Turner 1990), and LandSat 2005 imagery (ATLAS). Canals were categorized for each time interval to preserve canal data if surrounding land was completely lost in a later period. Agricultural land loss typically exists as large blocks of land loss, and was digitized based on previous reports (Okey 1918).

Interior loss was defined as loss that was not adjacent to a body of water existing in 1932, and was isolated using the Select by Location tool and then the Find/Replace tool to change these values to the ‘edge’ category. The remaining polygons were, therefore, assigned to the ‘interior loss’ category. For subsequent years, the water layer was merged with the ‘edge loss’ removed in the previous year, and the process was repeated. Land loss that occurred adjacent to interior loss in a previous interval was categorized as interior loss because the process that initiated the land loss in that area was submergence, even though edge erosion may account for subsequent

losses. An example of canal, edge, and interior land loss are in figure 5.4; canal and interior loss for the whole study area are also presented (Figure 5.5A and C).

A

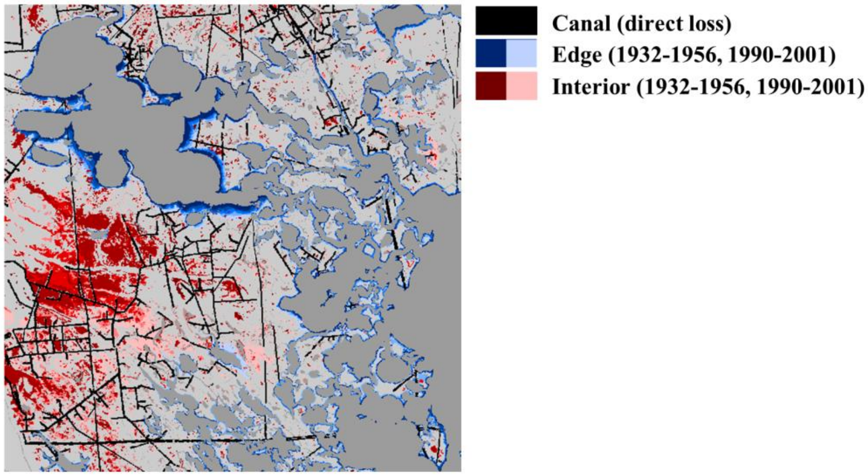

B

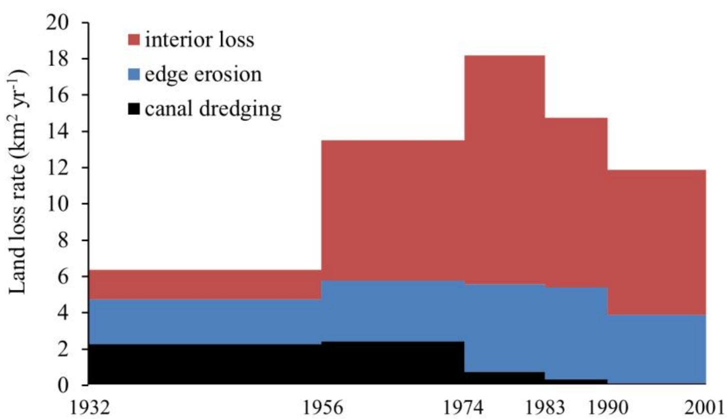

Figure 5.4 A. Example of land loss categorization into interior, edge, and direct canal loss. Darker colors for edge and interior indicate earlier loss. This area is delineated by the striped box shown in Figure 5.1. **B.** Land loss rates by time interval for the Barataria Basin.

The interior loss polygon values were reclassified so that each 10 × 10 m pixel represented 100 m^2. The Aggregate tool was then used to generalize the data to various scales based on the sum of the pixels included, yielding a raster with cell values representing the amount of land loss (in m^2) occurring between 1932 and 2001. Land loss was also calculated as

a percent loss of the original land, by dividing the m^2 loss by the total m^2 present in 1932. All raster pixels overlapped exactly using the Extent option to specify the study area.

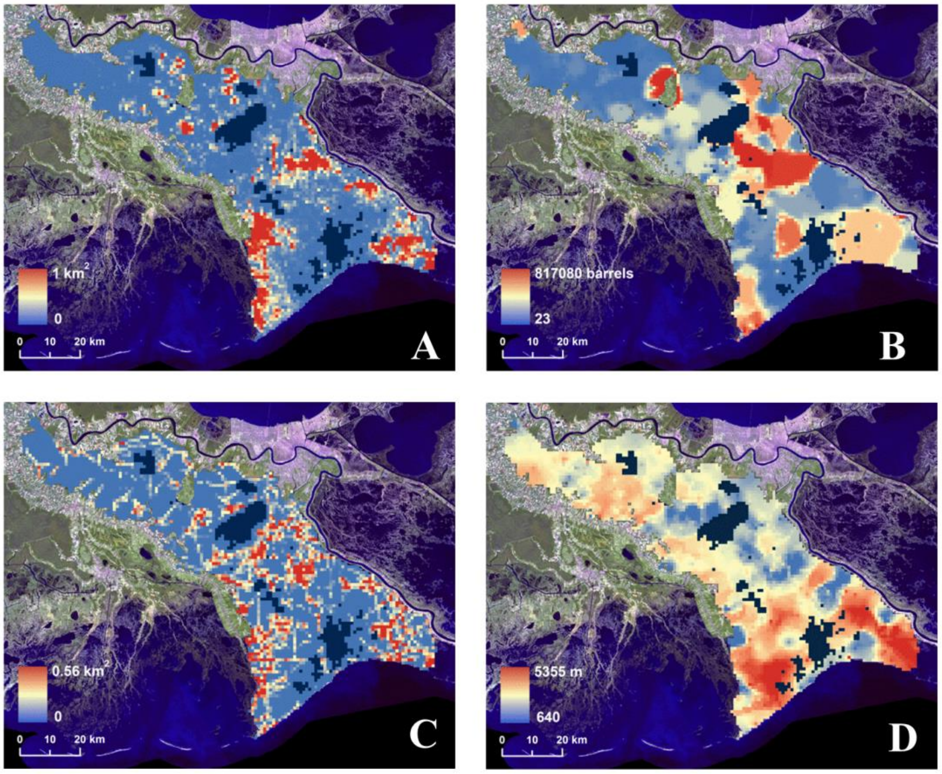

Figure 5.5 Land loss and anthropogenic variables included in analysis, shown at the 1 km^2 pixel size. **A**. Interior wetland loss, from 1932 to 2001. **B**. Petroleum production to 1977, in barrels per pixel. **C.** Direct wetland loss due to canal dredging, primarily for access to oil well heads. **D.** Depth of oil wells, averaged by area for multiple depths

2. Thickness of deltaic deposits

This layer represents the thickness (m) of deltaic deposits on top of the Pleistocene terrace. Polyline contours were digitized based on a published map (Blum et al. 2008). These depths were interpolated to estimate the area between the lines using an Inverse Distance Weighted technique at the desired pixel size within the same extent, creating pixels that were identical to those in other layers.

3. Lobe age

Former Mississippi River deltaic lobes were digitized from Roberts (1997) using the more recent dates from Blum and Roberts (2009). These were converted using Feature to Raster at the desired scale and extent.

4. Soil characteristics

Soil organic matter content (% by dry weight) and bulk density (g cm^{-3}) were obtained from the Louisiana Coastwide Reference Monitoring System at 363 sites (LDNR 2012). Data at 4 cm increments from 0 to 24 centimeters were averaged into one value. Inverse distance weighted interpolation was used to estimate values for areas between sample points (Tweel and Turner 2012).

5. Distance to coast

The Gulf of Mexico shoreline for the Barataria Basin was traced for the 1932 dataset. The Straight Line Distance tool was used to create pixel values that equaled the mean distance to shoreline.

6. Distance to distributary

Former Mississippi River distributaries were digitized based on US Army Corps of Engineers maps (USACE 1958) of deltaic plain geology and 2005 LandSat imagery (ATLAS 2010). Distributaries are clearly visible as raised areas, often with dead oak trees and flanking large, branching bayous. The Straight Line Distance tool was used to create a raster with values that equaled the mean distance to distributary.

7. Oil production

The cumulative oil field extraction was estimated using Louisiana Office of Conservation records for oil field production from its inception to 1977. This time period was acceptable for my analysis because it includes the period of the greatest oil production in Louisiana, and also the period of greatest wetland loss. Total petroleum production was taken as the sum of Crude Accumulation and Oil Production data fields- a record maintained by the Louisiana Office of Conservation. This data set does not take produced waters into consideration, because these data were not reported to the Office of Conservation for this time period (SONRIS 2010). Produced waters tend to be proportional to production of other fluids (Morton et al. 2005).

Oil fields were then mapped by generalizing oil well data (SONRIS 2010) using Dissolve by Field. The product was a multipoint layer, with points clustered by oil field. The oil well data were categorized in a Pivot Table (Microsoft Excel, Redmond, WA) to identify the number of wells per oil field as a new data column. These data were joined to the production data. I used Field Calculator to divide cumulative production by the number of wells per field, to give an average per-well production. These per-well point averages were then interpolated into pixels to yield a final layer of barrels of production per pixel. Although production obviously varies between wells, it was assumed that subsidence from fluid withdrawal within an oil field would be distributed throughout that field.

Because depth could potentially confound production data, I also investigated patterns of well depth across the study area and how they relate to oil production and land loss spatial patterns. For instance, the greatest surface expression (land loss) from fluid withdrawal would be expected in a shallow field with high production, and the least surface expression would be expected to result from a deep field with low production.

8. Distance to basin edge

Distance to basin edge, which also determined the upland boundary of the study area for Barataria basin, was digitized using 2005 LandSat imagery. These distances were coincident with levees that delineated developed areas, including agricultural as well as urban areas. This layer was also used as the extent for raster development of the other layers.

Compilation of spatial data

I combined the data for analysis. A Fishnet was created at each desired scale to equal that of the other rasters, so that each point was located at the center of the raster pixels. Land area for Barataria in 1932 was reclassified to include all data other than zero, and vectorized using the Raster to Features tool. The fishnets were clipped to this polygon layer to eliminate water pixels. Zonal Statistics from underlying rasters were extracted and exported to a separate spreadsheet. All spreadsheets were compiled using the common integer field "ID." These were then joined back to the original fishnet for analysis, so that each pixel contained values for the all of the study variables. Cells were converted to coarser scales using Aggregate to generalize the 1 km grid. The mean aggregate feature was used for all layers except those containing m^2 (land losses) and oil production where the sum yielded the desired units. Figures 5.5, 5.6, and 5.7 visualize input data at 1 km scale for anthropogenic, geologic, and spatial parameters, respectively.

Spatial analysis

The data were compiled at grid sizes of 1 km (n = 3376), 5 km (n = 142), 10 km (n = 34), and 20 km (n = 10). The data were first analyzed using the traditional regression method of Ordinary Least Squares (OLS) regression. There were too few samples at the 20 km scale to include all variables, and so only the top 4 variables from the nearest scale were tested. Ordinary

least squares regression was also used as a qualifying tool to look for overall trends in the dataset and to identify any co-varying parameters or parameters that should be excluded from the Geographically Weighted Regression (Rosenhein et al. 2011). Because one purpose of this study is to allow for the possibility of spatial non-stationarity, which could skew OLS models, I tested smaller areas within the study area to ensure that the models were properly specified.

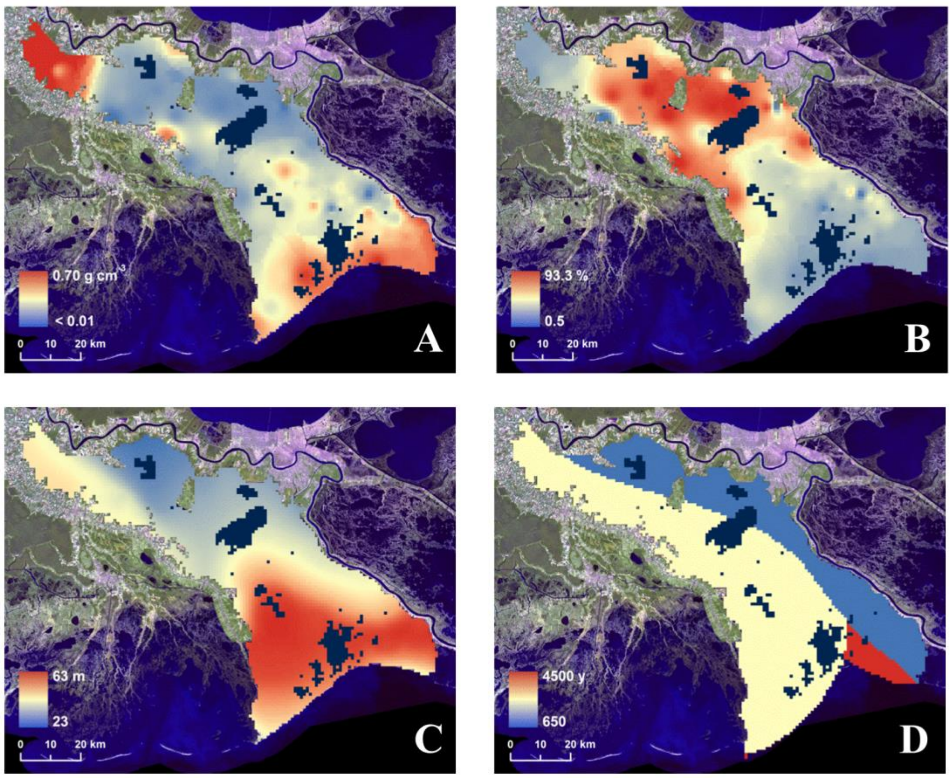

Figure 5.6 Geological and physical parameters included in analysis, shown at the 1 km^2 pixel size. **A**. Soil bulk density (g cm^{-3}) in top 24 cm, based on Coastwide Reference Monitoring System sites. **B**. Soil organic matter content (% of dry weight) from the same dataset. **C.** Thickness of Holocene delta deposits (m), from (Blum et al. 2008). **D**. Approximate age of most recent delta deposits (Blum and Roberts 2009).

Model assumptions were tested using statistics included in the analysis package. Moran's I values were calculated using standardized residuals from each model. Significant Moran's I values indicate model bias by identifying spatially clustered (non-random) model residuals. Similarly, the Koenker BP statistic was used to ensure that the standard errors were not biased, and the Jarque-Bera statistic tested if the assumption of normally distributed residuals

was met. Significant *p* values ($p < 0.05$) for these tests would indicate that model assumptions are not met. Failure to meet assumptions, however, does not preclude analysis of these data in a GWR analysis, as long as separate OLS investigations of subsections of the data meet the assumptions (Rosenhein et al. 2011). Additionally, non-stationarity may restrict model assumptions from being met. Geographically weighted regression yields the most meaningful results as a univariate analysis, so I used OLS to identify the most dominant variables and then examined how they vary spatially using GWR as a supplement to the traditional method.

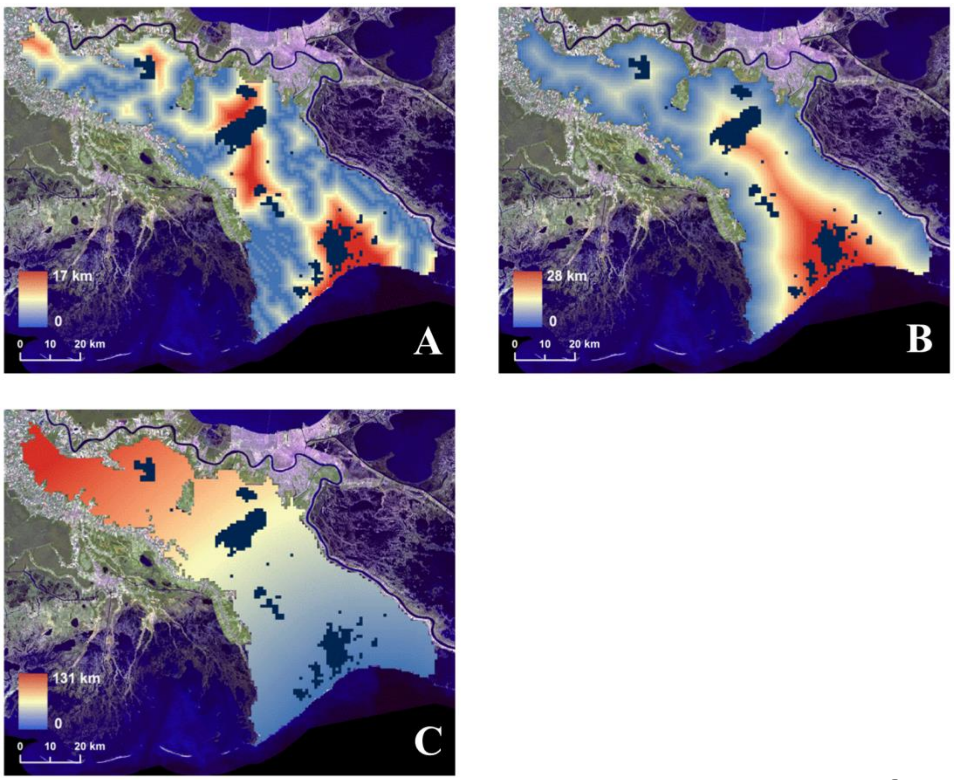

Figure 5.7 Distance-related variables used in analysis, shown at the 1 km^2 pixel size. **A**. Distance to former Mississippi River distributary. **B**. Distance to estuary upland edge. **C.** Distance to Gulf of Mexico.

Geographically Weighted Regression was used to see how the influence of the different parameters changed across space (ArcInfo 10.0, ESRI, Redlands, CA). The GWR provides local regression coefficients at each pixel in the study area. I used this to assess the strength and type of relationships between significant variables following OLS analysis. The local regression

slopes were then plotted against other variables to look for spatial thresholds in these relationships.

Results

Ordinary least squares (OLS)

The OLR analyses produced highly significant ($p<0.0001$) models at the 1, 5, and 10 km scales (Table 5.1, page 98). Marginally significant results ($p = 0.05$) at the 20 km scale may indicate insufficient degrees of freedom to produce a good model, because it was the best predictive model of the four scales tested (Figure 5.8). The smaller 1 and 5 km models, however, failed the three tests necessary to meet model assumptions. Therefore, the OLS model using 10 km pixels was the strongest overall OLS model. Canal density was a dominant variable at all scales tested, but soil bulk density was also significant at 1, 5, and 20 km scales (Table 5.1). The distance to the basin edge was significant at the 1 and 5 km scales, but not at the 10 km scale. Model prediction accuracy and r^2 values increased with increasing pixel size, demonstrating that extreme values are tempered by averaging datasets into larger pixels (Figure 5.8). In a reduced 10 km model, bulk density became significant as the model was adjusted to reduce co-variability. The 5 km model was closer to meeting model assumptions when the estuary was divided into southern (salt to intermediate marshes) and northern (freshwater marsh) portions and examined separately, but the southern section still indicated bias in the standard errors, and the northern section residuals were not normally distributed. Additionally, logarithmic and arcsine transformations of the 5 km data were not successful in resolving these model deficiencies.

As expected for variables sampled along a fresh- to saltwater estuarine gradient, there was co-variability among several parameters (Figure 5.9, page 99). Soil bulk density and

organic content were inversely correlated (r^2 = 0.76). Soil organic content increased, and bulk density decreased, with increasing distance to gulf (r^2 = 0.81 and 0.71, respectively). Soil parameters were similarly correlated to depth of Holocene stratum (Figure 5.9). Canal density and oil production were also related, but the relationship was noisier (r^2 = 0.25). The relationship between canal density and interior wetland loss was significant at the 10 km scale (Figure 5.10, page 100, r^2 = 0.41, $F_{(1, 32)}$ = 22.0, p < 0.001). The differing regression slopes for each marsh type, however, suggested non-stationarity.

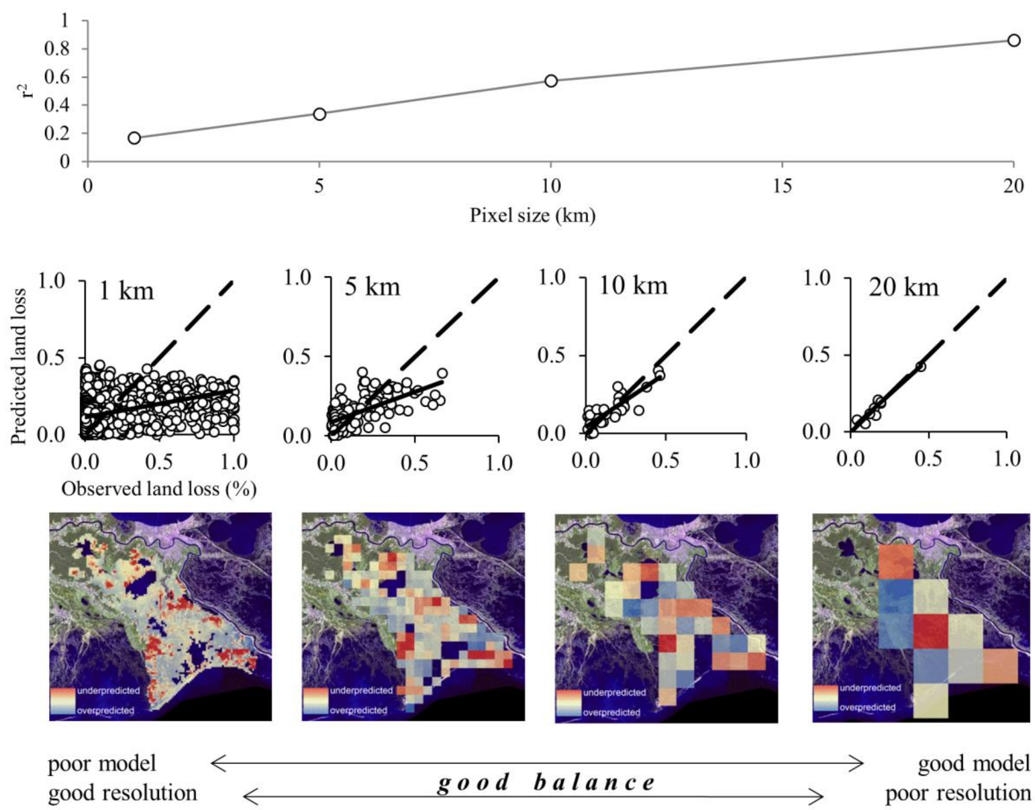

Figure 5.8. Comparison of model results from the OLS analyses for four sampling scales: 1 km, 5 km, 10 km, and 20 km showing increasing model performance, but reduced resolution, at the larger scales. The strongest model is the 10 km grid.

The variance inflation factors (Table 5.2) indicated that the distance to coast and soil organic material variables were co-variable in the multivariate model. Their removal and re-analysis provided a slightly stronger model at the 5 km scale (adj. r^2 0.34 to 0.35), but tests for

model assumptions still failed. At the 10 km scale, a sequential removal and re-analysis of the most co-variable parameters (organic matter and then distance to Gulf) did not improve the overall model (from an adj. r^2: 0.573 to r^2: 0.563), but did appear to distribute the explained variance to the remaining co-variables. When soil organic material (VIF: 7.46) and distance to Gulf (VIF: 6.33) variables were removed, soil bulk density became significant ($p = 0.002$). The variance inflation factors of the remaining seven variables did not exceed 3.1 (Table 5.2). The condition indices decreased from 54 to 25 between the full and reduced models, indicating that collinearity was sufficiently resolved. Squared semi-partial correlations (Type I) were helpful in identifying the relative contribution of variables at each stage in the model. Canal density accounted for between 18.8 and 19.6 percent of the total model variability in each of the three OLS tests at the 10 km scale (Figure 5.11, page 103). In the final model, bulk density and Holocene depth accounted for slightly less variability than canal density, and these three variables combine to account for 52% of the data variability.

Geographically weighted regression (GWR)

The results of the GWR analysis, used as a supplement to the OLS analysis, were helpful in identifying how relationships between variables changed across the landscape. The results of analyses at the 5 and 10 km scales produced similar trends in the model output. Canal density was more strongly correlated to interior land loss in the southern basin, and the strength of this correlation decreased with distance from the Gulf of Mexico (Figures 5.12 and 5.13, pages 104 and 106). Similarly, regression coefficients also decreased with distance from the Gulf, indicating a trend of weakening relationships along a north-to-south gradient. There were weak positive (10 km grid), and weak inverse (5 km grid) relationships between canals and land loss in the northern part of the estuary.

Table 5.1 Ordinary least squares regression model results at varying spatial scales. [1]A significant Koenker BP statistic indicates that standard errors are biased. [2]A significant Moran's I statistic indicates that model residuals are spatially clustered. [3]A significant Jarque-Bera statistic indicates that model residuals are not normally distributed

Pixel size	1	5	10	20	Interpretation
n	3376	142	34	10	
d.f.	3366	132	24	5	Too few d.f. to include all variables,
Adj. r^2	0.17	0.34	0.57	0.72	included top four at previous scale
AICc	-1409	-178	-65	-26	
Koenker BP[1]	<0.001	0.025	0.188	0.93	Standard errors are biased
Moran's I[2]	<0.001	<0.001	0.44	0.34	Residuals are spatially clustered
Jarque-Bera[3]	<0.001	<0.001	0.907	0.7	Residuals are not normally distributed
F	77.62	9.05	5.94	6.84	
p	<0.001	<0.001	<0.001	0.029	Significant at $p < 0.05$
Variable	***p***	***p***	***p***	***p***	
Intercept	0.28	0.97	0.16	0.61	
Holocene depth (m)	<0.01	0.23	0.05	0.62	Significant at $p < 0.05$
Delta lobe age (y)	0.26	0.75	0.08	0.29	
Distance to Gulf (m)	0.93	0.62	0.20	*	
Distance to distributary (m)	0.06	0.44	0.35	*	
Distance to development (m)	<0.01	<0.01	0.19	*	
Soil organic matter (% dry wt.)	0.08	0.99	0.62	*	
Soil bulk density (g cm^{-3})	<0.01	0.02	0.14	0.04	
Petroleum production (barrels)	<0.01	0.19	0.57	*	
Canal density (% of 1932 land)	<0.01	<0.01	<0.01	0.02	

A number of variables that I tested also exhibited trends along the north-to-south estuarine gradient, and I used this comparison to look for potential causal factors or thresholds that may correspond to ecological or geological parameters. There was an apparent threshold at the 40 m Holocene thickness where, at shallower thicknesses, the relationship between canal dredging and land loss weakened. Similarly, with respect to soil type, this transition takes place near 50% organic matter content and the relationship weakens as soil organic matter content increases (Figures 5.12 and 5.13, pages 104 and 106).

The GWR approach produced stronger models than OLS at both scales tested. In univariate models comparing interior land loss to canal density, the GWR produced an r^2 of 0.63, while the same model in OLS model produced an r^2 of 0.41 at the 10 km scale. At the 5 km scale, the GWR model produced an r^2 of 0.35, compared to 0.14 for the univariate model from the OLS analysis. The GWR analysis did confirm significant non-stationarity of the data, as was previously indicated by challenges meeting model assumptions in OLS at the 5 km scale.

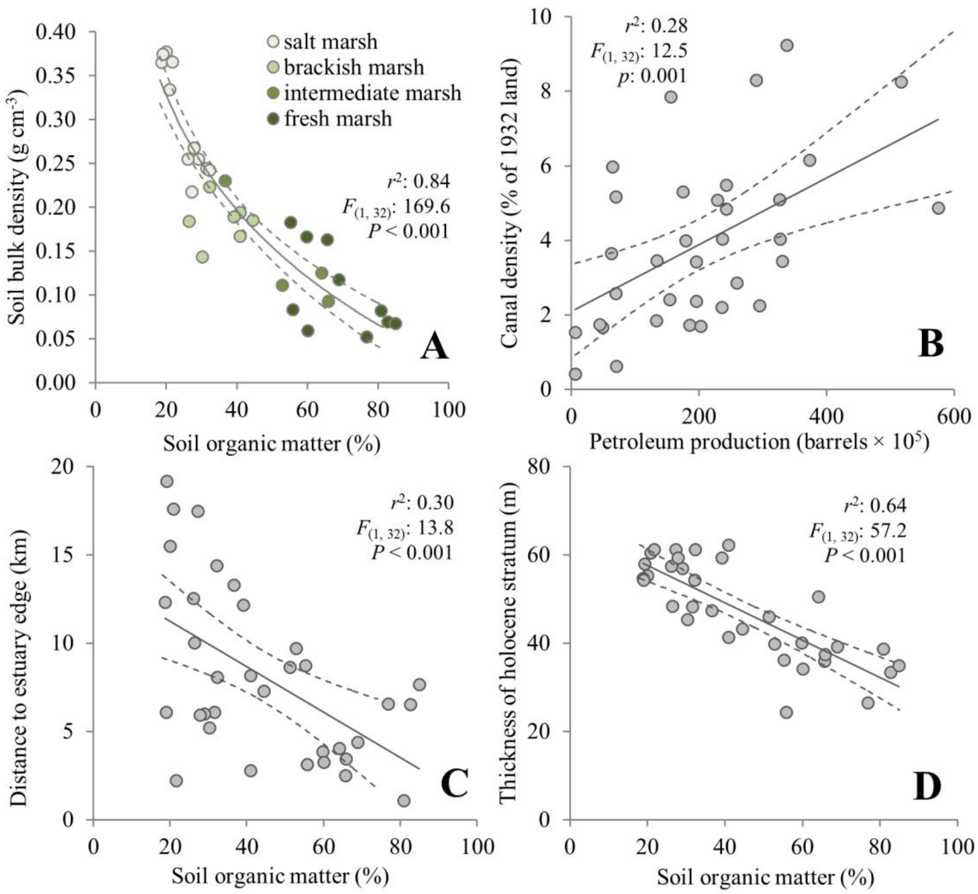

Figure 5.9 Covariability between selected parameters at the 10 km scale. **A.** Surface (0 to 24 cm) soil organic matter versus soil bulk density, categorized by marsh type. **B.** Petroleum production versus canal density . **C.** Soil organic matter versus distance to estuary edge. **D.** Soil organic matter versus thickness of Holocene stratum.

Discussion

Interior wetland loss is significantly correlated to canal dredging at multiple spatial scales in both OLS and GWR (Tables 5.1 and 5.2). This relationship explains the greatest proportion of variability in land loss of the variables tested. Holocene deposit thickness and soil bulk density are also significant factors in the strongest multivariate model. The GWR analysis identifies a distinct spatial threshold where the thicker delta deposits and more mineral-rich sediments appear to be more sensitive to canal dredging. This threshold also approximates a boundary between floating and freshwater marsh types, but the co-variability between these factors makes it difficult to isolate causation from correlation. Spatial variability in marsh sensitivity to canal dredging may be due to geological or biogeochemical processes, or perhaps more likely a combination of several factors.

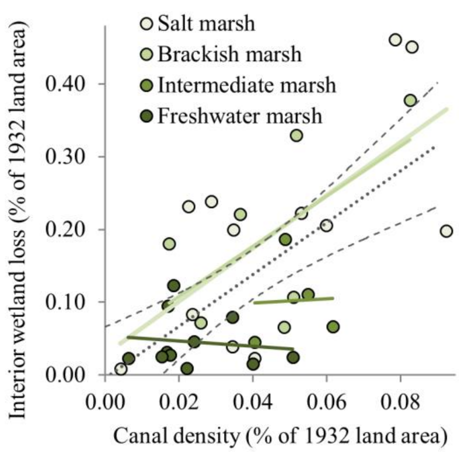

Figure 5.10 Relationship between canal density and interior wetland loss. The overall relationship is shown as a dotted line (± 95% CI), and broken down by marsh types (color-coded solid lines, salt and brackish marsh lines overlap). Varying relationships suggest non-stationarity is present in the dataset.

The areas of thicker Holocene deposits typically exhibit higher subsidence rates (Blum and Roberts 2009), which may render wetlands at the surface more sensitive to changes in surface hydrology. Marsh accretion rates are higher in these areas closer to the mouth of the estuary (Hatton et al. 1983, Chmura and Kosters 1994), and additional stress due to hydrologic

modifications may limit the capacity of marshes to maintain elevation by organic matter production. These feedbacks between hydrologic changes and biological processes are an important factor in maintaining marsh elevation, and marshes in microtidal estuaries (e.g., Louisiana) may be least able to adapt to increases in relative sea level (Kirwan et al. 2010). Spoil banks may also restrict the distribution of mineral sediment during tidal or cold front inundation events (Cahoon and Turner 1989) or during storm surge events (Day et al. 2012). This effect may be more significant in the lower estuary where mineral sediment comprises a larger proportion of the soil profile.

Sulfide toxicity is another possible cause for increased sensitivity to hydrologic modification in more saline marshes. Because canals and associated spoil banks can increase marsh hydroperiod and decrease groundwater exchange (Swenson and Turner 1987), changes in flooding regime would alter sediment biogeochemistry (Reddy and DeLaune 2008). The accumulation of sulfide and other toxins may harm plants during periods of prolonged waterlogging (Mendelssohn et al. 1981). Because of the presence of sulfate in seawater, this effect would be exacerbated in more saline marshes. Increased flooding duration has been linked to decreases in soil redox potential, sulfide toxicity, and reduced biomass production in *Spartina* marshes (Mendelssohn and McKee 1988). The indirectly caused toxicity effect from spoil banks may be further compounded by reduction of mineral sediment input during storm events, which contains iron that may precipitate sulfides (DeLaune and Pezeshki 1994). Coastal freshwater marshes, however, can tolerate prolonged flooding periods (Holm and Sasser 2008), and are not regularly exposed to sulfate-rich seawater (Odum 1988). Peak productivity of *Panicum hemitomon*, a grass common in freshwater marshes, has been reported in marshes flooded 85% of the time, and at flooding depths of tens of centimeters above the surface (Holm and Sasser 2008), which may indicate greater resilience to altered hydrology.

Table 5.2 Detailed OLS model results at the 10 km scale, showing model improvement by removal of co-variables. Amount of variance explained by each variable is shown as SSPC (squared semi-partial correlations, type I). [1]SSPC: Squared semi-partial correlations Type I, sum to r^2. [2]Higher VIF values indicate covariability.

Full model

r^2:	0.6945	Adj. r^2:	0.58		Condition index:	52
$F_{(9, 24)}$:	6.06	p:	0.0002			

Variable	Parameter estimate	± 95% CI	SE	p	SSPC[1]	VIF[2]
Intercept	0.263640	0.439240	0.212820	0.23	-	-
Holocene depth (m)	-0.005860	0.006170	0.002990	0.06	0.15	5.42
Delta lobe age (y)	0.000064	0.000259	0.000040	0.13	0.00	1.87
Distance to Gulf (m)	-0.000002	0.000003	0.000001	0.15	0.14	6.33
Distance to distributary (m)	-0.000007	0.000014	0.000007	0.30	0.05	1.69
Distance to development (m)	-0.000006	0.000011	0.000005	0.27	0.03	3.11
Soil organic matter (% dry wt.)	-0.000227	0.003853	0.001870	0.90	0.04	7.46
Soil bulk density (g cm^{-3})	0.550720	0.644650	0.312350	0.09	0.03	5.02
Petroleum production (barrels)	0.000000	0.000000	0.000000	0.63	0.05	1.86
Canal density (% of 1932 land)	3.411530	1.803450	0.873810	<0.001	0.19	1.97

Reduced model 1 Organic matter removed from the model

r^2:	0.6943	Adj. r^2:	0.60		Condition index:	44.2
$F_{(8, 25)}$:	7.1	p:	<0.0001			

Variable	Parameter estimate	± 95% CI	SE	p	SSPC[1]	VIF[2]
Intercept	0.249260	0.357100	0.173390	0.16	-	-
Holocene depth (m)	-0.005810	0.005990	0.002910	0.06	0.15	5.30
Delta lobe age (y)	0.000063	0.000079	0.000038	0.11	0.00	1.73
Distance to Gulf (m)	-0.000002	0.000003	0.000001	0.12	0.14	5.73
Distance to distributary (m)	-0.000008	0.000014	0.000007	0.26	0.05	1.59
Distance to development (m)	-0.000006	0.000010	0.000005	0.25	0.03	2.75
~~Soil organic matter (% dry wt.)~~	-	-	-	-	-	-
Soil bulk density (g cm^{-3})	0.573470	0.504880	0.245140	0.03	0.07	3.16
Petroleum production (barrels)	0.000000	0.000000	0.000000	0.61	0.05	1.86
Canal density (% of 1932 land)	3.418860	1.759630	0.854380	<0.001	0.20	1.97

Reduced model 2 Organic matter and Distance to Gulf removed from the model

r^2:	0.6619	Adj. r^2:	0.57		Condition index:	24.8
$F_{(7, 26)}$:	7.27	p:	<0.0001			

Variable	Parameter estimate	± 95% CI	SE	p	SSPC[1]	VIF[2]
Intercept	-0.003880	0.162710	0.079150	0.96	-	-
Holocene depth (m)	-0.002710	0.004660	0.002270	0.24	0.15	3.13
Delta lobe age (y)	0.000043	0.000070	0.000039	0.18	0.00	1.70
~~Distance to Gulf (m)~~	-	-	-	-	-	-
Distance to distributary (m)	-0.000008	0.000014	0.000007	0.24	0.05	1.59
Distance to development (m)	-0.000006	0.000010	0.000005	0.24	0.02	2.74
~~Soil organic matter (% dry wt.)~~	-	-	-	-	-	-
Soil bulk density (g cm^{-3})	0.775850	0.447900	0.217900	<0.01	0.18	2.32
Petroleum production (barrels)	0.000000	0.000000	0.000000	0.88	0.08	1.78
Canal density (% of 1932 land)	3.350110	1.808890	0.880010	<0.001	0.19	1.97

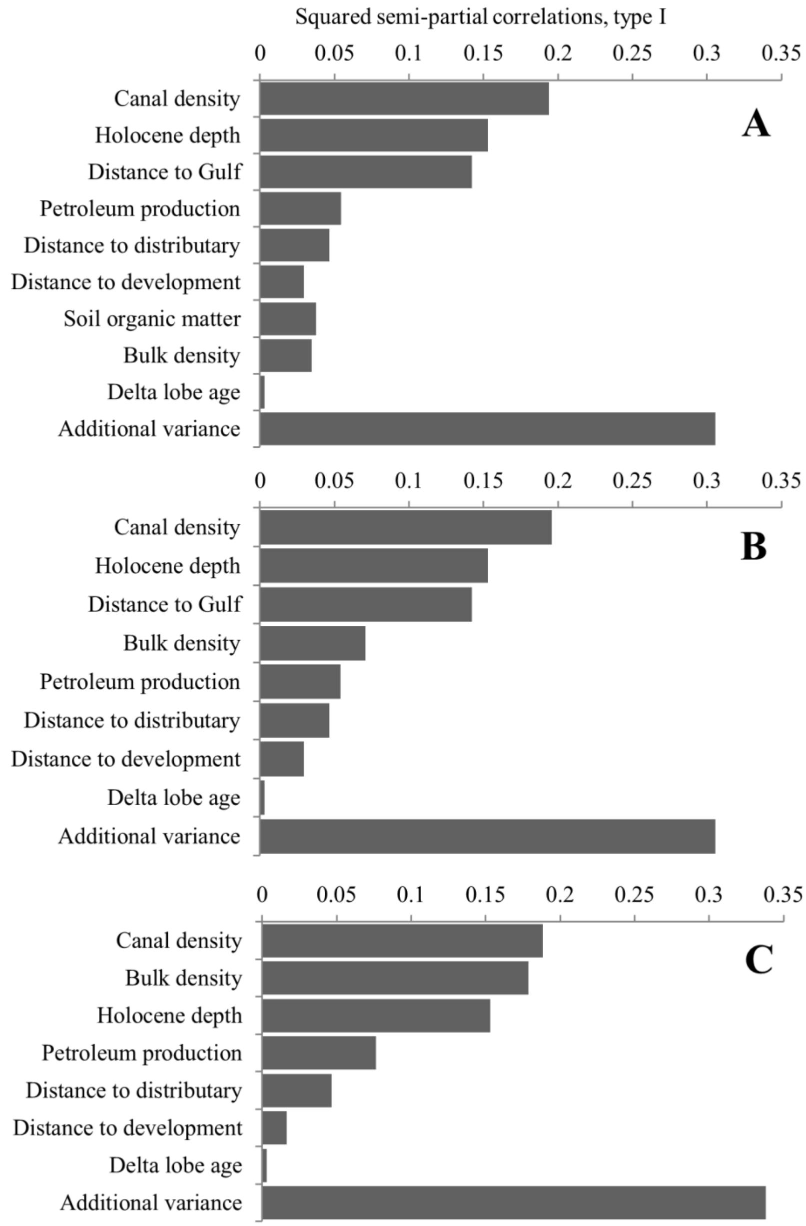

Figure 5.11 Squared semi-partial correlations (Type I) for variables used in an OLS multiple regression analysis. The values for variables sum to r^2 and indicate the proportion of variance explained by each variable. Unexplained variance ($1 - r^2$) is also shown. The effect of sequential removal of co-varying parameters is shown as **A.** Full model, **B.** The percent organic matter parameter is removed, **C.** The percent organic matter and distance to Gulf parameters are removed.

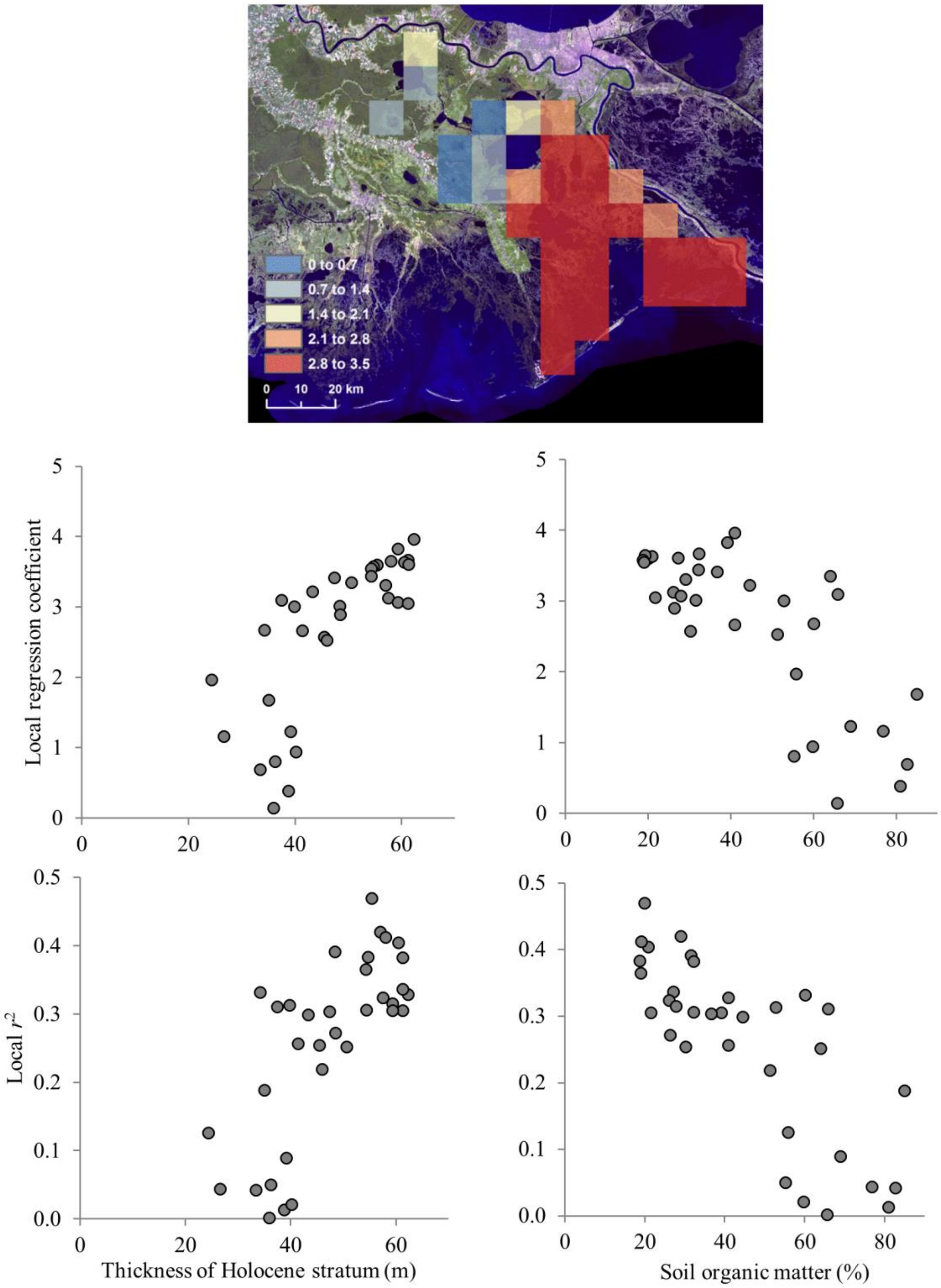

Figure 5.12 Geographically weighted regression results at the 10 km scale. The map depicts the decreasing northward trend in local regression coefficients (β). The graphs depict how local regression coefficients (top) and local r^2 values (bottom) vary with respect to Holocene stratum thickness (left) and soil organic matter (right).

Spatial variability in estuarine suspended sediment concentrations is another possible difference between salt and freshwater portions of Barataria Basin. Suspended sediment concentrations tend to be greater in the lower estuary (E. Swenson, unpublished data). Restriction of tidal flooding could block suspended sediments from reaching marshes (Reed et al. 2006, Kuhn et al. 1999). Similarly, spoil banks could block storm surge sedimentation. However, vertical accretion in salt marshes is driven primarily by organic processes (Turner et al. 2002), and so reductions in allochthonous sedimentation may not fully explain land loss patterns.

I did not find oil production to be significantly correlated to interior land loss at any scale, although researchers studying smaller areas have reported a relationship to land loss hotspots (Morton et al. 2005). I found the highest rates of land loss in the study area in the southwest Barataria Basin in an area of deeper than average well depths (4-5 km) in relatively unproductive oil fields (Bayou Ferblanc and Bay Jaque fields). I observed a similar pattern of deep well depths and relatively low production in the Bastian Bay oil field, in the southeast corner of the study area. A separate study investigated land loss patterns near productive wells and wells that were drilled but never productive, and found no significant difference in surrounding land loss rates (Spicer 2007). While fluid withdrawal may be locally significant, it does not appear to drive patterns of land loss at the basin scale.

The smaller spatial scales exhibited significant clustering of residuals, indicating bias in the models that could result from spatial non-stationarity of one or more variables. Non-stationarity among the relationship between canals and land loss was demonstrated at both the 5 km and 10 km scales. The larger scales, despite less statistical power, yielded stronger models at

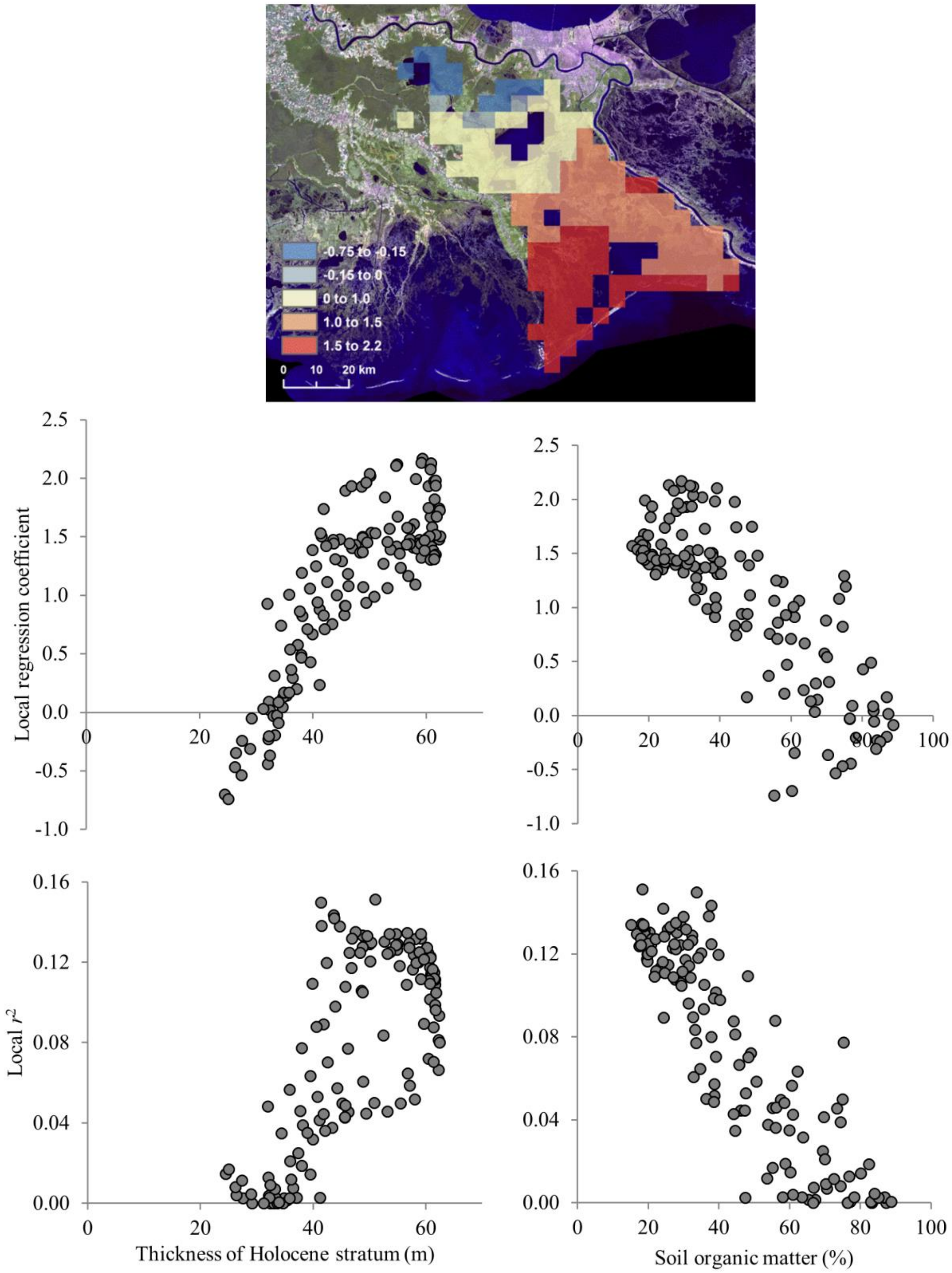

Figure 5.13 Geographically weighted regression results at the 5 km scale. The map depicts decreasing northward trend in local regression coefficients (β). Graphs depict how local regression coefficients (top) and local r^2 values (bottom) vary with respect to Holocene stratum thickness (left) and percent soil organic matter (right).

the expense of spatial resolution. This may be due to the decrease in variance that arises when data are aggregated into larger scales (Wiens 1989). Moderate spatial scales (10 km in this example) provided the best balance between avoiding model bias and maintaining interpretable spatial resolution, but the appropriate scale could vary widely depending on the variables and source data being analyzed (Wiens 1989). Even if the smallest pixel size were statistically viable, this scale may be inappropriate for measuring land loss in coastal Louisiana because of the patch size of land loss areas. In the Barataria Basin study area, the largest interior land loss patch size was 15.5 km^2, which would nearly fill a pixel of 4 km per side. Additionally, 46.1% of the interior land loss in this basin has occurred in patches greater than 1 km^2, and so regression of these data as the dependent variable should aim to include the independent variables in the same pixel.

Successful coastal restoration will depend on addressing the variety of causes of land loss in coastal Louisiana. Application of the results from this study is helpful in identifying areas where coastal marshes are most sensitive to the effects of canal dredging. This methodology could be adapted to test additional variables at varying spatial scales. With land loss rates expected to increase due to sea level rise projections, limited coastal restoration resources could be used more efficiently by accounting for this and other spatially varying relationships.

References

ATLAS. 2010. Louisiana Statewide GIS. CADGIS Research Laboratory, Louisiana State University. www.atlas.lsu.edu

Barras, J. A. 2007. Land Area Changes in Coastal Louisiana after Hurricanes Katrina and Rita. Science and the Storms. GS Farris, GJ Smith, MP Crane, CR Demas, LL Robbins and DL Lavois, eds. Science and the storms: the USGS response to the hurricanes of 2005. p. 97-112.

Blum, M. D. and H. H. Roberts. 2009. Drowning of the Mississippi Delta Due to Insufficient Sediment Supply and Global Sea-Level Rise. Nature Geoscience 2:488-491.

Blum, M. D., J. H. Tomkin, A. Purcell, and R. R. Lancaster. 2008. Ups and Downs of the Mississippi Delta. Geology 36:675-678.

Britsch, L. D. and J. B. Dunbar. 2006. Land Loss in Coastal Louisiana 1932 to 2001. Vicksburg, Mississippi Engineer Research and Development Center, US Army Corps of Engineers, New Orleans.

Brunsdon, C., S. Fotheringham, and M. Charlton. 2002. Geographically Weighted Regression. Journal of the Royal Statistical Society: Series D (The Statistician) 47:431-443.

Cahoon, D. R. and R. E. Turner. 1989. Accretion and Canal Impacts in a Rapidly Subsiding Wetland Ii. Feldspar Marker Horizon Technique. Estuaries and Coasts 12:260-268.

Cowan, J. H. and R. E. Turner. 1988. Modeling Wetland Loss in Coastal Louisiana: Geology, Geography, and Human Modifications. Environmental Management 12:827-838.

Craig, N. J., R. E. Turner, and J. W. Day. 1979. Land Loss in Coastal Louisiana (USA). Environmental Management 3:133-144.

Davis, D. W. 1973. Louisiana Canals and Their Influence on Wetland Development. Ph.D. Dissertation. Louisiana State University and Agricultural and Mechanical College.

Day, J., R. Hunter, R. F. Keim, R. DeLaune, G. Shaffer, E. Evers, D. Reed, C. Brantley, P. Kemp, J. Day, and M. Hunter. 2012. Ecological Response of Forested Wetlands with and without Large-Scale Mississippi River Input: Implications for Management. Ecological Engineering 46:57-67.

Day, J. W., L. D. Britsch, S. R. Hawes, G. P. Shaffer, D. J. Reed, and D. Cahoon. 2000. Pattern and Process of Land Loss in the Mississippi Delta: A Spatial and Temporal Analysis of Wetland Habitat Change. Estuaries and Coasts 23:425-438.

Deegan, L. A., H. M. Kennedy, and C. Neill. 1984. Natural Factors and Human Modifications Contributing to Marsh Loss in Louisiana's Mississippi River Deltaic Plain. Environmental Management 8:519-527.

DeLaune, R. and S. Pezeshki. 1994. The Influence of Subsidence and Saltwater Intrusion on Coastal Marsh Stability: Louisiana Gulf Coast, USA. Journal of Coastal Research SI 12:77-89.

Dunbar, J. B., L. Britsch, and E. Kemp. 1992. Land Loss Rates: Louisiana Coastal Plain. US Army Engineer Waterways Experiment Station, Vicksburg, Mississippi. Report GO-90-2, Part 3.

Fearnley, S., S. Penland, and L. D. Britsch. 2009. Mapping the Geomorphology and Processes of Coastal Land Loss in the Pontchartrain Basin: 1932 to 1990 and 1990 to 2001. Journal of Coastal Research 54:48-58.

Hatton, R., R. DeLaune, and W. Patrick Jr. 1983. Sedimentation, Accretion, and Subsidence in Marshes of Barataria Basin, Louisiana. Limnology and Oceanography 28:494-502.

Holm, G. and C. Sasser. 2008. The Management and Ecology of the Wetland Grass, Maidencane. Journal of Aquatic Plant Management 46:51-60.

Kirwan, M. L., G. R. Guntenspergen, A. D'Alpaos, J. T. Morris, S. M. Mudd, and S. Temmerman. 2010. Limits on the Adaptability of Coastal Marshes to Rising Sea Level. Geophysical Research Letters 37:L23401.

Kolb, C. R. and J. R. van Lopik. 1966. Depositional Environments of the Mississippi River Deltaic Plain Region-Southeastern Louisiana. L.S. Shirley and J. A. Ragsdale, eds. Deltas in their Geologic Framework. Houston Geological Society. p.17-61.

Kosters, E. C. 1989. Organic-Clastic Facies Relationships and Chronostratigraphy of the Barataria Interlobe Basin, Mississippi Delta Plain. Journal of Sedimentary Research 59:98-113.

Kuhn, N. L., I. A. Mendelssohn, and D. J. Reed. 1999. Altered Hydrology Effects on Louisiana Salt Marsh Function. Wetlands 19:617-626.

LDNR. 2012. Coastwide Reference Monitoring System. Louisiana Department of Natural Resources, Baton Rouge, Louisiana. www.lacoast.gov/crms

Lee, J. M. and R. E. Turner. 1990. Hydrology and Land Loss / Accretion: Barataria Map. Center for Wetland Resources, Louisiana State University.

Mendelssohn, I. A., K. McKee, and W. Patrick Jr. 1981. Oxygen Deficiency in Spartina Alterniflora Roots: Metabolic Adaptation to Anoxia. Science 214:439-441.

Mendelssohn, I. A. and K. L. McKee. 1988. Spartina Alterniflora Die-Back in Louisiana: Time-Course Investigation of Soil Waterlogging Effects. The Journal of Ecology 76:509-521.

Morton, R. A., J. C. Bernier, J. A. Barras, and N. F. Ferina. 2005. Historical Subsidence and Wetland Loss in the Mississippi Delta Plain. Gulf Coast Association of Geological Societies Transactions 55:555-571.

Nyman, J. A., M. Carloss, R. D. DeLaune, and W. H. P. Jr. 1994. Erosion Rather Than Plant Dieback as the Mechanism of Marsh Loss in an Estuarine Marsh. Earth Surface Processes and Landforms 19:69-84.

Odum, W. E. 1988. Comparative Ecology of Tidal Freshwater and Salt Marshes. Annual Review of Ecology and Systematics 19:147-176.

Okey, C. W. 1918. The Wet Lands of Southern Louisiana and Their Drainage. USDA Bulletin 652. 67 p.

O'Neil, T. 1949. The Muskrat in the Louisiana Coastal Marshes. Louisiana Wildlife and Fisheries Commission, New Orleans, Louisiana. 152 p.

Raymond, P. A., N. H. Oh, R. E. Turner, and W. Broussard. 2008. Anthropogenically Enhanced Fluxes of Water and Carbon from the Mississippi River. Nature 451:449-452.

Reddy, K. R. and R. D. DeLaune. 2008. Biogeochemistry of Wetlands: Science and Applications. Boca Raton, Florida. CRC Press. 800 p.

Reed, D. J., M. S. Peterson, and B. J. Lezina. 2006. Reducing the Effects of Dredged Material Levees on Coastal Marsh Function: Sediment Deposition and Nekton Utilization. Environmental Management 37:671-685.

Roberts, H. H. 1997. Dynamic Changes of the Holocene Mississippi River Delta Plain: The Delta Cycle. Journal of Coastal Research 13:605-627.

Rosenshein, L., L. Scott, and M. Pratt. 2011. Finding a Meaningful Model. ESRI ArcUser, Winter 2011:40-45.

Simenstad, C., J. Toft, H. Higgins, J. Cordell, M. Orr, P. Williams, L. Grimaldo, Z. Hymanson, and D. Reed. 2000. Sacramento/San Joaquin Delta Breached Levee Wetland Study (Breach). Preliminary report. Seattle (WA): Wetland Ecosystem Team, University of Washington, School of Fisheries. 46 p.

SONRIS. 2010. Petroleum Production Data to 1977. Louisiana Office of Conservation. Baton Rouge, Louisiana.

Spicer, J. 2007. A Comparison of Channel Morphology, Marsh Elevation, and Biological Processes in Natural and Dredged Tidal Salt Marshes in Louisiana. Ph.D. Dissertation. Louisiana State University.

Swenson, E. M. and R. E. Turner. 1987. Spoil Banks: Effects on a Coastal Marsh Water-Level Regime. Estuarine, Coastal and Shelf Science 24:599-609.

Turner, R. E. 1997. Wetland Loss in the Northern Gulf of Mexico: Multiple Working Hypotheses. Estuaries and Coasts 20:1-13.

Turner, R. E. 2001. Estimating the Indirect Effects of Hydrologic Change on Wetland Loss: If the Earth Is Curved, Then How Would We Know It? Estuaries 24:639-646.

Turner, R. E. and N. N. Rabalais. 1994. Coastal Eutrophication near the Mississippi River Delta. Nature 368:619-621.

Tweel, A. W. and R. E. Turner. 2012a. Watershed Land Use and River Engineering Drive Wetland Formation and Loss in the Mississippi River Birdfoot Delta. Limnology and Oceanography 57:18-28.

USACE. 1958. Geology of the Mississippi River Deltaic Plain, Southeastern Louisiana. US Army Engineer Waterways Experiment Station. Vicksburg, Mississippi. Volume 2.

Walker, H. J., J. M. Coleman, H. H. Roberts, and R. S. Tye. 1987. Wetland Loss in Louisiana. Geografiska Annaler. Series A. Physical Geography 69:189-200.

Wiens, J. A. 1989. Spatial Scaling in Ecology. Functional Ecology 3:385-397.

CHAPTER 6
SYNTHESIS: FUTURE CHANGES AND CONSIDERATIONS FOR COASTAL MANAGEMENT

Introduction

The research presented in this dissertation demonstrates the spatial and temporal variability in this system, and how landscape changes are driven by processes whose influence varies spatially. The four research areas I examined are a linked series of investigations of the internal and external forcing mechanisms driving landscape change in coastal wetlands. Here I address the four main questions posed in the introduction chapter and discuss how the cumulative effects of these findings contribute to the overall scientific understanding of processes driving coastal wetland landscapes, as well as their implications for coastal restoration and impacts from climate change.

Second chapter summary

Question one: How have changes in the Mississippi River suspended sediment load influenced land area in the birdfoot delta and how do these changes relate to patterns observed elsewhere on the coast?

This research chapter sought to quantify the linkage between anthropogenic watershed modification and wetland formation and loss at the mouth of the river. I found that these land change processes were primarily sediment-driven, and that the amount of wetlands sustained by the river has been directly proportional to the sediment load in the river as it fluctuated over the past two centuries. Following agricultural development in Europe (Bruckner 1986), and later in colonial America (Kirwan et al. 2011), the Mississippi River sediment load increased as large tracts of land were converted to European-style agriculture (Chapter two). The sediment load to the river delta was later reduced as dams were constructed, and also as soil conservation

practices improved (Keown et al. 1981). This increase, decrease, and then relative stabilization of sediment load were directly reflected at the mouth of the river as land formation, loss, and relative stabilization. These sediment-driven landscape changes were not seen elsewhere along the Louisiana coast, and this difference is demonstrated by thick autogenic organic soils characteristic of most of the deltaic and chenier plain wetlands, but not the birdfoot delta. Similarly, the timing of land loss elsewhere along the coast does not correspond to the modern reduction in sediment supply from the river- at least not on the same timescale. Certainly shifting delta lobes on a millennial timescale correspond to patterns of wetland formation and loss, as submarine shoals mark the extent of former delta landscapes, but the effects of the recent reduction in riverine sediment loads do not appear to extend beyond active delta wetlands. This distinction is that deltaic sedimentation processes built the platform for wetland plants to thrive, but that sediment loading was already greatly reduced on the deltaic plain as the river avulsed in search of a new path to the Gulf. At this point, the maintenance of elevation was taken over by mostly organic processes, and these 'living surfaces' are evidenced by the prevalence of peat up to 6 m thick and 3000 years old in these areas (Gagliano et al. 1981).

Third and fourth chapter summaries

Questions two and three: How much mineral sediment was deposited by hurricanes in Louisiana wetlands during 2005 and 2008 and how does this deposition vary spatially? How do these depositional events relate to long-term trends in hurricane landfall and wetland sediment characteristics?

One significant source of sediment to wetlands in abandoned delta lobes and the chenier plain is infrequent, but powerful, tropical cyclone events (Chapters three and four). Prior to the analysis I present here, there have been few estimates of the total amount of sediment deposited

on wetlands by hurricanes and tropical storms, or how this varied spatially and temporally (Turner et al. 2006). There have been numerous site-specific studies that have reported up to tens of centimeters of sediment being deposited during storm surge events, but the contribution of these events to the overall sediment budget for coastal wetlands is uncertain. My research demonstrated that the processes of mineral sedimentation in abandoned delta lobes and the chenier plain are driven largely by these tropical cyclone events (Chapter four). By comparison to overbank flooding events before river leveeing and the modern reduction in sediment loads, tropical cyclone events contribute a greater amount of sediment per unit area, and also distribute sediment over a larger area. This dominance of marine-driven sedimentation in abandoned lobes, rather than by overbank flooding, is also apparent in the spatial distribution of wetland soil types (Figure 2.8, page 29). These soils exhibit a clear trend of decreasing mineral content with distance from the Gulf (Tweel and Turner 2012a, Chabreck 1972, Kolb and van Lopik 1966). The notion that sediments passing through the mouth of the river are 'lost' is overly simplistic (Winer 2011, CLEAR 2008: 'uselessly', CPRA 2012: 'wasted'), because wave energy from hurricanes is capable of suspending coarse sand from depths of 140 m (and therefore finer sediments from even deeper) and transporting these sediments to shallower depths where they come to rest as wave energy diminishes (Tweel and Turner 2012b).

Other types of infrequent storm surge events may also contribute significantly to the sediment budget for coastal wetlands (e.g., Barra et al. 2004, Schuerch et al. 2012). Widespread casualties, property damage, and thick sediment deposits from the recent tsunamis in 2011 and 2004 are examples of how quickly and intensely some events can modify the coastal landscape (Bourgeois 2009, Goto et al. 2011). Large boulders are often transported far inland by tsunami waves (Bourgeois 2009, Dawson 1994). In a Chilean salt marsh, an 8 cm sand layer was

deposited by a single tsunami in 1960, and accretion since this event has averaged 0.5 cm yr^{-1} (Barra et al. 2004). Similar observations have been made in Japanese salt marshes, with return intervals of large events estimated at 365-553 years (Nanayama et al. 2007). Near shore, tsunami events may deposit less sediment in a given area, and cover a smaller spatial extent, but there are many variables (e.g., sediment source, event duration/proximity), and much uncertainty remains as to their relative contribution to coastal sediment budgets (Morton et al. 2007).

Fifth chapter summary

Questions four and five: What variables are related to the patterns of land loss in coastal Louisiana wetlands and how do these relationships vary across the landscape? Is geographically weighted regression a suitable tool for identifying variability in ecosystem response to stressors?

These varying coastal processes should be considered within the context of the larger set of variables linked to the suite of geological and ecological processes in coastal Louisiana to understand the implications of these sedimentation research areas for coastal restoration and future ecosystem changes. The patterns of landscape change on this coast are best characterized by their variability, rather than by coast-wide metrics or long term averages. The multivariate analysis in Chapter Four represents an effort to quantify the processes that drive this variability. This methodology is ideal for investigating spatial variability in ecosystem stressors, and could have wide applications beyond coastal wetland landscapes. For this analysis, there were two main conclusions. The most salient observation is that the patterns of interior land losses since the 1930s were strongly correlated to canal density at multiple analysis scales. Secondly, I identified that this relationship varied spatially - canals closer to the Gulf are more strongly correlated to land loss than canals in the more freshwater marshes located inland.

Several mechanisms for this spatial non-stationarity were proposed. In contrast to the large study scale, a biogeochemical pathway may provide the best explanation. The increase in hydroperiod due to canal spoil banks could have an exacerbated effect on organic accretion in saline marshes due to the prevalence of sulfate-rich seawater that could develop sulfide toxicity during periods of prolonged flooding (Mendelssohn et al. 1981). This would explain the lesser sensitivity in freshwater, sulfate-poor, marshes where methanogenesis is a dominant redox pathway. Secondly, higher accretion rates in the lower estuary may be affected by changes in hydroperiod, which could push them to even faster accretion rates that are not sustainable. A third possible reason is that estuarine suspended sediment concentrations are higher in the lower estuary, and so spoil banks may inhibit the deposition of this during normal tidal cycles. This spatial variability is one example of how variable this coast is, and that restoration actions should strive to incorporate these nuances into long term planning. For instance, canal restoration projects in the more saline marshes would be expected to have greater benefit to surrounding marshes than those in the upper estuary where wetland losses have been minimal.

Geologic Factors Leading to Development of Coastal Louisiana Wetlands

The formation of this coast must be considered within the context of its geologic and ecological development on a millennial timescale when discussing the implications of these results on current restoration initiatives. These wetlands rest on a platform built by the Mississippi River as it shifted courses in search of easier outlets to the sea. In abandoned delta lobes and the chenier plain, which comprise about 90% of coastal Louisiana wetlands, marsh soils are dominated by peats that maintain elevation primarily by the accretion of organic materials. Some of the first geologists to study surficial deposits in abandoned delta lobes recognized this when they noted that “the marsh surface is, in reality, built ‘down’ rather than

‘up’” (Kolb and van Lopik 1966). The dominance of organic material in its contribution to vertical accretion in coastal marshes of former delta lobes has been quantified in more recent analyses (Turner et al. 2002, Kosters 1989).

Periodic flooding of the Mississippi River caused freshwater and sediments to overflow its banks and enter estuaries such as the Barataria Basin and Breton Sound. Sediments in suspension were deposited as water velocities decreased, leaving behind a wedge of sediments that decreased in thickness with distance from the river (Kolb and van Lopik 1966). Natural levees are the dominant landscape feature resulting from these flooding events. These natural levees range in width from approximately 7 km at 300 river-km (Baton Rouge = 370) to less than a km near the mouth of the river south of Venice, LA, (Kolb and van Lopik 1966). In the interior portions of abandoned delta lobes, the prevalence of hiatal peat surfaces, commonly 2 m thick, but range up to 6 m thick, is indicative of environments with low input of clastic sediments (Kosters 1989). Continuous peat formation has been more prevalent in the upper freshwater portions of Barataria Basin, and peat layers in the southern, more saline, portion of the basin are punctuated by layers of inorganic-rich sediments (Kosters et al. 1987). This is consistent with other reports that inorganic layers in inactive delta lobes primarily result from marine processes, rather than riverine flooding events (Figure 4.7, page 75, Turner et al. 2007). Inorganic sediments are present in the more freshwater reaches, but appear as thicker clay layers that were formed as the river shifted courses and slowly filled interdistributary water bodies (Kosters et al. 1987).

Coastal Restoration

Sediment starvation

A prevailing view of Louisiana coastal restoration is that the marshes are sediment "starved" as a result of their isolation from overbank flooding of the Mississippi River by levee construction, and, therefore, restoration initiatives should aim to offset this sediment deficit by the introduction of mineral sediments (CPRA 2012, Morang et al. 2012, CLEAR 2008). Few studies, however, have attempted to quantify how much sediment once flowed over the natural levees and through crevasses into coastal marshes during these spring flood events, or the proportion of total inorganic sedimentation resulting from such floods. Kesel (1989) proposed that on average two percent of the total annual suspended load would have been available for overbank flow. This estimated percentage was then distributed over an average flood area of 10,000 km^2 to estimate an annual sedimentation rate of 0.028 g cm^{-2} yr^{-1} due to river flooding (2% of 141 MMT yr^{-1} over 10,000 km^2, or 2% of 'pre-dam' 463 MMT yr^{-1} load: 0.093 g cm^{-2} yr^{-1}). However, this estimate may overestimate the contribution of river floods to wetland sedimentation in abandoned delta lobes for several reasons.

One possible cause of overestimation is that the pre-disturbance sediment load of the Mississippi River is often estimated from samples collected in the late 1800s (Meade and Moody 2010, Kesel 1989, Kesel et al. 1992). However, these samples were collected during a period when the watershed was undergoing rapid conversion to an agricultural landscape (Tweel and Turner 2012a). This type of watershed modification led to increased erosion, and a subsequent increase in the amount of sediment carried by the river to the Gulf of Mexico (Tweel and Turner 2012a, Turner and Rabalais 2003, Keown et al. 1981). The sediment load prior to the proliferation of European-style agriculture (before 1800) was more likely somewhere between

the present (post-dam) load and the peak in the late 1800s. A model prediction of this load is 174 MMT yr^{-1} (Syvitski et al. 2003, Tweel and Turner 2012a), which suggests that the modern loads represent about 80% of historical loads, rather than the 30-35% often presented (Kesel 1989, Blum and Roberts 2012, Meade and Moody 2010). From either reference point, however, the reduction in sediment transport due to reservoir construction has been significant. Overbank flooding from the updated pre-disturbance (pre-1800) sediment load, would then have been 3.5 MMT yr^{-1}, or 0.035 g cm^{-2} yr^{-1} for the 10,000 km^2 flood area, with the thickness of this deposit decreasing with distance from the river channel.

A second consideration is that the suspended sediment concentrations at New Orleans are lower than at Tarbert landing, and this difference has been attributed to deposition in the river channel between the two stations (Allison et al. 2012, Winkley 1977). Estimates for overbank flooding were derived from sediment data collected at Tarbert Landing, and so may be greater than what was available at New Orleans and below. Other possible causes for overestimation of the sediment budget for overbank flooding include flood stages that have increased due to channel confinement (Belt 1973), and the need to include estuarine and wetland trapping efficiency. The fine silts and clays carried in the river have relatively long settling times ($> 4 \times 10^{-5}$ m s^{-1}), and can be easily resuspended (Booth et al. 2000).

Restriction of inorganic sediment supply due to river leveeing does not appear to sufficiently account for patterns of wetland loss in the last century. While reductions in sediment supply have been correlated to land loss in the birdfoot delta (Chapter two), the patterns and timing of loss in the deltaic and chenier plains occurred later than at the mouth of the river (Couvillion et al. 2011), and bear no detectable spatial relationship to the location of the river channel (Chapter five). There have been extensive wetland losses in the chenier plain which

never received overbank floodwaters from the Mississippi River, and these losses were similar in timing and magnitude to deltaic plain losses. These patterns align with the timing of deltaic plain wetland loss, and therefore suggest that the construction of river levees was not the primary driver of this landscape change. Additionally, the Biloxi Marsh and Marsh Island, which were formed by former delta lobes, have been isolated from riverine flooding for several millennia and have persisted with relatively low rates of land loss (Couvillion et al. 2011). Conversely, marshes near Lake Penchant have experienced an increase in fluvial inputs in the past several decades, yet have also experienced high land losses during the same period (Swarzenski et al. 2008). The areas of more stable marshes areas do, however, also overlie thinner (~30 m) Holocene deposits (Blum and Roberts 2009). In a multivariate analysis of Barataria Basin the thickness of these deposits was not found to be the dominant driver of land loss patterns (canal dredging: 19% of variability), but did explain about 15% of the variability of interior land loss patterns (Figure 5.11, page 103).

Wetlands closer to the river would receive more sediment during floods than wetlands farther away, yet there is no identifiable spatial relationship between the river channel and patterns of land loss or soil type (Chapter five). Instead, marsh soil type patterns in abandoned delta lobes increase in mineral content the closer they are to marine influence (Figure 2.8, page 29; Chabreck 1972, Kolb and van Lopik 1966, Tweel and Turner 2012b). This trend reflects the significance of marine processes (e.g., tides, hurricanes) in sediment budget of these wetlands. Recent analysis shows that hurricane storm surges are likely the dominant source of these inorganic sediments (Chapter four). This result stands in contrast to what occurs in active deltas, such as the birdfoot delta, which have seen reductions in sediment loads that are reflected in changes in land area (Tweel and Turner 2012a). Table 6.1 summarizes pre-disurbance and

modern inorganic sediment loading to Barataria Basin, based on the findings presented here and in the literature.

Rationale for canal restoration

The other anthropogenic factor that has been attributed to large-scale wetland loss is hydrologic modification due to canal dredging for pipelines and access to oil and gas canals (Chapter five, Turner 1997, Boesch et al. 1994, Penland et al. 2001). This has resulted in fragmentation of coastal wetland habitats, increased wetland edge exposure, and a decreased proportion of interior marshes (Table A.1, page 131). While canal dredging is acknowledged in the 2012 Master Plan as a factor that has caused land loss, none of the 145 restoration projects proposed in the most recent Master Plan address this cause-and-effect linkage in a restoration strategy (CPRA 2012). In the Hydrologic Restoration project group, projects involve the installation or improvement of hard structures such as sills or barriers (Master Plan Appendix A 2012). Three projects that included the gapping of spoil banks were screened out of consideration. The rationale why two canal backfilling projects were also screened out of the recommended project list appears to be because of size, rather than cost to benefit ratio.

Table 6.1 Summary of estimated inorganic sediment loading to Barataria Basin at time of European settlement and modern periods.

	Pre-disturbance		Modern		
To Barataria Basin (wetlands and water)	**MMT (tons × 10^6 yr^{-1})**	**%**	**MMT**	**%**	**Reference or Explanation**
Hurricanes	2.21	48	2.21	67 to 86	Chapter 5
Overbank flooding	1.27	28	0.00	0	Kesel 1989, prorated for new load esimates (Chapter 2)
Crevasses	0.47	10	0.00	0	and % of levee adjacent to Barataria
Intracoastal waterway	0.00	0	0.16	5 to 6	Mean streamflow at USGS gage 07381235, 140 mg L^{-1}
Naomi siphon	0.00	0	0.04 to 0.2	1 to 8	Estimated based on proportional discharge to Davis Pond
Pointe a la Hache siphon	0.00	0	0.04 to 0.2	1 to 8	Estimated based on proportional discharge to Davis Pond
Davis Pond diversion	0.00	0	0.1 to 0.5	3 to 20	Swenson unpubl., Allison et al. 2012
Tidal movement	? (+ or -)		? (+ or -)		
Cold fronts	? (+ or -)		? (+ or -)		
From uplands	?		0.01	0.4	Based on yield for 7 coastal basins, prorated for watershed size (Rosen 2013, Wu 2005)
TOTAL	**3.95**		**2.56 to 3.28**		Modern values are 65% to 83% of pre-disturbance loads

Restoration of wetlands in coastal Louisiana should aim, I think, to reverse, where practicable, the anthropogenic modifications to both ecological and geological processes. Recent analysis shows a strong relationship between land loss and canal dredging, and no apparent relationship to any distance parameter related to the river or distributary (Chapter five). Louisiana's coastal wetlands have approximately 357 km^2 of canals and channels in the deltaic plain, plus additional direct wetland loss from spoil placement and canals in the chenier plain (Penland et al. 2001). Public data identify over 18,000 oil and gas wells in the Louisiana Coastal zone that lie within the wetland landscape (i.e. excluding bays and ponds) and are listed as "dry and plugged" or "shut in, no future utility." Although many canals provide access to more than one well, there are many canals that are no longer used that would be good candidates for hydrologic restoration. Spoil banks of actively used canals could also be gapped to relieve hydrologic stress on the coastal landscape while still providing access to support the oil and gas industry.

Canals in Jean Lafitte National Park have been restored with good success (Baustian and Turner 2006), and at a per-area cost well below most other projects listed in Appendix A (CPRA 2012). Estimates for the construction costs of dredging spoil banks into adjacent canals range from to \$3,400-\$16,800 ha^{-1} (Baustian et al. 2009), plus additional hydrologic benefit to adjacent marshes. Average construction costs for planned diversions under the moderate sea level scenario range from \$680,000 to \$1,620,000 ha^{-1} at 50 and 20 years, respectively, and approximately \$580,000 ha^{-1} for construction costs of direct marsh creation (CPRA 2012 Appendix A). The benefits would include direct wetland creation (Baustian and Turner 2006), restoration of natural hydroperiods to surrounding wetlands (Swenson and Turner 1987), increased habitat for fish and invertebrates (Rozas and Reed 1994), and storm surge reduction via reduced fragmentation and shallower channels- all of which help meet the goals of the

Master Plan. Coastal restoration would benefit greatly from the addition of canal backfilling and spoil bank gapping projects to the Louisiana Comprehensive Master Plan. Future changes in climate, sea level, and human/economic dimensions of coastal Louisiana present new uncertainties beyond the challenges of restoring historical impacts to the Louisiana coast.

Climate change

Climate change will likely affect coastal ecosystems in many ways, both directly and indirectly, but many of these effects are intertwined and the net landscape effect is highly uncertain (Gedan et al. 2011, Syvitski et al. 2005). Examples of direct impacts to coastal wetlands include sea level rise or changes in hurricane or winter storm frequency. Indirect impacts may include secondary effects such as changes in river discharge or water quality resulting from shifts in precipitation patterns, or even tertiary impacts such as changes in watershed vegetation cover that would, in turn, affect water quality (Michener et al. 1997). Marshes with differing tidal ranges and sediment inputs may be more resilient than others, with marshes in high tide range areas expected to withstand increases in sea level more readily (D'Alpaos et al. 2011, Kirwan et al. 2010).

Certainly, ecotones will migrate landward in response to sea level rise (Syvitski et al. 2005). Developed upland boundaries, however, may constrain this process (Michener et al. 1997), and the rate of relative sea level rise will be a major factor in how coastal ecosystems are affected (Feagin et al. 2010). Marsh accretion rates will increase to attempt to maintain their position in the tidal frame, and this biological-physical feedback will ultimately determine marsh survival (Redfield 1972, Kirwan et al. 2010). Part of this feedback cycle could depend on changes in mineral sediment loading, which would vary with changes in storm frequency or intensity (Chapter four, Schuerch et al. 2012). Increases in storm intensity could also lead to

increased damage to coastal communities (Emanuel 2005) and accelerated geomorphic change (Morton and Barras 2011). Transgression and reworking of eroding marshes at the seaward extent of estuaries would supply the more inland marshes with additional sediment. Vegetative canopy can baffle and trap sediment, but decreases in canopy due to waterlogging can trigger a positive feedback that also leads to reduced sedimentation (Voss et al. 2013). Current restoration plans to divert nutrient-rich Mississippi River water into estuaries may exacerbate these vulnerabilities by weakening marsh soils due to increasing soil decomposition rates (Kearney et al. 2011, Swarzenski et al 2008) or shifting plant species composition (Howes et al. 2010). Fed by an intensive agricultural system that covers 40% of the watershed (Raymond et al. 2008), nutrient loads in the Mississippi River are higher than ever (Broussard and Turner 2009). This brings into consideration whether the re-introduction of flood water is the restoration of a historical process or the initiation of a novel ecosystem with uncertain characteristics. The complexity and feedback mechanisms inherent to these interactions make it difficult to predict the response of coastal wetlands to climate change. Researchers and managers are faced with the challenging task of weighing the costs and benefits against the large uncertainties that remain.

Conclusions

Coastal restoration plans must be flexible enough to adapt to changing scientific understanding of how ecosystems respond to human intervention. The 2012 Comprehensive Master Plan places great weight on the assumptions that (1) coastal marshes are starved of mineral sediment and must be restored by reintroduction of river water (2) that the addition of nutrients supplied by Mississippi River water will help, or at least not harm, coastal marshes (CPRA 2012). Research presented here and elsewhere raises new questions about how physical, chemical, and biological systems interact and regulate coastal systems, and how these driving

factors can vary considerably over relatively short distances (Tweel and Turner 2012a, Tweel and Turner 2012b, Kearney et al. 2011, Turner 2009). The success of coastal restoration in Louisiana and elsewhere will be greatly aided if this spatial variability and remaining scientific uncertainties are included in planning. Doing this will supply resource managers with the tools needed to accurately compare the costs, benefits, and risks of restoration options.

References

Allison M. A., C. R. Demas, B. A. Ebersole, B. A. Kleiss, C. D. Little, E. A. Meselhe, M. J. Powell, T. C. Pratt, and B. M. Vosburg. 2012. A Water and Sediment Budget for the Lower Mississippi-Atchafalaya River in Flood Years 2008-2010: Implications for Sedimetn Discharge to the Oceans and Coastal Restoration in Louisiana. Journal of Hydrology 432:84-97.

Barra, R., M. Cisternas, C. Suarez, A. Araneda, O. Piñones, and P. Popp. 2004. PCBs and HCHs in a Salt-Marsh Sediment Record from South-Central Chile: Use of Tsunami Signatures and ^{137}Cs Fallout as Temporal Markers. Chemosphere 55:965-972.

Baustian, J. J. and R. Eugene Turner. 2006. Restoration Success of Backfilling Canals in Coastal Louisiana Marshes. Restoration Ecology 14:636-644.

Baustian, J. J., R. E. Turner, N. F. Walters, and D. P. Muth. 2009. Restoration of Dredged Canals in Wetlands: A Comparison of Methods. Wetlands Ecology and Management 17:445-453.

Belt Jr., C. 1975. The 1973 Flood and Man's Constriction of the Mississippi River. Science 189:681-684.

Blum, M. D. and H. H. Roberts. 2012. The Mississippi Delta Region: Past, Present, and Future. Annual Review of Earth and Planetary Sciences 40:655-683.

Boesch, D. F., M. N. Josselyn, A. J. Mehta, J. T. Morris, W. K. Nuttle, C. A. Simenstad, and D. J. Swift. 1994. Scientific Assessment of Coastal Wetland Loss, Restoration and Management in Louisiana. Journal of Coastal Research SI 20. 103 p.

Booth, J., R. Miller, B. McKee, and R. Leathers. 2000. Wind-Induced Bottom Sediment Resuspension in a Microtidal Coastal Environment. Continental shelf research 20:785-806.

Bourgeois, J. 2009. Geologic Effects and Records of Tsunamis. A. R. Robinson and E. N. Bernard, eds. The Sea. Harvard University Press, Cambridge, Massachusetts. p. 55-91.

Broussard, W. and R. E. Turner. 2009. A Century of Changing Land-Use and Water-Quality Relationships in the Continental Us. Frontiers in Ecology and the Environment 7:302-307.

Brückner, H. 1986. Man's Impact on the Evolution of the Physical Environment in the Mediterranean Region in Historical Times. GeoJournal 13:7-17.

Chabreck, R. H. 1972. Vegetation, Water and Soil Characteristics of the Louisiana Coastal Region. Louisiana Agricultural Experiment Station Bulletin 664. 72 p.

CLEAR. 2008. Coastal Louisiana Ecosystem Assessment and Restoration (Clear) Program. Volume 4. Final Report to Department of Natural Resources, Coastal Restoration Division. Baton Rouge, Louisiana. www.clear.lsu.edu

Couvillion, B. R., J. A. Barras, G. D. Steyer, W. Sleavin, M. Fischer, H. Beck, N. Trahan, B. Griffin, and D. Heckman. 2011. Land Area Change in Coastal Louisiana (1932 to 2010). US Department of the Interior, US Geological Survey. 12 p.

CPRA. 2012. Louisiana's Comprehensive Master Plan for a Sustainable Coast. Coastal Protection and Restoration Authority, Baton Rouge, Louisiana. www.coastalmasterplan.louisiana.gov

D'Alpaos, A., S. Mudd, and L. Carniello. 2011. Dynamic Response of Marshes to Perturbations in Suspended Sediment Concentrations and Rates of Relative Sea Level Rise. Journal of Geophysical Research 116:F04020.

Dawson, A. 1994. Geomorphological Effects of Tsunami Run-up and Backwash. Geomorphology 10:83-94.

Emanuel, K. 2005. Increasing Destructiveness of Tropical Cyclones over the Past 30 Years. Nature 436:686-688.

Feagin, R. A., M. L. Martinez, G. Mendoza-Gonzalez, and R. Costanza. 2010. Salt Marsh Zonal Migration and Ecosystem Service Change in Response to Global Sea Level Rise: A Case Study from an Urban Region. Ecology and Society 15:14-28.

Gagliano, S. M., K. J. Meyer-Arendt, and K. M. Wicker. 1981. Land Loss in the Mississippi River Deltaic Plain. Transactions Gulf Coast Association Geological Society 31:295-300.

Gedan, K. B., M. L. Kirwan, E. Wolanski, E. B. Barbier, and B. R. Silliman. 2011. The Present and Future Role of Coastal Wetland Vegetation in Protecting Shorelines: Answering Recent Challenges to the Paradigm. Climatic change 106:7-29.

Goto, K., C. Chagué-Goff, S. Fujino, J. Goff, B. Jaffe, Y. Nishimura, B. Richmond, D. Suguwara, W. Szczuciński, and D. R. Tappin. 2011. New Insights of Tsunami Hazard from the 2011 Tohoku-Oki Event. Marine Geology 290:46-50.

Howes, N. C., D. M. FitzGerald, Z. J. Hughes, I. Y. Georgiou, M. A. Kulp, M. D. Miner, J. M. Smith, and J. A. Barras. 2010. Hurricane-Induced Failure of Low Salinity Wetlands. Proceedings of the National Academy of Sciences 107:14014-14019.

Kearney, M. S., J. C. A. Riter, and R. E. Turner. 2011. Freshwater River Diversions for Marsh Restoration in Louisiana: Twenty-Six Years of Changing Vegetative Cover and Marsh Area. Geophysical Research Letters 38:L16405.

Keown, M. P., E. A. Dardeau Jr, and E. M. Causey. 1981. Characterization of the Suspended Sediment Regime and Bed-Material Gradation of the Mississippi River Basin. US Army Engineer Waterways Experiment Station, Vicksburg, Mississippi.

Kesel, R. H. 1988. The Decline in the Suspended Load of the Lower Mississippi River and Its Influence on Adjacent Wetlands. Environmental Geology 11:271-281.

Kesel, R. H. 1989. The Role of the Mississippi River in Wetland Loss in Southeastern Louisiana, USA. Environmental Geology 13:183-193.

Kesel, R. H., E. G. Yodis, and D. J. McCraw. 1992. An Approximation of the Sediment Budget of the Lower Mississippi River Prior to Major Human Modification. Earth Surface Processes and Landforms 17:711-722.

Kirwan, M. L., G. R. Guntenspergen, A. D'Alpaos, J. T. Morris, S. M. Mudd, and S. Temmerman. 2010. Limits on the Adaptability of Coastal Marshes to Rising Sea Level. Geophysical Research Letters 37:L23401.

Kirwan, M. L., A. B. Murray, J. P. Donnelly, and D. R. Corbett. 2011. Rapid Wetland Expansion During European Settlement and Its Implication for Marsh Survival under Modern Sediment Delivery Rates. Geology 39:507-510.

Kolb, C. R. and J. R. van Lopik. 1966. Depositional Environments of the Mississippi River Deltaic Plain Region-Southeastern Louisiana. L. S. Shirley and J. A. Ragsdale, eds. Deltas in their Geologic Framework. Houston Geological Society. p. 17-61.

Kosters, E., G. Chmura, and A. Bailey. 1987. Sedimentary and Botanical Factors Influencing Peat Accumulation in the Mississippi Delta. Journal of the Geological Society, London 144:423-434.

Kosters, E. C. 1989. Organic-Clastic Facies Relationships and Chronostratigraphy of the Barataria Interlobe Basin, Mississippi Delta Plain. Journal of Sedimentary Research 59:98-113.

Meade, R. H. and J. A. Moody. 2010. Causes for the Decline of Suspended-Sediment Discharge in the Mississippi River System, 1940–2007. Hydrological Processes 24:35-49.

Mendelssohn, I. A., K. McKee, and W. Patrick Jr. 1981. Oxygen Deficiency in Spartina Alterniflora Roots: Metabolic Adaptation to Anoxia. Science 214:439-441.

Michener, W. K., E. R. Blood, K. L. Bildstein, M. M. Brinson, and L. R. Gardner. 1997. Climate Change, Hurricanes and Tropical Storms, and Rising Sea Level in Coastal Wetlands. Ecological Applications 7:770-801.

Morang, A., J. P. Waters, and S. M. Khalil. 2012. Gulf of Mexico Regional Sediment Budget. Journal of Coastal Research SI 60:14-29.

Morton, R. A. and J. A. Barras. 2011. Hurricane Impacts on Coastal Wetlands: A Half-Century Record of Storm-Generated Features from Southern Louisiana. Journal of Coastal Research 27:27-43.

Morton, R. A., G. Gelfenbaum, and B. E. Jaffe. 2007. Physical Criteria for Distinguishing Sandy Tsunami and Storm Deposits Using Modern Examples. Sedimentary Geology 200:184-207.

Nanayama, F., R. Furukawa, K. Shigeno, A. Makino, Y. Soeda, and Y. Igarashi. 2007. Nine Unusually Large Tsunami Deposits from the Past 4000 Years at Kiritappu Marsh Along the Southern Kuril Trench. Sedimentary Geology 200:275-294.

Penland, S., L. Wayne, D. Britsch, S. Williams, A. Beall, and V. Butterworth. 2001. Process Classification of Coastal Land Loss between 1932 and 1990 in the Mississippi River Delta Plain, Southeastern Louisiana, Open-File Report 00-418. United States Geological Survey.

Raymond, P. A., N. H. Oh, R. E. Turner, and W. Broussard. 2008. Anthropogenically Enhanced Fluxes of Water and Carbon from the Mississippi River. Nature 451:449-452.

Redfield, A. C. 1972. Development of a New England Salt Marsh. Ecological Monographs 42:201-237.

Rosen, T. 2013. Long-term Total Suspended Sediment Yield of Coastal Louisiana Rivers with Spatiotemporal Analysis of the Atchafalaya River Basin and Delta Complex. M.S. Thesis. Louisiana State University.

Rozas, L. P. and D. J. Reed. 1994. Comparing Nekton Assemblages of Subtidal Habitats in Pipeline Canals Traversing Brackish and Saline Marshes in Coastal Louisiana. Wetlands 14:262-275.

Schuerch, M., J. Rapaglia, V. Liebetrau, A. Vafeidis, and K. Reise. 2012. Salt Marsh Accretion and Storm Tide Variation: An Example from a Barrier Island in the North Sea. Estuaries and Coasts 35:486-500.

SONRIS. 2012. Petroleum Production Data to 1977. Louisiana Office of Conservation. Baton Rouge, Louisiana.

Swarzenski, C. M., T. W. Doyle, B. Fry, and T. G. Hargis. 2008. Biogeochemical Response of Organic-rich Freshwater Marshes in the Louisiana Delta Plain to Chronic River Water Influx. Biogeochemistry 90:49-63.

Swenson, E. M. and R. E. Turner. 1987. Spoil Banks: Effects on a Coastal Marsh Water-Level Regime. Estuarine, Coastal and Shelf Science 24:599-609.

Syvitski, J. P., C. J. Vörösmarty, A. J. Kettner, and P. Green. 2005. Impact of Humans on the Flux of Terrestrial Sediment to the Global Coastal Ocean. Science 308:376-380.

Syvitski, J. P. M., S. D. Peckham, R. Hilberman, and T. Mulder. 2003. Predicting the Terrestrial Flux of Sediment to the Global Ocean: A Planetary Perspective. Sedimentary Geology 162:5-24.

Turner, R., E. Swenson, and C. Milan. 2002. Organic and Inorganic Contributions to Vertical Accretion in Salt Marsh Sediments. M. P. Weinstein and D. A. Kreeger, eds. Concepts and Controversies in Tidal Marsh Ecology. Kluwer Publishers. p. 583-595.

Turner, R. E. 1997. Wetland Loss in the Northern Gulf of Mexico: Multiple Working Hypotheses. Estuaries and Coasts 20:1-13.

Turner, R. E. 2009. Doubt and the Values of an Ignorance-Based World View for Restoration: Coastal Louisiana Wetlands. Estuaries and Coasts 32:1054-1068.

Turner, R. E., J. J. Baustian, E. M. Swenson, and J. S. Spicer. 2006. Wetland Sedimentation from Hurricanes Katrina and Rita. Science 314:449-452.

Turner, R. E. and N. N. Rabalais. 2003. Linking Landscape and Water Quality in the Mississippi River Basin for 200 Years. BioScience 53:563-572.

Tweel, A. W. and R. E. Turner. 2012a. Watershed Land Use and River Engineering Drive Wetland Formation and Loss in the Mississippi River Birdfoot Delta. Limnology and Oceanography 57:18-28.

Tweel, A. W. and R. E. Turner. 2012b. Landscape-Scale Analysis of Wetland Sediment Deposition from Four Tropical Cyclone Events. PloS ONE 7:e50528.

Voss, C. M., R. R. Christian, and J. T. Morris. 2013. Marsh Macrophyte Responses to Inundation Anticipate Impacts of Sea-Level Rise and Indicate Ongoing Drowning of North Carolina Marshes. Marine Biology 160:1-14.

Winer, H. S. 2011. Re-Engineering the Mississippi River as a Sediment Delivery System. Journal of Coastal Research SI 21:229-234.

Winkley, B. R. 1977. Man-Made Cutoffs on the Lower Mississippi River, Conception, Construction, and River Response. US Army Engineer District. Vicksburg, Mississippi.

Wu, K. 2005. Long-term Freshwater Input and Sediment Load from Three Tributaries to Lake Pontchartrain, Louisiana. Ph.D. Dissertation. Louisiana State University.

APPENDIX A
OIL AND GAS DEVELOPMENT IN THE COASTAL ZONE AND BARATARIA BASIN

This section presents a geographical summary of oil and gas development the Louisiana Coastal Zone (to 2007) and examples from Barataria Basin, Louisiana (to 2001).

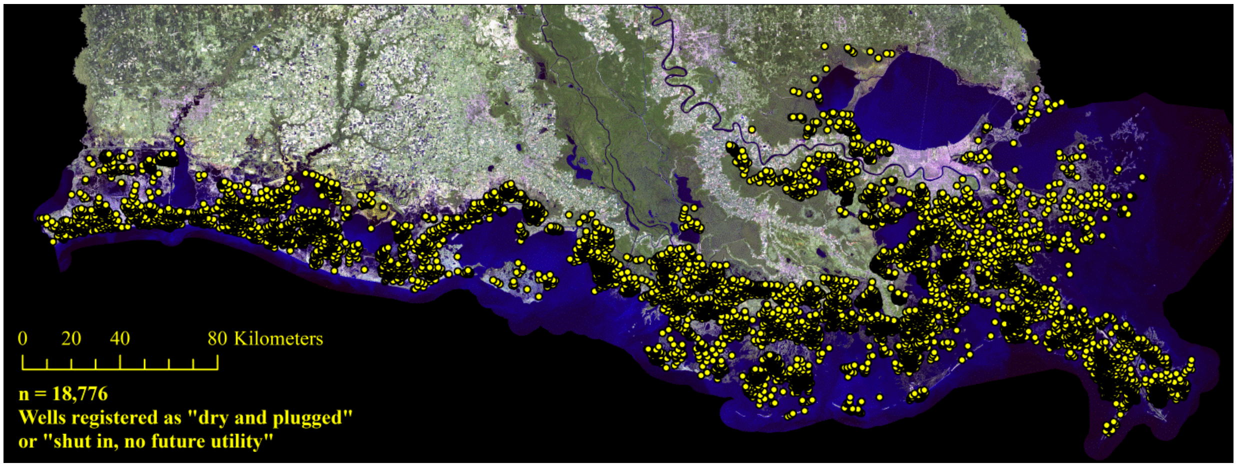

Figure A.1 Oil wells registered with the State of Louisiana that are coded as “dry and plugged” or “shut in, no future utility” that intersect the Coastal Zone and land area of 1932, excluding developed areas.

Table A.1 Summary statistics for land area in Barataria Basin from 1932 to 2001.

Year	Edge (km)	Area (km^2)	Edge:Area ratio	μ patch size (km^2)	# patches	μ distance to edge (m)
1932	6675	3577	1.87	5.31	673	750
1958	9237	3426	2.70	2.91	1175	482
1974	12298	3208	3.83	1.42	2244	352
1983	13291	3047	4.36	0.91	3332	289
1990	13773	2948	4.67	0.71	4135	278
2001	13965	2819	4.95	0.54	5132	267

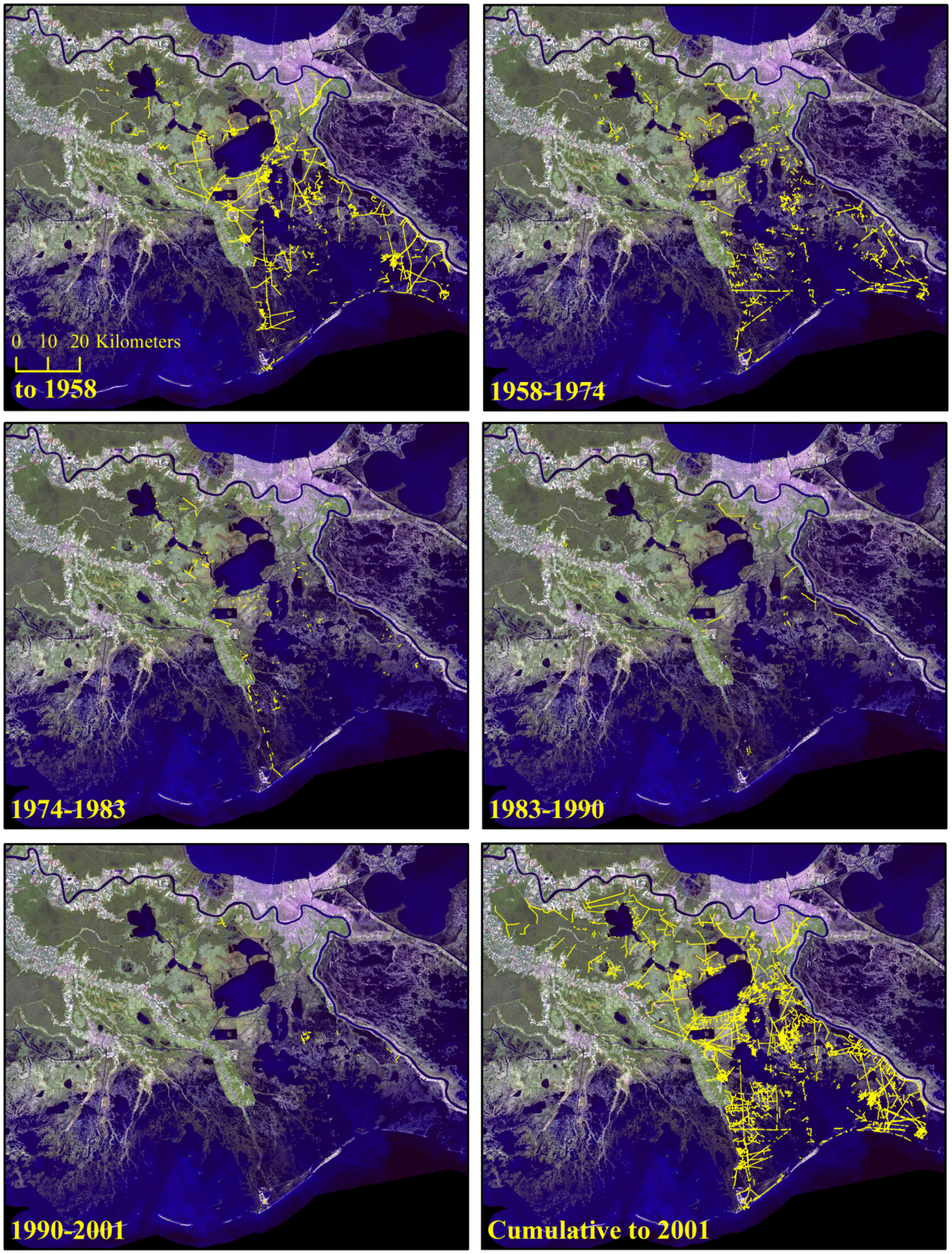

Figure A.2 Canal development in Barataria Basin to 2001.

APPENDIX B
COPYRIGHT PERMISSIONS

CHAPTER 2

Gmail by Google

Andrew Tweel <atweel@gmail.com>

ASLO Copyright Permission

Jo Davis <jdavis@sgmeet.com>
To: "atweel1@lsu.edu" <atweel1@lsu.edu>

Tue, Feb 5, 2013 at 4:50 PM

To: Mr. Andrew W. Tweel,

On behalf of the Association for the Sciences of Limnology and Oceanography, we are happy to grant permission to use the figures from Limnology & Oceanography per your application below for free publication not to be sold.

When reproducing the article/figure(s), please cite according to the references that follow:

All copyrighted works, whether displayed electronically or in print, should be properly acknowledged as follows:

"Copyright (Year) by the Association for the Sciences of Limnology and Oceanography, Inc."

Once permission is granted to use an article or any part thereof of a work from L&O, the full citation must include:
1. Name(s) of the author(s);
2. Journal title (Association for the Sciences of Limnology & Oceanography or L&O)
3. Publication date
4. Volume number
5. Issue number
6. Chapter or article name
7. Pages on which the articles, data, and/ or figure(s) appear

For your records, the Association for the Sciences of Limnology and Oceanography is a nonprofit organization. (Taxpayer I.D. Number: 38-1710020)

If you have additional requests or have any questions in regard to this request, you can contact me directly via e-mail at jdavis@sgmeet.com.

Sincerely,

Jo Davis
ASLO Business Office
Database Supervisor

CHAPTER 3

plos.org | create account | sign in

PLOS | ONE

Articles | For Authors | About Us | Search

advanced search

Open-Access License

No Permission Required

PLOS applies the Creative Commons Attribution License (CCAL) to all works we publish (read the human-readable summary or the full license legal code). Under the CCAL, authors retain ownership of the copyright for their article, but authors allow anyone to download, reuse, reprint, modify, distribute, and/or copy articles in PLOS journals, so long as the original authors and source are cited. **No permission is required from the authors or the publishers.**

In most cases, appropriate attribution can be provided by simply citing the original article (e.g., Kaltenbach LS et al. (2007) Huntingtin Interacting Proteins Are Genetic Modifiers of Neurodegeneration. *PLOS Genet* 3(5): e82. doi:10.1371/journal.pgen.0030082). If the item you plan to reuse is not part of a published article (e.g., a featured issue image), then please indicate the originator of the work, and the volume, issue, and date of the journal in which the item appeared. For any reuse or redistribution of a work, you must also make clear the license terms under which the work was published.

This broad license was developed to facilitate open access to, and free use of, original works of all types. Applying this standard license to your own work will ensure your right to make your work freely and openly available. Learn more about open access. For queries about the license, please contact us.

PLOS

Ambra 2.5.3 Managed Colocation provided by **Internet Systems Consortium**.

Privacy Policy | Terms of Use | Advertise | Media Inquiries

Journals

PLOS Biology
PLOS Medicine
PLOS Computational Biology
PLOS Genetics
PLOS Pathogens
PLOS ONE
PLOS Neglected Tropical Diseases

plos.org

Blogs

Collections

Send us feedback

VITA

Andrew Tweel was born in Columbus, Ohio. He attended Colorado College in Colorado Springs, Colorado, graduating in 2004 with a Bachelor of Arts in Biology and a minor in Environmental Issues. Following graduation, he worked at Archbold Biological Station in Lake Placid, Florida, studying plant demography and fire ecology. He later worked at MacArthur Research Center, near Okeechobee, Florida, studying nutrient cycling in subtropical wetlands. Following a brief stint as a handyman, he worked at Waquoit Bay National Estuarine Research Reserve in Falmouth, Massachusetts. Here he studied vegetation and nekton communities with respect to hydrologic restoration of a salt marsh, and also led a tagging study to determine the migratory behaviors of native sea-run brook trout. He also, mostly unsuccessfully, fly-fished for these secretive trout. Following his interest in wetlands, he began his doctorate in the Department of Oceanography and Coastal Sciences in 2008.